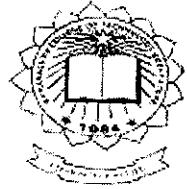




P-3515



**DESIGN AND DEVELOPMENT OF HIGH EFFICIENT
MICROSTRIP ANTENNA FOR WLAN 802.11b/g APPLICATIONS**

By

RIA MARIA GEORGE

Reg. No. 0920107018

of

KUMARAGURU COLLEGE OF TECHNOLOGY

(An Autonomous Institution affiliated to Anna University, Coimbatore)

COIMBATORE - 641049

A PROJECT REPORT

Submitted to the

**FACULTY OF ELECTRONICS AND COMMUNICATION
ENGINEERING**

In partial fulfillment of the requirements

for the award of the degree

of

MASTER OF ENGINEERING


IN


COMMUNICATION SYSTEMS

APRIL 2011

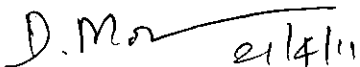
BONAFIDE CERTIFICATE

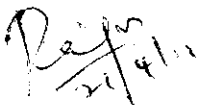
Certified that this project report entitled “**DESIGN AND DEVELOPMENT OF HIGH EFFICIENT MICROSTRIP ANTENNA FOR WLAN 802.11b/g APPLICATIONS**” is the bonafide work of **Ms.Ria Maria George** [Reg. no. 0920107018] who carried out the research under my supervision. Certified further, that to the best of my knowledge the work reported herein does not form part of any other project or dissertation on the basis of which a degree or award was conferred on an earlier occasion on this or any other candidate.


Project Guide
Mr.S.Venkatesh


Head of the Department
Dr. (Mrs.) Rajeswari Mariappan

The candidate with university Register no. 0920107018 is examined by us in the project viva-voce examination held on ...21-04-2011.....


Internal Examiner


External Examiner



CERTIFICATE

This is to certify that **Ms. Ria Maria George** has successfully completed and submitted the project work titled “**Design and Development of High Efficient Microstrip Antenna for WLAN 802.11 b/g Applications**” towards the partial fulfilment of requirements for the award of M.E. Degree in Communication Systems at Kumaraguru College of Technology, affiliated to Anna university, Coimbatore is a bonafide record of the work carried out under our guidance at SFO Technologies Pvt. Ltd (JKH Technology Center), Cochin.


31/3/11
Dr. Suresh Nair.K.R.

Chief Technology Officer


Mr .Ahamed Ameen .P

Project Manager

ACKNOWLEDGEMENT

A project of this nature needs co-operation and support from many for successful completion. In this regards, I would like to express my thanks and appreciation to the many people who have contributed to the successful completion of this project.

I express my profound gratitude to our beloved Director **Dr.J. Shanmugam**, Kumaraguru College of Technology for his kind support and necessary facilities to carry out the work.

I would like to thank **Prof.Dr.S.Ramachandran Ph.D** , Principal for providing us an opportunity to carry out this project work.

I express my gratitude to **Dr.Rajeswari Mariappan Ph.D** Head of the Department, Electronics and Communication Engineering, who gave her continual support for me throughout the course of this project.

My heartfelt thanks to **Ms.D.Mohanageetha (Ph.D)**, Associate Professor and Project Coordinator, for her contribution and innovative ideas at various stages of the project and for her help to successful completion of this project work.

I express my gratitude to **Mr. S. Venkatesh (Ph.D)**, Assistant Professor and my internal project guide, for his valuable guidance, innovative ideas and constant encouragement throughout this project.

I express my sincere gratitude to **Dr.Suresh Nair K. R**, Chief Technology Officer, SFO Technologies JKH Technology Centre, for providing exhaustive facilities, constant encouragement and many valuable suggestions provided throughout the project work.

I would like to express my sincere thanks to **Mr. Ahamed P. Ameen**, Project Manager SFO Technologies and my external project guide for his valuable guidance and support throughout this project.

I express my sincere gratitude to my family members, friends and to all my staff members of Electronics and Communication Engineering department for their support throughout the course of my project.

Last but not the least I would like to thank the God almighty without whose grace nothing would have been possible so far.

ABSTRACT

WLAN 802.11 b/g devices use 2.4 GHz frequency for communication and in order to achieve better range and continuity, the antenna needs to be highly efficient. This calls for requirement of antennas with better VSWR or Return Loss (RL) as well as Omni- directional radiation pattern. For existing antenna RL is around -2.5 dB and this shows a poor matching characteristics. The project aims to design and develop microstrip antennas with better Return Loss or VSWR and good Omni directional radiation pattern. The simulation is done for different substrate materials as well as antenna shapes to achieve optimum characteristics. The CAD tool used is HFSS (AnSoft). The antenna showing the best characteristics will be fabricated and studied. The fabricated antennas will be characterized for return loss and radiation pattern (limited way in open air).

TABLE OF CONTENT

CHAPTER NO	TITLE	PAGE NO
	ABSTRACT	iv
	LIST OF FIGURES	ix
	LIST OF TABLES	xiii
	LIST OF ABBREVIATIONS	xiv
1	INTRODUCTION	1
	1.1 Problem Definition	1
	1.2 Scope of work	2
	1.3 Company Profile	2
	1.4 Overview of Microstrip Antenna	3
	1.5 Antenna Characteristics	4
	1.5.1 Radiation pattern	4
	1.5.2 Polarization	4
	1.5.3 Radiation Intensity	5
	1.5.4 Radiated Power	5
	1.5.5 Effective Angle	6
	1.5.6 Directivity	6
	1.5.7 Gain	6
	1.5.8 Efficiency	6
	1.5.9 Effective Area	7
	1.5.10 VSWR	7
	1.5.11 Return loss	7
2	MICROSTRIP PATCH ANTENNA	8
	2.1 Introduction	8

2.2	Advantages and Disadvantages	10
2.3	Feed Techniques	11
2.3.1	Microstrip Line Feed	11
2.4	Method of Analysis	12
2.4.1	Transmission Line Mode	12
3	HIGH FREQUENCY STRUCTURE SIMULATOR	16
4	SIMULATIONS AND RESULT	19
4.1	Dipole Antenna using different substrate materials	19
4.1.1	FR4 of 1mm thickness	20
4.1.2	FR4 of 1.6mm thickness	21
4.1.3	DUROID 5880 of 1.575mm thickness	22
4.1.4	ROGERS RO 4350 of 1.524mm thickness	23
4.2	Rectangular Inset Feed Patch Antenna using different substrate materials	24
4.2.1	FR4 of 1mm thickness	25
4.2.2	FR4 of 1.6mm thickness	26
4.2.3	DUROID 5880 of 1.575mm thickness	27
4.2.4	ROGERS RO 4350 of 1.524mm thickness	28
4.3	Elliptical Inset Feed Patch Antenna using different substrate materials	29
4.3.1	FR4 of 1mm thickness	30
4.3.2	FR4 of 1.6mm thickness	31
4.3.3	DUROID 5880 of 1.575mm thickness	31
4.3.4	ROGERS RO 4350 of 1.524mm thickness	33
4.4	Planar Inverted F-Antenna (PIFA) using different substrate materials	34
4.4.1	FR4 of 1mm thickness	35
4.4.2	FR4 of 1.6mm thickness	36
4.4.3	DUROID 5880 of 1.575mm thickness	37

4.4.4	ROGERS RO 4350 of 1.524mm thickness	38
4.5	F- Monopole Antenna using different substrate materials	39
4.5.1	F-antenna of 10x15mm ² integrated on substrate dimension- 45x80mm ²	39
4.5.1.1	FR4	40
4.5.1.2	DUROID 5880 of 1.575mm thickness	41
4.5.1.3	ROGERS RO 4350 of 1.524mm thickness	42
4.5.2	F-antenna of 9x15mm ² integrated on FR4 substrate (1mm) dimension of 50x35mm ² and cutout 15x15mm ²	43
4.5.3	F-antenna of 9x15mm ² integrated on substrate dimension of 50x35mm ² and cutout 50x18mm ²	45
4.5.3.1	FR4 of 1mm thickness	46
4.5.3.2	FR4 of 1.6mm thickness	47
4.5.4	F-antenna of 9x15mm ² integrated on FR4 substrate (1mm) dimension 47x40mm ² and cutout 15x15mm ²	48
4.5.5	F-antenna of 9x15mm ² integrated on substrate dimension of 47x40mm ² and cutout 47x18mm ²	50
4.5.5.1	FR4 of 1mm thickness	51
4.5.5.2	FR4 of 1.6mm thickness	52
4.6	Spiral Shaped Monopole an using Duroid 5870 Substrate antenna using different substrate materials	53
4.6.1	FR4 of 1mm thickness	54
4.6.2	FR4 of 1.6mm thickness	55
4.6.3	DUROID 5880 of 1.575mm thickness	56
4.6.4	ROGERS RO 4350 of 1.524mm thickness	57
5	FABRICATION AND MEASURED RESULTS	59
5.1	Measured Return loss and VSWR	61
5.1.1	F-antenna of 9x15mm ² integrated on FR4 of 1.6mm thickness substrate dimension- 50x35mm ²	61

5.1.2. F-antenna of $9 \times 15 \text{mm}^2$ integrated on FR4 of 1.6mm thickness substrate dimension- $47 \times 40 \text{mm}^2$	61
5.1.3 Planar Spiral of $5 \times 10 \text{mm}^2$ & FR4- $35 \times 50 \text{mm}^2$	62
5.2 Measured Radiation Pattern	63
5.2.1 F-antenna of $9 \times 15 \text{mm}^2$ integrated on FR4 substrate dimension- $47 \times 40 \text{mm}^2$	63
5.2.2. Planar Spiral of $5 \times 10 \text{mm}^2$ & FR4- $35 \times 50 \text{mm}^2$	64
5.3 Range Results	66
6 CONCLUSION	69
BIBLIOGRAPHY	72

LIST OF FIGURES

FIGURE NO	CAPTION	PAGE NO
1.1a	Photograph of Antenna in the device	1
1.1b	Return Loss characteristics of the antenna	2
2.1	Structure of a Microstrip Patch Antenna	8
2.2	Common Shapes of Microstrip Patch elements Microstrip	9
2.3	Line Feed	11
2.4	Microstrip Line	12
2.5	Electric Field Lines	12
2.6	Microstrip Patch Antennas	13
2.7	Top View of Antenna	14
2.8	Side View of Antenna	14
3.1	Main Screen of HFSS	17
3.2	The Process of Creating Design	18
4.1	Structure of dipole antenna on HFSS	19
4.1.1	Simulated results of Dipole antenna with FR4 of thickness 1mm	20
4.1.2	Simulated results of Dipole antenna with FR4 of thickness 1.6mm	21
4.1.3	Simulated results of Dipole antenna with Duroid 5880	22
4.1.4	Simulated results of Dipole antenna with RO 4350	23
4.2	Structure of rectangular inset feed patch antenna on HFSS	24
4.2.1	Simulated results of Rectangular inset feed patch antenna with FR4 of thickness 1mm	25
4.2.2	Simulated results of Rectangular inset feed patch antenna with FR4 of thickness 1.6mm	26
4.2.3	Simulated results of Rectangular inset feed patch antenna with Duroid 5880	27

4.2.4	Simulated results of Rectangular inset feed patch antenna with RO 4350	28
4.3	Structure of elliptical inset feed patch antenna on HFSS	29
4.3.1	Simulated results of Elliptical inset feed patch antenna with FR4 of thickness 1mm	30
4.3.2	Simulated results of Elliptical inset feed patch antenna with FR4 of thickness 1.6mm	31
4.3.3	Simulated results of Elliptical inset feed patch antenna with Duroid 5880	32
4.3.4	Simulated results of Elliptical inset feed patch antenna with RO 4350	33
4.4	Structure of PIFA antenna on HFSS	34
4.4.1	Simulated results of PIFA antenna with FR4 of thickness 1mm	35
4.4.2	Simulated results of PIFA antenna with FR4 of thickness 1.6mm	36
4.4.3	Simulated results of PIFA antenna with Duroid 5880	37
4.4.4	Simulated results of PIFA antenna with RO 4350	38
4.5.1	Structure of F- antenna of substrate dimension $45 \times 80 \text{mm}^2$ on HFSS.	39
4.5.1.1	Simulated results of F antenna of $10 \times 15 \text{mm}^2$ integrated on substrate dimension- $45 \times 80 \text{mm}^2$ with FR4	40
4.5.1.2	Simulated results of F antenna of $10 \times 15 \text{mm}^2$ integrated on substrate dimension- $45 \times 80 \text{mm}^2$ with Duroid 5880	41
4.5.1.3	Simulated results of F antenna of $10 \times 15 \text{mm}^2$ integrated on substrate dimension- $45 \times 80 \text{mm}^2$ with RO 4350	42
4.5.2	Structure of F- antenna of substrate dimension $50 \times 35 \text{mm}^2$ and cutout $15 \times 15 \text{mm}^2$ on HFSS	43
4.5.2.1	Simulated results of F antenna of substrate dimension $50 \times 35 \text{mm}^2$ and cutout $15 \times 15 \text{mm}^2$ with FR4 of thickness 1mm	44

4.5.3	Structure of F- antenna of substrate dimension 50x35mm ² and cutout 50x18mm ² on HFSS	45
4.5.3.1	Simulated results of F antenna of substrate dimension 50x35mm ² and cutout 50x18mm ² with FR4 of thickness 1mm	46
4.5.3.2	Simulated results of F antenna of substrate dimension 50x35mm ² and cutout 50x18mm ² with FR4 of thickness 1.6mm	47
4.5.4	Structure of F- antenna of substrate dimension 47x40mm ² and cutout 15x15mm ² on HFSS	48
4.5.4.1	Simulated results of F antenna of substrate dimension 47x40mm ² and cutout 15x15mm ² with FR4 of thickness 1mm	49
4.5.5	Structure of F- antenna of substrate dimension 47x40mm ² and cutout 47x18mm ² on HFSS	50
4.5.5.1	Simulated results of F antenna of substrate dimension 47x40mm ² and cutout 47x18mm ² with FR4 of thickness 1mm	51
4.5.5.2	Simulated results of F antenna of substrate dimension 47x40mm ² and cutout 47x18mm ² with FR4 of thickness 1.6mm	52
4.6	Structure of Spiral Antenna on HFSS	53
4.6.1	Simulated results of Spiral antenna with FR4 of thickness 1mm	54
4.6.2	Simulated results of Spiral antenna with FR4 of thickness 1.6mm	55
4.6.3	Simulated results of Spiral antenna with Duroid 5880	56
4.6.4	Simulated results of Spiral antenna with RO 4350	57
5.1	Device used for fabrication	59
5.2	Different antenna shapes fabricated	59
5.3	Fabricated F-antennas of substrate dimension 47x40mm ²	60

	and 50x35mm ²	
5.4	Planar spiral antenna of substrate dimension 35x50mm ²	60
5.5	Network Analyzer used for measurement of Return Loss and VSWR	60
5.1.1	Measured Results of F-antenna of 9x15mm ² integrated on FR4 of 1.6mm thickness substrate dimension- 35x50mm ²	61
5.1.2	Measured Results of F-antenna of 9x15mm ² integrated on FR4 of 1.6mm thickness substrate dimension- 47x40mm ²	61
5.1.3	Measured Results of Spiral of 5x10mm ² & FR4-35x50mm ²	62
5.2.1	Measured Radiation Pattern of F-antenna of 9x15mm ² integrated on FR4 substrate dimension- 47x40mm ² in (a) E-co plane (b) H-co plane (c) E-cross plane (d) H-cross plane	63
5.2.2	Measured Radiation Pattern of Spiral antenna of 5x10mm ² & FR4-35x50mm ² in (a) E-co plane (b) H-co plane (c) E-cross plane (d) H-cross plane	65
5.3.1	Device set-up for Range measurement	66
5.3.2	WLAN Power up test	67
5.3.3	Ping Test	67
5.3.4	Test File Download test	68
6.1	Comparison of simulated and measured Return Loss of Spiral antenna	70
6.2	Simulated Radiation Pattern of Spiral Antenna in terms of Theta and Phi plane	70
6.3	Measured Radiation Pattern of Spiral antenna in E-co plane and H-co plane resp.	71

LIST OF TABLES

TABLE NO	CAPTION	PAGE NO
4.1	Microstrip Dipole Antenna Design Parameters	19
4.2	Microstrip Rectangular Patch Antenna Design Parameters	24
4.3	Microstrip Elliptical Patch Antenna Design Parameters	29
4.4	Microstrip PIFA Antenna Design Parameters	34
4.5.1	Microstrip F Antenna of substrate dimension $45 \times 80 \text{mm}^2$ Design Parameters	39
4.5.2	Microstrip F Antenna of substrate dimension $50 \times 35 \text{mm}^2$ and cutout $15 \times 15 \text{mm}^2$ Design Parameters	43
4.5.3	Microstrip F Antenna of substrate dimension $50 \times 35 \text{mm}^2$ and cutout $50 \times 18 \text{mm}^2$ Design Parameters	45
4.5.4	Microstrip F Antenna of substrate dimension $47 \times 40 \text{mm}^2$ and cutout $15 \times 15 \text{mm}^2$ Design Parameters	48
4.5.5	Microstrip F Antenna of substrate dimension $47 \times 40 \text{mm}^2$ and cutout $47 \times 18 \text{mm}^2$ Design Parameters	50
4.6	Microstrip Spiral Antenna Design Parameters	53
4.7	Best results based on different substrates for different antenna shapes	58
6.1	Comparison of simulated and measured result of F and spiral antenna	72

LIST OF ABBREVIATIONS

RL	-----	Return Loss
VSWR	-----	Voltage Standing Wave Ratio
CAD	-----	Computer Aided Drafting
RF	-----	Radio Frequency
TEM	-----	Transverse-Electric-Magnetic
MIC	-----	Microwave Integrated Circuits
FEM	-----	Finite Element Method
QFP	-----	Quad Flat Package
BGA	-----	Ball Grid Array
SFP	-----	Small Form-Factor Pluggable
XFP	-----	10 Gigabit Small Form Factor Pluggable
EMI	-----	Electromagnetic Interference
EMC	-----	Electromagnetic Compatibility
PIFA	-----	Planar Inverted F- Antenna

CHAPTER 1

INTRODUCTION

1.1 PROBLEM DEFINITION

In Wireless devices, the recent trend is to use microstrip antennas which are placed inside the enclosure. For communication systems to reliably operate, a good signal needs to be received. A weak signal will cause loss of data. Eg: In mobile devices the plastic cover acts like a radom for the antenna and in many cases bringing in loss of power transmitted as well as received. It is expected that the antenna associated with any such communication device needs to be well matched and radiate and receive maximum power with Omni directional radiation pattern.

The problem under study here is related to the Wi-Fi 802.11b/g data communication of a device used for remote inventory stock taking applications. The device is used to scan the bar codes associated with products in the inventory and the device consolidates these data and sends to the Wi-Fi router. The device contains a Wi-Fi Transceiver and an antenna. It is reported from field that the range performance of this device is not satisfactory. The transmit power as well as the receive sensitivity of the wireless module used is of standard commercially available one. Thus the study was directed only towards the antenna performance and to arrive at some improvement methods.

The existing antenna in the device is shown in Fig.1.1a. The Return Loss characteristics of the antenna is measured and shown as Fig.1.1b.

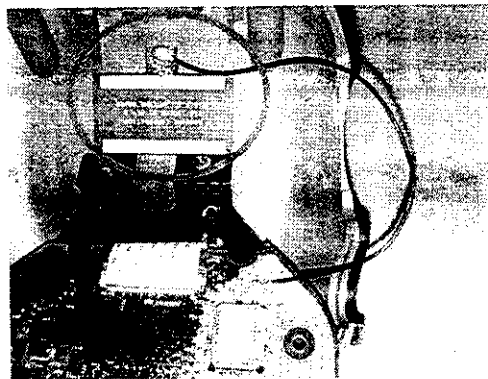


Figure 1.1a Photograph of Antenna in the device

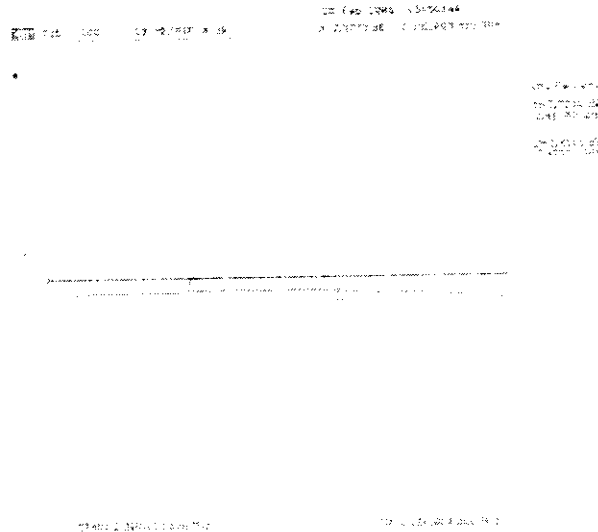


Figure 1.1b Return Loss characteristics of the antenna

This is a dipole antenna having RL around 2.5 dB and thus gives a poor matching characteristics. The range measurement shows that, this provides a range of about 144 feet in “line of sight” propagation and 96 feet in “non-line of sight” propagation. The project aims to design and develop microstrip antennas with better Return Loss or VSWR , good omni directional radiation pattern and better range in “non- line of sight” propagation.

1.2 SCOPE OF WORK:

The VSWR is a measure of the impedance matching. The impedance is dependent on the geometry and dielectric constant. Therefore, it is planned to do design and simulations for different substrate materials as well as antenna shapes to achieve optimum characteristics. The CAD tool planned to be used is HFSS (AnSoft). The antenna showing the best characteristics which will suit our application will be fabricated and studied. The pattern shall be generated and Gerber output will be used to transfer the geometry on the substrate. In house PCB machine is planned to be used for this purpose. The fabricated antennas will be characterized for return loss and radiation pattern (limited way in open air).

1.3 COMPANY PROFILE

SFO Technologies, Kochi is a 200 Million USD company with Design, manufacturing and testing facilities in Electronics, Power, RF & Wireless, Photonics and Mechanical domains. The number of employees is around 4000 with the operations at

Cochin, Bangalore, Mysore and Trivandrum. The customer list includes top Fortune 500 companies.

SFO offers:

- Integrated capabilities for product design:
 1. Electronics, Fiber Optics, RF & Wireless, Power Supplies, Embedded Firmware, Mechanical, Industrial Design and Application Software.
 2. Rapid prototyping, test and validation, third party compliance
- Domain expertise in healthcare, communication, industrial and automotive applications.
- Design partner for GE, HP, PMC, TI, Microvision, Schneider, Gunnebo, Lambda, Agilent, Tyco, Toshiba to name a few.

SFO Technologies has set high quality standard at all its facilities which are ISO 9001, ISO 14001, IS13485, CMMI level 5, AS9100, TL9000, certified.

1.4 OVERVIEW OF MICROSTRIP ANTENNA

A microstrip antenna consists of conducting patch on a ground plane separated by dielectric substrate. This concept was undeveloped until the revolution in electronic circuit miniaturization and large-scale integration in 1970. After that many authors have described the radiation from the ground plane by a dielectric substrate for different configurations. The early work of Munson on micro strip antennas for use as a low profile flush mounted antennas on rockets and missiles showed that this was a practical concept for use in many antenna system problems. Various mathematical models were developed for this antenna and its applications were extended to many other fields. The number of papers, articles published in the journals for the last ten years, on these antennas shows the importance gained by them. The micro strip antennas are the present day antenna designer's choice.

Low dielectric constant substrates are generally preferred for maximum radiation. The conducting patch can take any shape but rectangular and circular configurations are the most

commonly used configuration. Other configurations are complex to analyze and require heavy numerical computations. A microstrip antenna is characterized by its Length, Width, Input impedance, and Gain and radiation patterns. Various parameters of the microstrip antenna and its design considerations were discussed in the subsequent chapters. The length of the antenna is nearly half wavelength in the dielectric; it is a very critical parameter, which governs the resonant frequency of the antenna. There are no hard and fast rules to find the width of the patch.

1.5 ANTENNA CHARACTERISTICS

An antenna is a device that is made to efficiently radiate and receive radiated electromagnetic waves. There are several important antenna characteristics that should be considered when choosing an antenna for your application as follows:

1.5.1 Radiation pattern: An antenna radiation pattern is the angular distribution of the power radiated by an antenna. If an antenna radiates fields $E(r, \theta, \phi)$ and $H(r, \theta, \phi)$, then the time average far field power density radiated at the point r has the form

$$\begin{aligned} S_{av}(r, \theta, \phi) &= \left(\frac{1}{2}\right) \text{Re} \{E(r) \times H(r)^*\} \\ &= \frac{|E(r)|^2}{2\eta} \hat{r} \\ &\cong f(\theta, \phi) \frac{1}{r^2} \hat{r}, r \rightarrow \infty \end{aligned}$$

Where we have lumped all the angle dependence into $f(\theta, \phi)$. This angular dependence is the radiation pattern of the antenna. It is customary to normalize the radiation pattern to a maximum value of unity, so that the radiation pattern is defined to be $f(\theta, \phi)/f_{max}$. While the power density pattern is most important, one can also look at the field intensity, phase, or polarization patterns of an antenna.

1.5.2 Polarization: The far-field can be decomposed in several ways. You can work with the basic decomposition in (E_θ, E_ϕ) . However, with linear polarized antennas, it is sometimes more convenient to decompose the far-fields into (E_{co}, E_{cross}) which is a decomposition based on an antenna measurement set-up. For circular polarized antennas, a decomposition into left and right hand polarized field components (E_{lhp}, E_{rhp}) is most appropriate. Below you can find how the different components are related to each other.

$$\vec{E}_{ff}(\theta, \varphi) = E_{\theta}(\theta, \varphi)\hat{i}_{\theta} + E_{\varphi}(\theta, \varphi)\hat{i}_{\varphi} = E_{co}(\theta, \varphi)\hat{i}_{co} + E_{cross}(\theta, \varphi)\hat{i}_{cross} = E_{lhp}(\theta, \varphi)\hat{i}_{lhp} + E_{rhp}(\theta, \varphi)\hat{i}_{rhp}$$

$$H_{\varphi} = \frac{E_{\theta}}{Z_{\omega}}$$

$$H_{\theta} = -\frac{E_{\varphi}}{Z_{\omega}}$$

$$Z_{\omega} = \sqrt{\frac{\mu}{\epsilon}}$$

Z_{ω} is the characteristic impedance of the open half sphere under consideration. The fields can be normalized with respect to:

$$\max(\sqrt{|E_{\theta}|^2 + |E_{\varphi}|^2})$$

1.5.3 Radiation Intensity: The radiation intensity, U is the power radiated from an antenna per unit solid angle, is given by:

$$U(\theta, \varphi) = \frac{1}{2}(\mathbf{E}_{ff}(\theta, \varphi) \times \mathbf{H}_{ff}^*(\theta, \varphi)) = \frac{1}{2Z_{\omega}}(|E_{\theta}(\theta, \varphi)|^2 + |E_{\varphi}(\theta, \varphi)|^2)$$

For a certain direction, the radiation intensity will be maximal and equals:

$$U_{max}(\theta, \varphi) = \max(U(\theta, \varphi))$$

1.5.4 Radiated Power: Radiated power is the amount of time-averaged power (in watts) exiting a radiating antenna structure through a radiation boundary, is represented by:

$$P_{rad} = \int_{\Omega} U(\theta, \varphi) \cdot d\Omega = \frac{1}{2} \int_{\Omega} \mathbf{E}_{ff} \times \mathbf{H}_{ff}^* \cdot d\Omega$$

1.5.5 Effective Angle: This parameter is the solid angle through which all power emanating from the antenna would flow if the maximum radiation intensity is constant for all angles over the beam area. It is measured in steradians and is represented by:

$$\Omega_A = \frac{P_{rad}}{U_{max}}$$

1.5.6 Directivity: Directivity is defined as the ratio of an antenna's radiation intensity in a given direction to the radiation intensity averaged over all directions. Directivity is dimensionless and is represented by:

$$D(\theta, \varphi) = 4\pi \frac{U(\theta, \varphi)}{P_{rad}}$$

The maximum directivity is given by:

$$D = 4\pi \frac{U_{max}}{P_{rad}} = \frac{4\pi}{\Omega_A}$$

1.5.7 Gain: Gain is four pi times the ratio of an antenna's radiation intensity in a given direction to the total power accepted by the antenna. Peak gain, in turn, is the maximum gain over all the user-specified directions of the far-field infinite sphere. The gain of the antenna is represented by:

$$G(\theta, \varphi) = 4\pi \frac{U(\theta, \varphi)}{P_{inj}}$$

where P_{inj} is the real power, in watts, injected into the circuit. The maximum gain is given by:

$$G = 4\pi \frac{U_{max}}{P_{inj}}$$

1.5.8 Efficiency: The radiation efficiency is the ratio of radiated power to the real power injected into the circuit, given by:

$$\eta = \frac{P_{rad}}{P_{inj}} = \frac{G}{D}$$

1.5.9 Effective Area: The effective area, in square meters, of the antenna circuit is given by:

$$A_{eff}(\theta, \varphi) = \frac{\lambda^2}{4\pi} G(\theta, \varphi)$$

1.5.10 VSWR: It is a measure of how well a load is impedance-matched to a source. The mismatch of a load Z_L to a source Z_0 results in a reflection coefficient of

$$\Gamma = \frac{(Z_L - Z_0)}{(Z_L + Z_0)}$$

The magnitude of the reflection coefficient is given by:

$$\rho = |\Gamma|$$

$$VSWR = \frac{(1 + \rho)}{(1 - \rho)}$$

1.5.11 Return Loss: In telecommunications, return loss or reflection loss is the loss of signal power resulting from the reflection caused at a discontinuity in a transmission line or optical fiber. This discontinuity can be a mismatch with the terminating load or with a device inserted in the line. It is usually expressed as a ratio in decibels (dB);

$$RL(dB) = 10 \log_{10} \frac{P_i}{P_r}$$

where $RL(dB)$ is the return loss in dB, P_i is the incident power and P_r is the reflected power.

Return loss is the negative of the magnitude of the reflection coefficient in dB. Since power is proportional to the square of the voltage, return loss is given by,

$$RL(dB) = -20 \log_{10} |\Gamma|$$

CHAPTER 2

2. MICROSTRIP PATCH ANTENNA

Microstrip antennas are attractive due to their light weight, conformability and low cost. These antennas can be integrated with printed strip-line feed networks and active devices. This is a relatively new area of antenna engineering. The radiation properties of micro strip structures have been known since the mid 1950's.

The application of this type of antennas started in early 1970's when conformal antennas were required for missiles. Rectangular and circular micro strip resonant patches have been used extensively in a variety of array configurations. A major contributing factor for recent advances of microstrip antennas is the current revolution in electronic circuit miniaturization brought about by developments in large scale integration. As conventional antennas are often bulky and costly part of an electronic system, micro strip antennas based on photolithographic technology are seen as an engineering breakthrough.

2.1 INTRODUCTION

In its most fundamental form, a Microstrip Patch antenna consists of a radiating patch on one side of a dielectric substrate which has a ground plane on the other side as shown in Figure 2.1. The patch is generally made of conducting material such as copper or gold and can take any possible shape. The radiating patch and the feed lines are usually photo etched on the dielectric substrate.

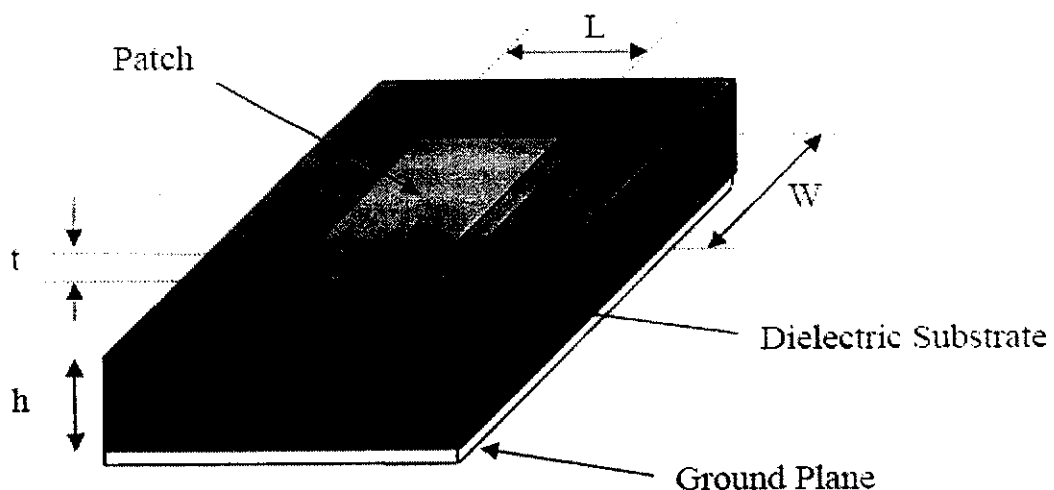


Figure 2.1. Structure of a Microstrip Patch Antenna

In order to simplify analysis and performance prediction, the patch is generally square, rectangular, circular, triangular, and elliptical or some other common shape as shown in Figure 2.2

For a rectangular patch, the length L of the patch is usually $0.3333\lambda_0 < L < 0.5\lambda_0$, where λ_0 is the free-space wavelength. The patch is selected to be very thin such that $t \ll \lambda_0$ (where t is the patch thickness). The height h of the dielectric substrate is usually $0.003\lambda_0 \leq h \leq 0.05\lambda_0$. The dielectric constant of the substrate (ϵ_r) is typically in the range $2.2 \leq \epsilon_r \leq 12$.

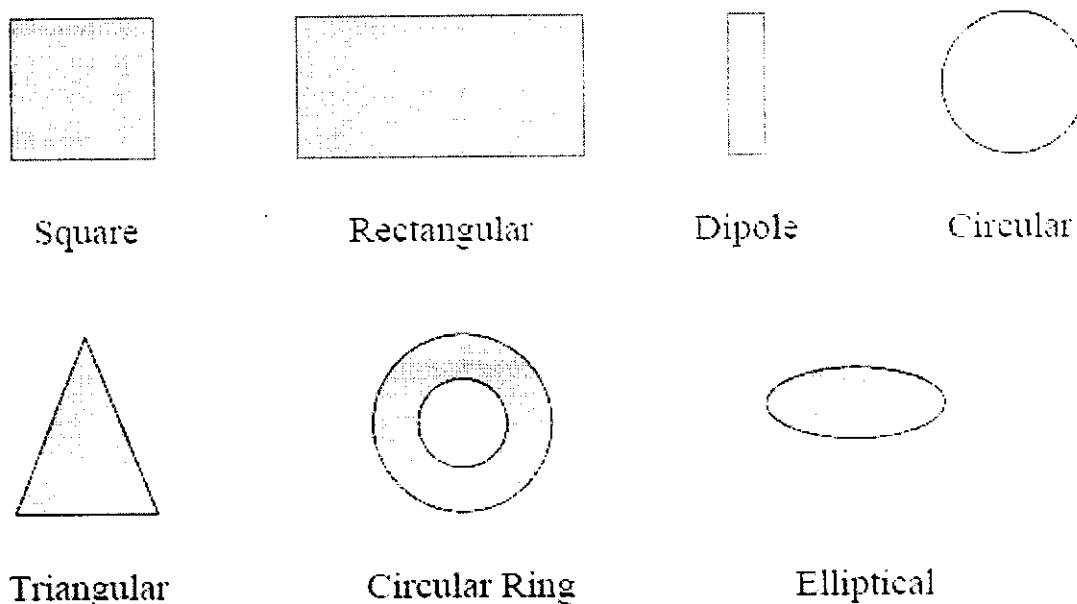


Figure 2.2 Common Shapes of Microstrip Patch elements

Microstrip patch antennas radiate primarily because of the fringing fields between the patch edge and the ground plane. For good antenna performance, a thick dielectric substrate having a low dielectric constant is desirable since this provides better efficiency, larger bandwidth and better radiation. However, such a configuration leads to a larger antenna size. In order to design a compact Microstrip patch antenna, substrates with higher dielectric constants must be used which are less efficient and result in narrower bandwidth. Hence a trade-off must be realized between the antenna dimensions and antenna performance.

2.2 ADVANTAGES AND DISADVANTAGES

Microstrip patch antennas are increasing in popularity for use in wireless applications due to their low-profile structure. Therefore they are extremely compatible for embedded antennas in handheld wireless devices such as cellular phones, pagers etc... The telemetry and communication antennas on missiles need to be thin and conformal and are often in the form of Microstrip patch antennas. Another area where they have been used successfully is in Satellite communication. Some of their principal advantages are given below:

- Light weight and low volume.
- Low profile planar configuration which can be easily made conformal to host surface.
- Low fabrication cost, hence can be manufactured in large quantities.
- Supports both, linear as well as circular polarization.
- Can be easily integrated with MICs.
- Capable of dual and triple frequency operations.
- Mechanically robust when mounted on rigid surfaces.

Microstrip patch antennas suffer from more drawbacks as compared to conventional antennas. Some of their major disadvantages are given below:

- Narrow bandwidth
- Low efficiency
- Low Gain
- Extraneous radiation from feeds and junctions
- Poor end fire radiator except tapered slot antennas
- Low power handling capacity
- Surface wave excitation

Microstrip patch antennas have a very high antenna quality factor (Q). It represents the losses associated with the antenna where a large Q leads to narrow bandwidth and low efficiency. Q can be reduced by increasing the thickness of the dielectric substrate. But as the thickness increases, an increasing fraction of the total power delivered by the source goes into a surface wave. This surface wave contribution can be counted as an unwanted power loss since it is ultimately scattered at the dielectric bends and causes degradation of the antenna characteristics. Other problems such as lower gain and lower power handling capacity can be overcome by using an array configuration for the elements.

2.3 FEED TECHNIQUES

Microstrip patch antennas can be fed by a variety of methods. These methods can be classified into two categories- contacting and non-contacting. In the contacting method, the RF power is fed directly to the radiating patch using a connecting element such as a microstrip line. In the non-contacting scheme, electromagnetic field coupling is done to transfer power between the microstrip line and the radiating patch. The four most popular feed techniques used are the microstrip line, coaxial probe (both contacting schemes), aperture coupling and proximity coupling (both non-contacting schemes).

2.3.1 Microstrip Line Feed

In this type of feed technique, a conducting strip is connected directly to the edge of the Microstrip patch as shown in Figure 2.3. The conducting strip is smaller in width as compared to the patch and this kind of feed arrangement has the advantage that the feed can be etched on the same substrate to provide a planar structure.

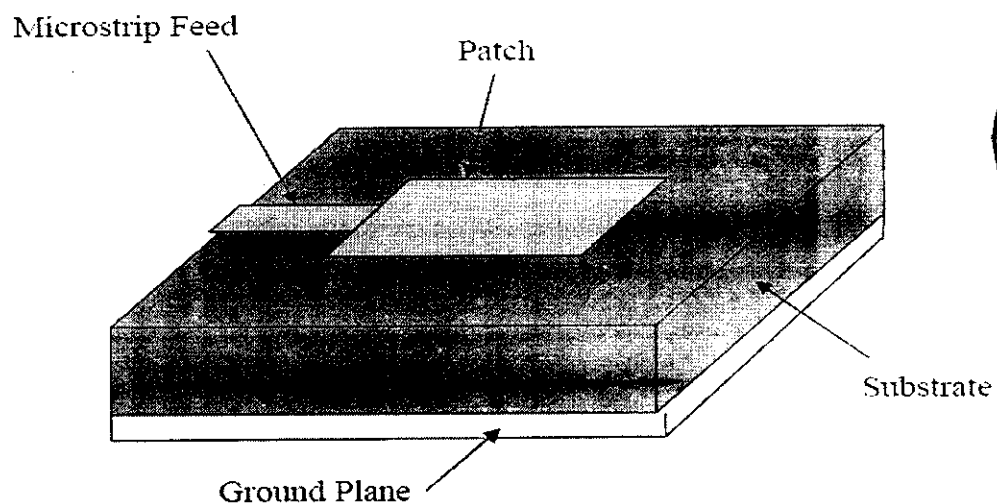


Figure 2.3 Microstrip Line Feed

The purpose of the inset cut in the patch is to match the impedance of the feed line to the patch without the need for any additional matching element. This is achieved by properly controlling the inset position. Hence this is an easy feeding scheme, since it provides ease of fabrication and simplicity in modelling as well as impedance matching. However as the thickness of the dielectric substrate being used, increases, surface waves and spurious feed radiation also increases, which hampers the bandwidth of the antenna. The feed radiation also leads to undesired cross polarized radiation.

2.4 METHODS OF ANALYSIS

The preferred models for the analysis of Microstrip patch antennas are the transmission line model, cavity model, and full wave model (which include primarily integral equations/Moment Method). The transmission line model is the simplest of all and it gives good physical insight but it is less accurate. The cavity model is more accurate and gives good physical insight but is complex in nature. The full wave models are extremely accurate, versatile and can treat single elements, finite and infinite arrays, stacked elements, arbitrary shaped elements and coupling. These give less insight as compared to the two models mentioned above and are far more complex in nature.

2.4.1 Transmission Line Model

This model represents the microstrip antenna by two slots of width W and height h , separated by a transmission line of length L . The microstrip is essentially a non homogeneous line of two dielectrics, typically the substrate and air.

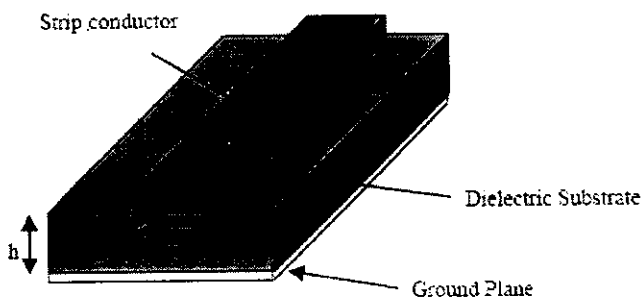


Figure 2.4 Microstrip Line

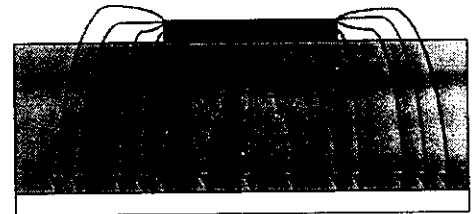


Figure 2.5 Electric Field Lines

Hence, as seen from Figure 2.5, most of the electric field lines reside in the substrate and parts of some lines in air. As a result, this transmission line cannot support pure TEM mode of transmission, since the phase velocities would be different in the air and the substrate. Instead, the dominant mode of propagation would be the quasi-TEM mode. Hence, an effective dielectric constant (ϵ_{reff}) must be obtained in order to account for the fringing and the wave propagation in the line. The value of ϵ_{reff} is slightly less than ϵ_r because the fringing fields around the periphery of the patch are not confined in the dielectric substrate but are also spread in the air as shown in Figure 2.5 above. The expression for ϵ_{reff} is given by Balanis as:

$$\epsilon_{reff} = \frac{\epsilon_r + 1}{2} + \frac{\epsilon_r - 1}{2} \left[1 + 12 \frac{h}{W} \right]^{-\frac{1}{2}}$$

Where

ϵ_{reff} = Effective dielectric constant

ϵ_r = Dielectric constant of substrate

h = Height of dielectric substrate

W = Width of the patch

Consider Figure 2.6 below, which shows a rectangular microstrip patch antenna of length L , width W resting on a substrate of height h . The co-ordinate axis is selected such that the length is along the x direction, width is along the y direction and the height is along the z direction.

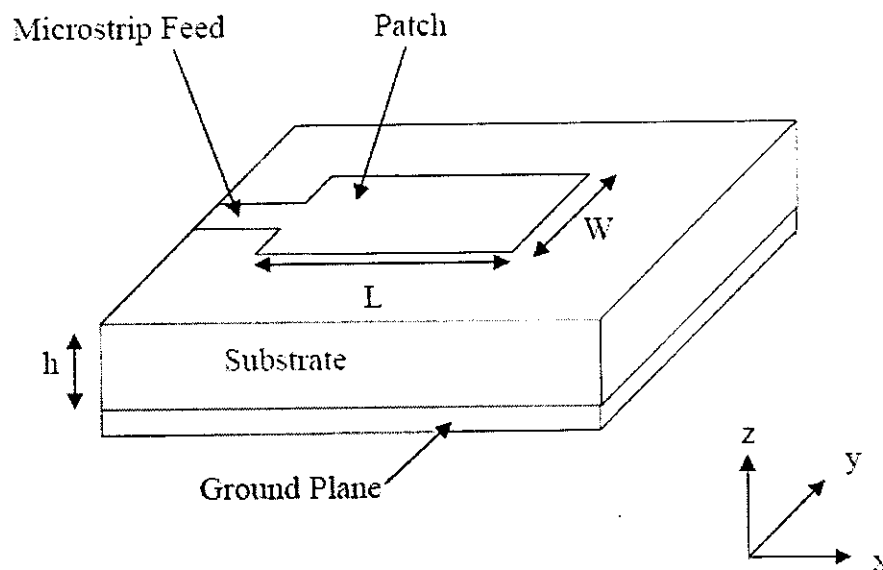


Figure 2.6 Microstrip Patch Antenna

In order to operate in the fundamental TM_{10} mode, the length of the patch must be slightly less than $\lambda/2$ where λ is the wavelength in the dielectric medium and is equal to $\lambda_0/\sqrt{\epsilon_{reff}}$ where λ_0 is the free space wavelength. The TM_{10} mode implies that the field varies one $\lambda/2$ cycle along the length, and there is no variation along the width of the patch. In the Figure 2.7 shown below, the microstrip patch antenna is represented by two slots, separated by a transmission line of length L and open circuited at both the ends. Along the width of the patch, the voltage is maximum and current is minimum due to the open ends. The fields at the

edges can be resolved into normal and tangential components with respect to the ground plane.

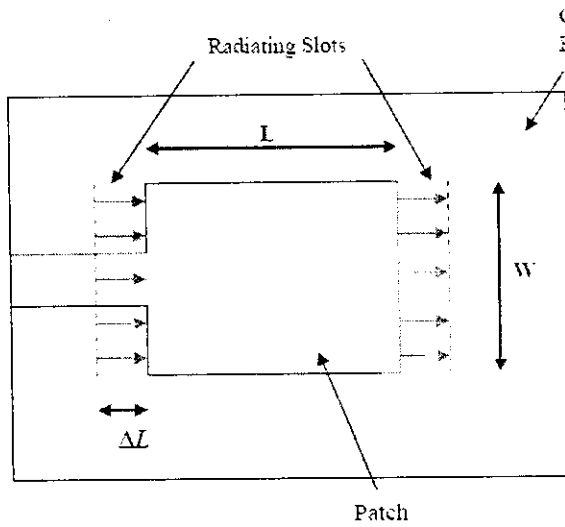


Figure 2.7 Top View of Antenna

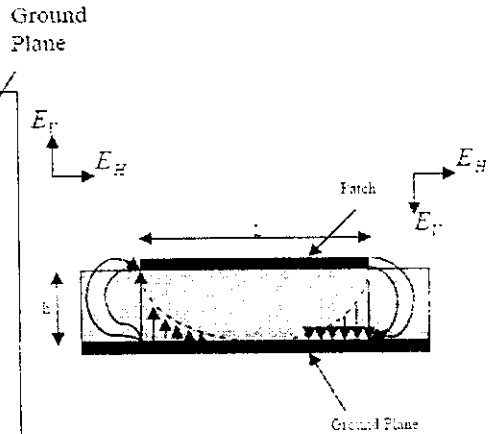


Figure 2.8 Side View of Antenna

It is seen from Figure 2.8 that the normal components of the electric field at the two edges along the width are in opposite directions and thus out of phase since the patch is $\lambda/2$ long and hence they cancel each other in the broadside direction. The tangential components (seen in Figure 2.8), which are in phase, means that the resulting fields combine to give maximum radiated field normal to the surface of the structure. Hence the edges along the width can be represented as two radiating slots, which are $\lambda/2$ apart and excited in phase and radiating in the half space above the ground plane. The fringing fields along the width can be modelled as radiating slots and electrically the patch of the microstrip antenna looks greater than its physical dimensions. The dimensions of the patch along its length have now been extended on each end by a distance ΔL , which is given empirically by Hammerstad as:

$$\Delta L = 0.412h \frac{(\epsilon_{r_{eff}} + 0.3) \left(\frac{W}{h} + 0.264 \right)}{(\epsilon_{r_{eff}} - 0.258) \left(\frac{W}{h} + 0.8 \right)}$$

The effective length of the patch L_{eff} now becomes

$$L_{eff} = L + 2\Delta L$$

For a given resonance frequency f_o , the effective length is given by

$$L_{eff} = \frac{c}{2f_c \sqrt{\epsilon_{reff}}}$$

For a rectangular Microstrip Patch antenna, the resonance frequency for any TM_{mn} mode is given by:

$$f_o = \frac{c}{2\sqrt{\epsilon_{reff}}} \left[\left(\frac{m}{L} \right)^2 - \left(\frac{n}{W} \right)^2 \right]^{\frac{1}{2}}$$

Where m and n are modes along L and W respectively. For efficient radiation, the width W is given by:

$$W = \frac{c}{2f_c \sqrt{\frac{(\epsilon_r + 1)}{2}}}$$

CHAPTER 3

HIGH FREQUENCY STRUCTURE SIMULATOR (HFSS)

HFSS is a high-performance full-wave electromagnetic (EM) field simulator for arbitrary 3D volumetric passive device modelling that takes advantage of the familiar Microsoft Windows graphical user interface. It integrates simulation, visualization, solid modelling, and automation in an easy-to-learn environment where solutions to your 3D EM problems are quickly and accurately obtained. Ansoft HFSS employs the FEM, adaptive meshing, and brilliant graphics to give you unparalleled performance and insight to all of your 3D EM problems. Ansoft HFSS can be used to calculate parameters such as S- Parameters, Resonant Frequency, and Fields. Typical uses include:

Package Modelling – BGA, QFP, Flip-Chip

PCB Board Modelling – Power /Ground planes, Mesh Grid Grounds, Backplanes

Silicon/GaAs - Spiral Inductors, Transformers

EMC/EMI– Shield Enclosures, Coupling, Near- or Far-Field Radiation

Antennas/Mobile Communications– Patches, Dipoles, Horns, Conformal Cell Phone

Antennas, Quadrafilar Helix, Specific Absorption Rate(SAR), Infinite Arrays, Radar Cross

Section(RCS), Frequency Selective Surfaces(FSS)

Connectors – Coax, SFP/XFP, Backplane, Transitions

Waveguide – Filters, Resonators, Transitions, Couplers

Filters – Cavity Filters, Microstrip, Dielectric

HFSS is an interactive simulation system whose basic mesh element is a tetrahedron. This allows you to solve any arbitrary 3D geometry, especially those with complex curves and shapes, in a fraction of the time it would take using other techniques.

The name HFSS stands for High Frequency Structure Simulator. Ansoft pioneered the use of the FEM for EM simulation by

developing/ implementing technologies such as tangential vector finite elements, adaptive meshing, and Adaptive Lanczos-Pade Sweep (ALPS). Today, HFSS continues to lead the industry with innovations such as Modes-to-Nodes and Full- Wave Spice™.

Ansoft HFSS has evolved over a period of years with input from many users and industries. In industry, Ansoft HFSS is the tool of choice for high-productivity research, development, and virtual prototyping.

The Ansoft HFSS window has several optional panels:

A Project Manager which contains a design tree which lists the structure of the project.

A Message Manager that allows you to view any errors or warnings that occur before you begin a simulation.

A Property Window that displays and allows you to change model parameters or attributes.

A Progress Window that displays solution progress.

The 3D Modeler Window which contains the model and model tree for the active design. For more information about the 3D Modeler Window.

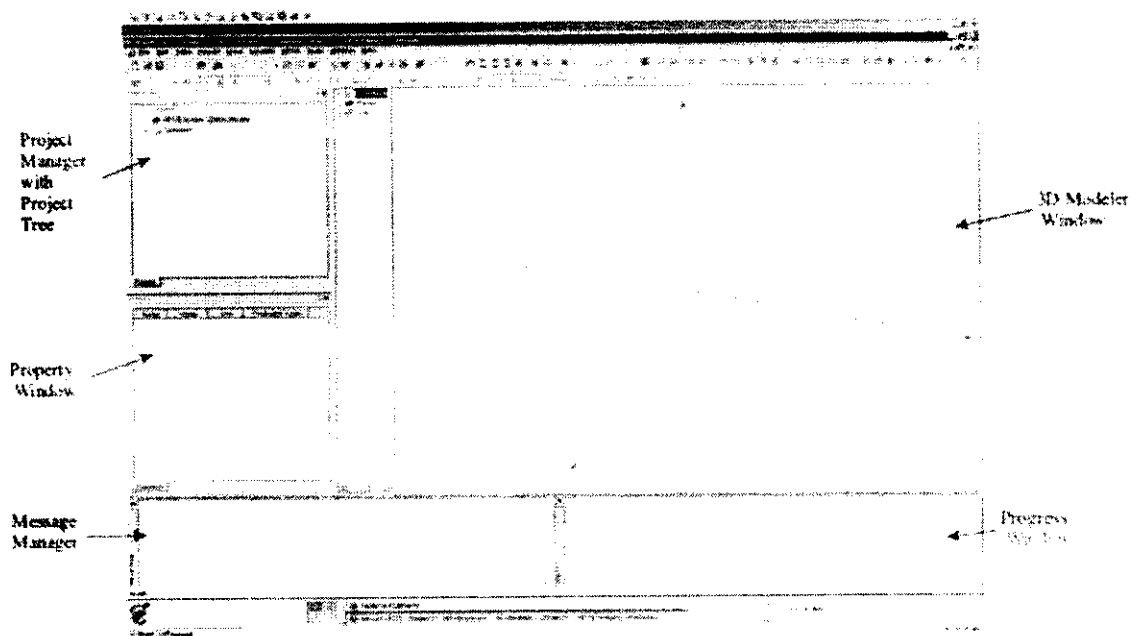


Figure 3.1 Main Screen of HFSS

The Ansoft HFSS Desktop provides an intuitive, easy-to-use interface for developing passive RF device models. Creating designs, involves the following:

1. Parametric Model Generation – creating the geometry, boundaries and excitations
2. Analysis Setup – defining solution setup and frequency sweeps
3. Results – creating 2D reports and field plots
4. Solve Loop - the solution process is fully automated

To understand how these processes co-exist, examine the illustration shown below.

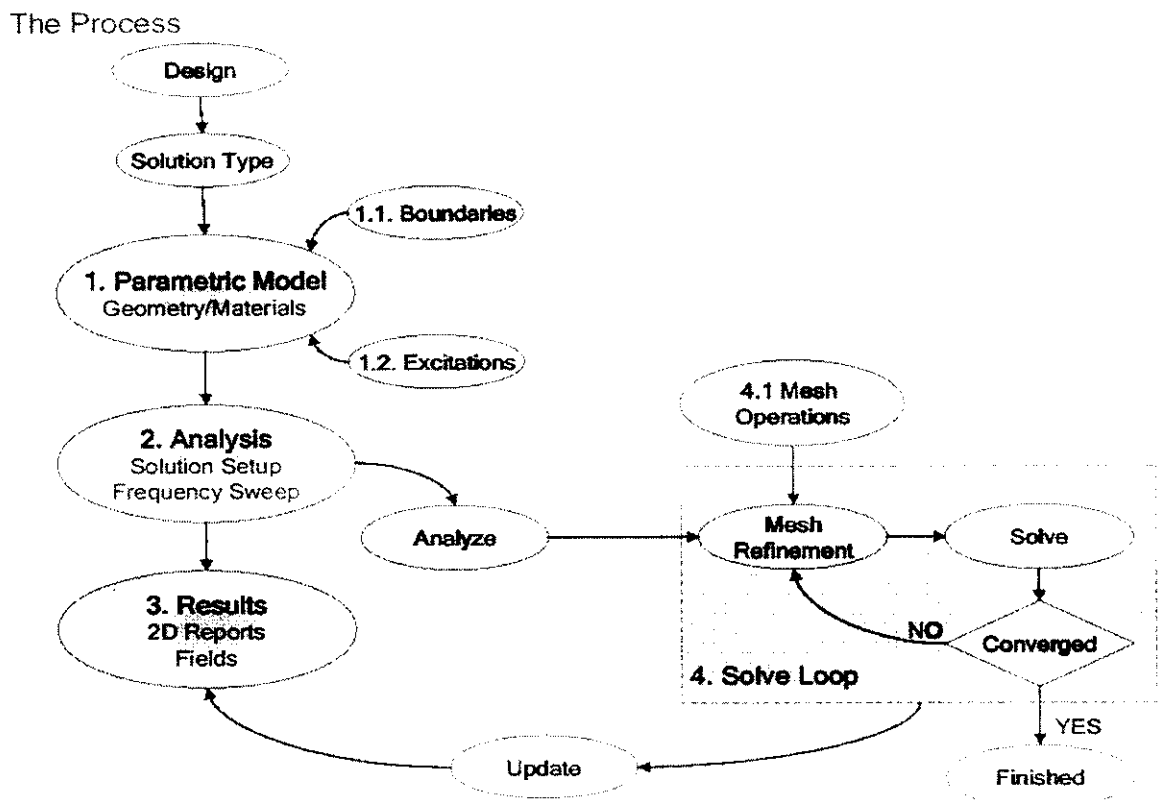


Figure 3.2 The Process of Creating Design

CHAPTER 4

SIMULATIONS AND RESULTS

Different types of antenna shapes were simulated, fabricated and studied. The different shapes include planar dipole, rectangular patch, elliptical patch, planar inverted F antenna, F monopole and spiral. These antennas were designed at a frequency of 2.4GHz. The array of F-antenna was also simulated and fabricated.

4.1 DIPOLE ANTENNA USING DIFFERENT SUBSTRATE MATERIALS

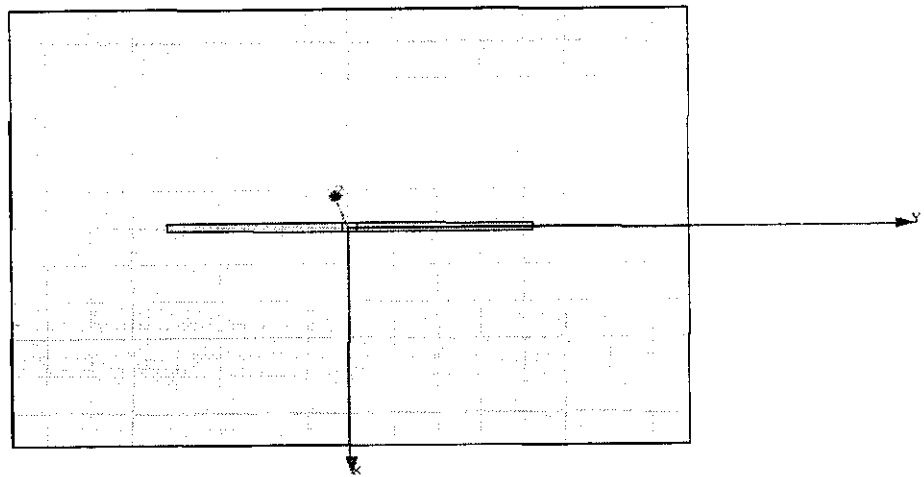


Figure 4.1 Structure of dipole antenna on HFSS.

Table 4.1 Microstrip Dipole Antenna Design Parameters

Parameter	Value (cm)
Dipole length	5.03
Antenna width	0.13
Port gap width	0.13
SubX	7.5
SubY	10.1

4.1.1. FR4 of 1mm thickness

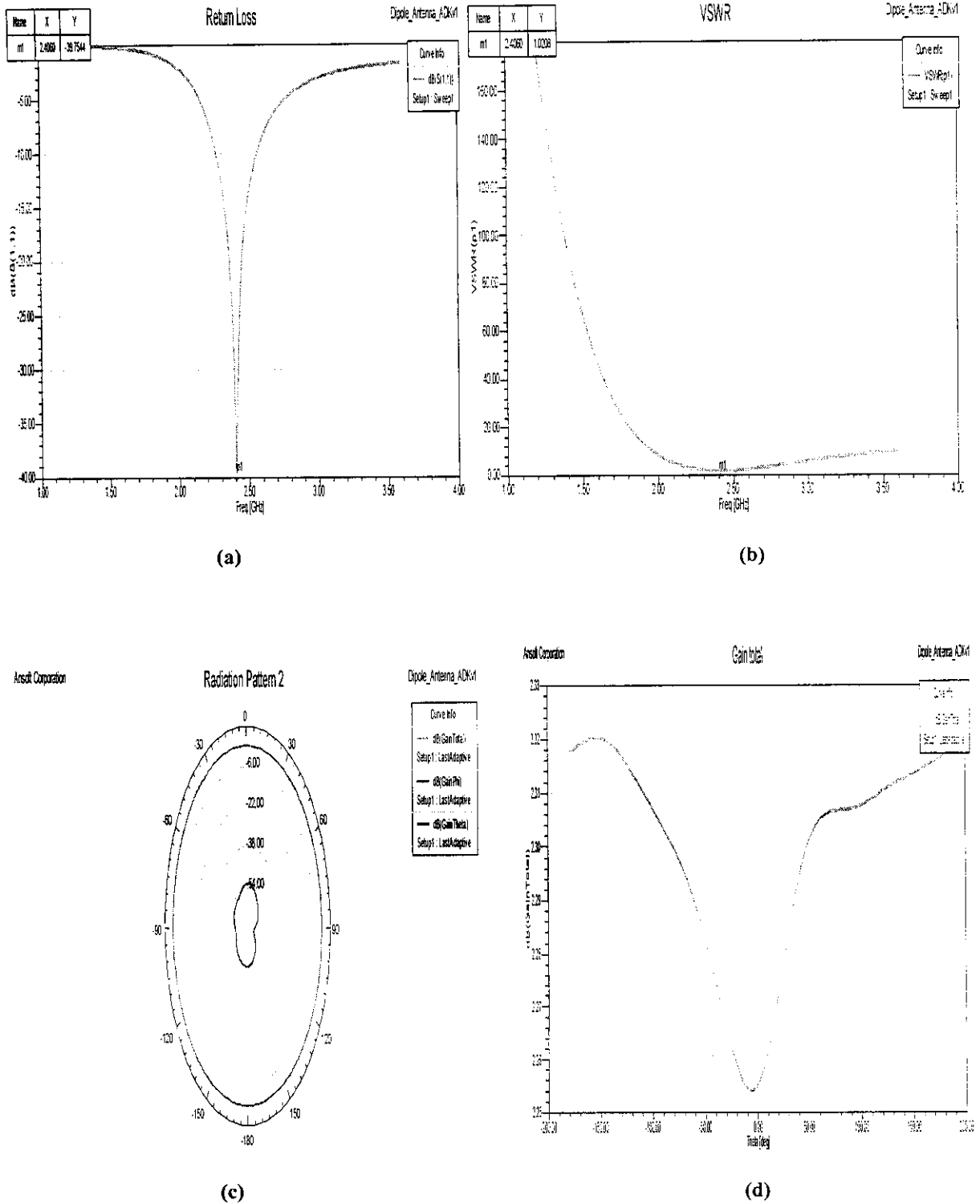


Figure 4.1.1: Simulated results of Dipole antenna with FR4 of thickness 1mm (a) Return Loss (b) VSWR (c) Radiation Pattern (d) Gain

4.1.2. FR4 of 1.6mm thickness

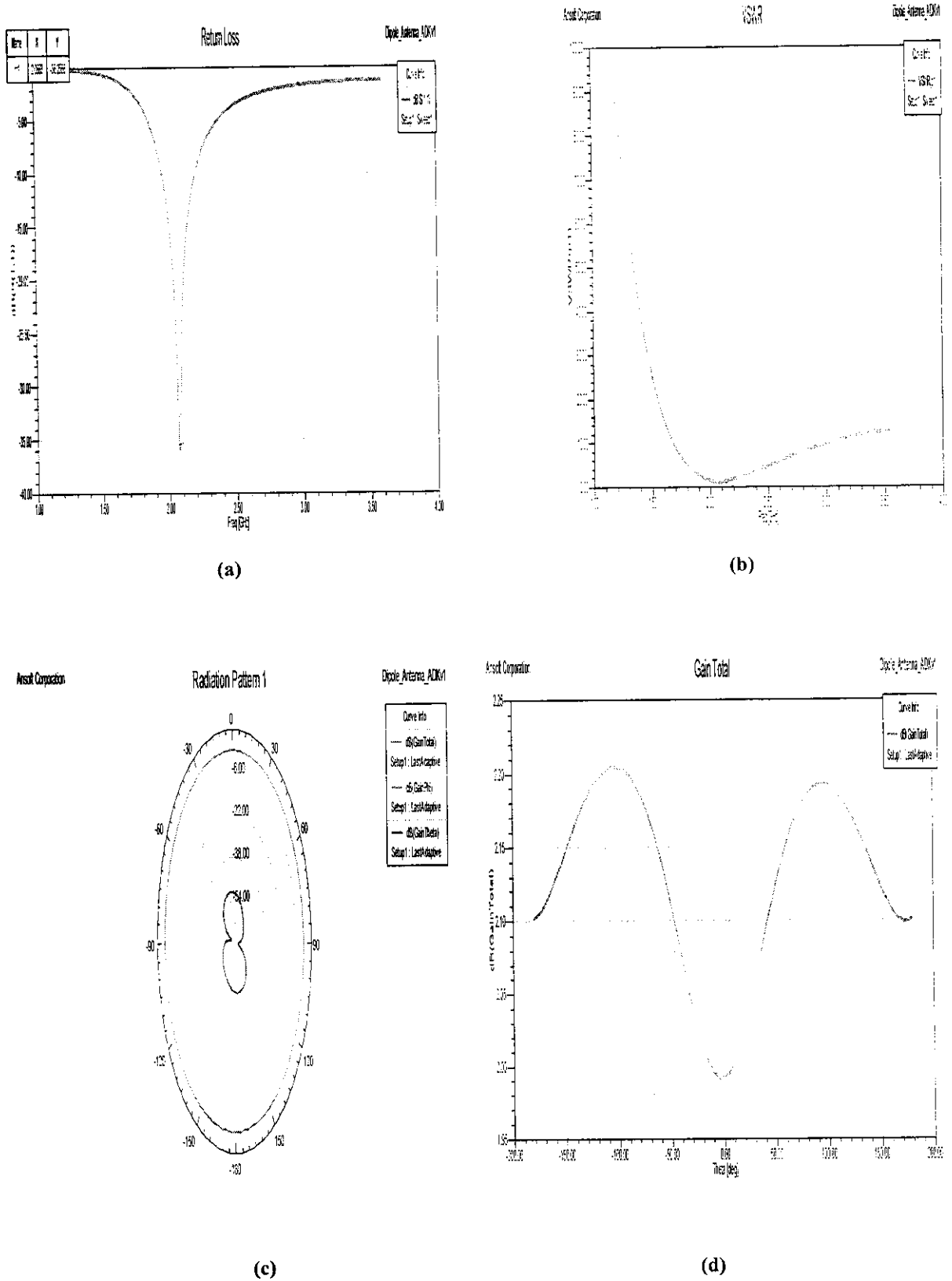


Figure 4.1.2: Simulated results of Dipole antenna with FR4 of thickness 1.6mm (a) Return Loss (b) VSWR (c) Radiation Pattern (d) Gain

4.1.3. DUROID 5880 of 1.575mm thickness

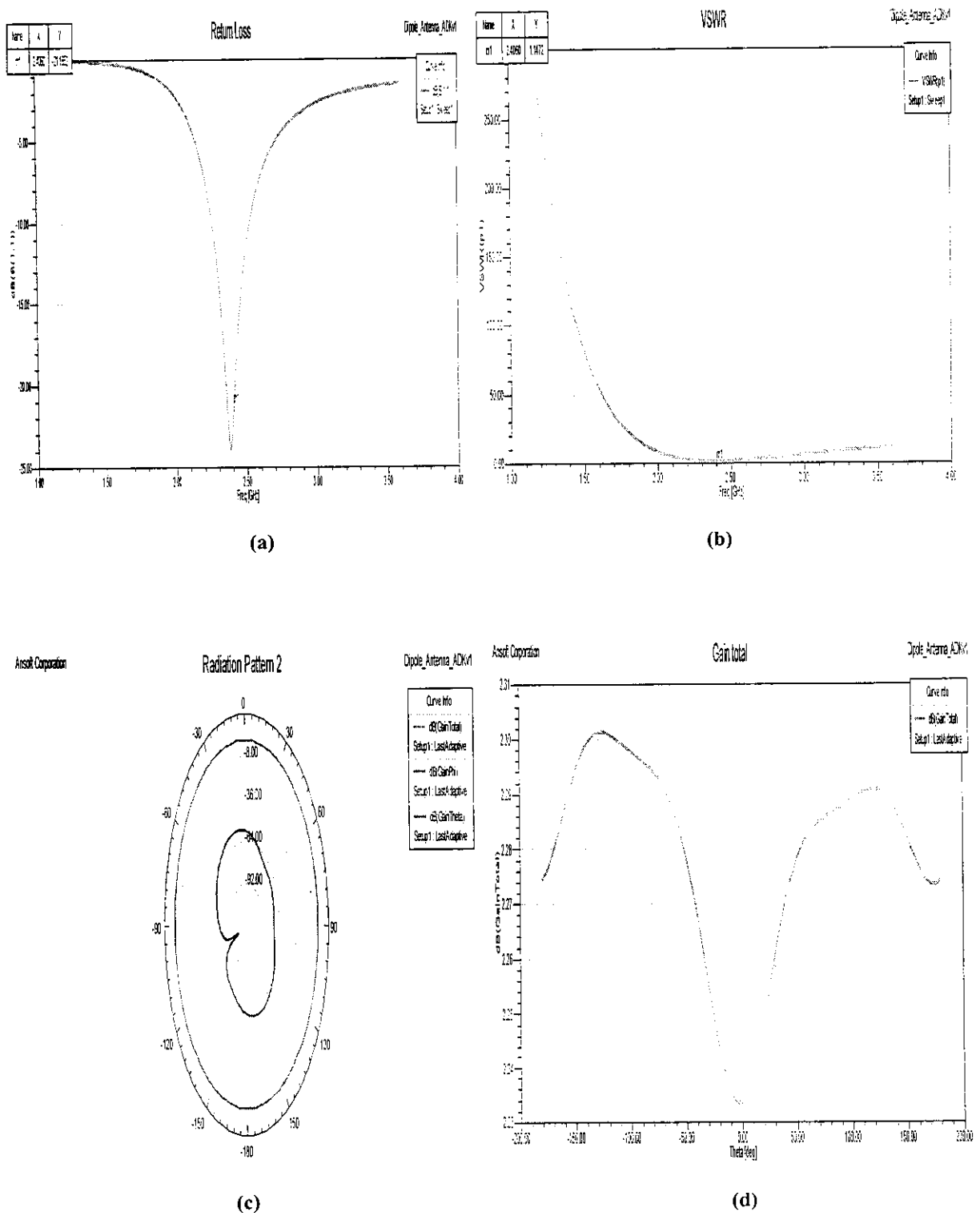
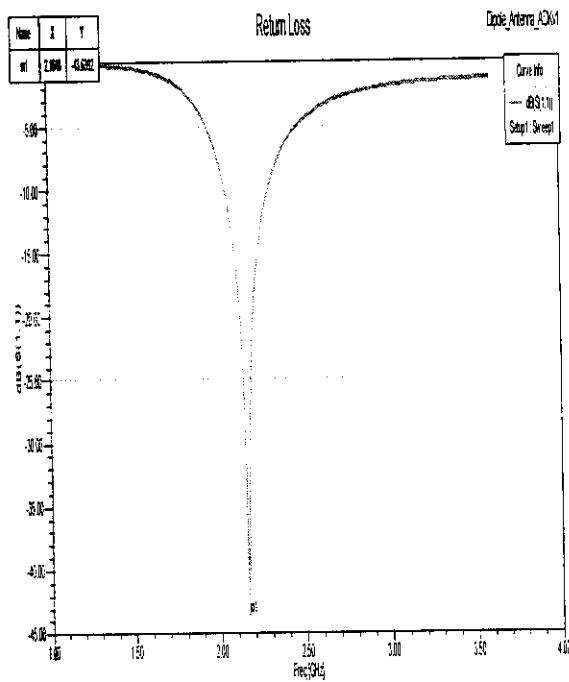
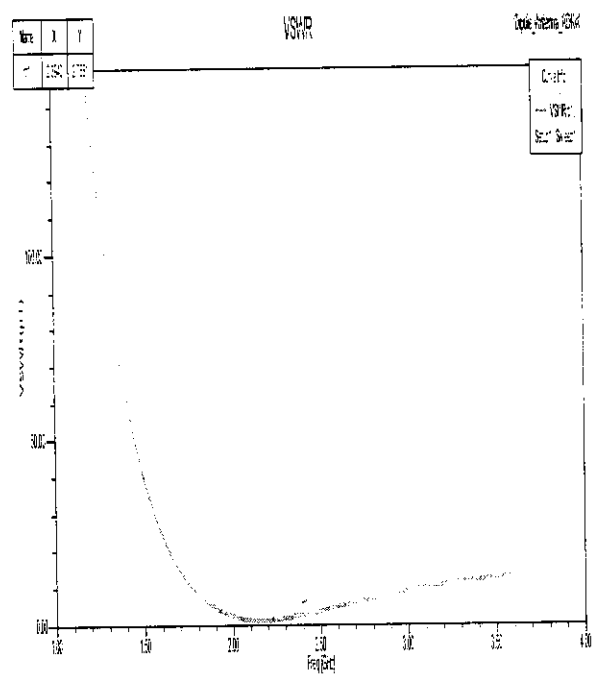


Figure 4.1.3: Simulated results of Dipole antenna with Duroid 5880 (a) Return Loss (b) VSWR (c) Radiation Pattern (d) Gain

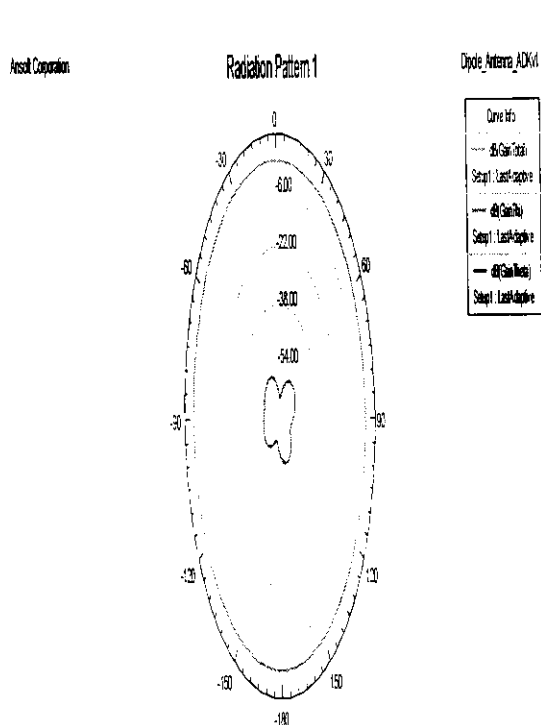
4.1.4. ROGERS RO 4350 of 1.524mm thickness



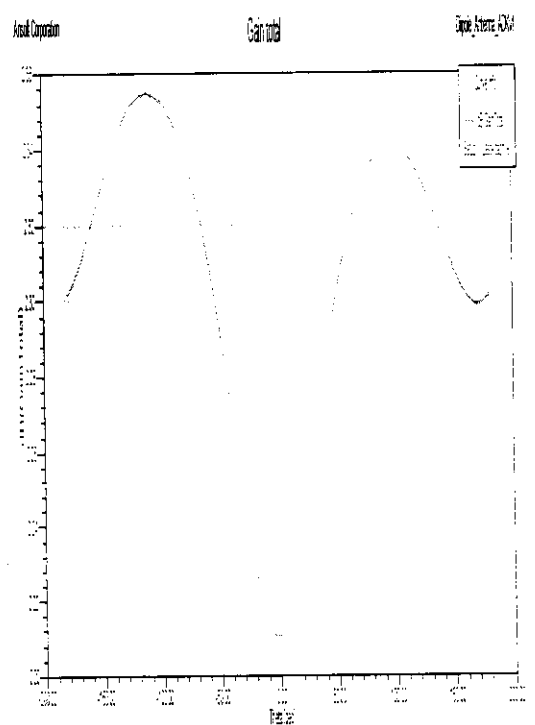
(a)



(b)



(c)



(d)

Figure 4.1.4: Simulated results of Dipole antenna with RO 4350 (a) Return Loss (b) VSWR (c) Radiation Pattern (d) Gain

4.2 RECTANGULAR INSET FEED PATCH ANTENNA USING DIFFERENT SUBSTRATE MATERIAL

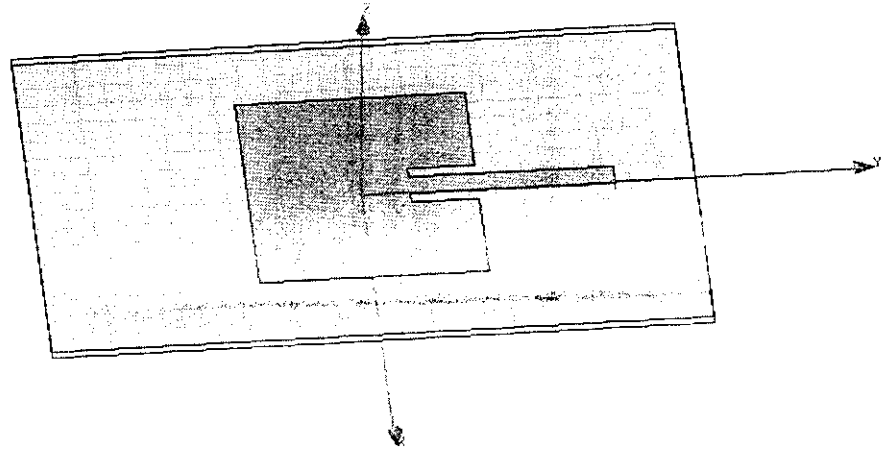
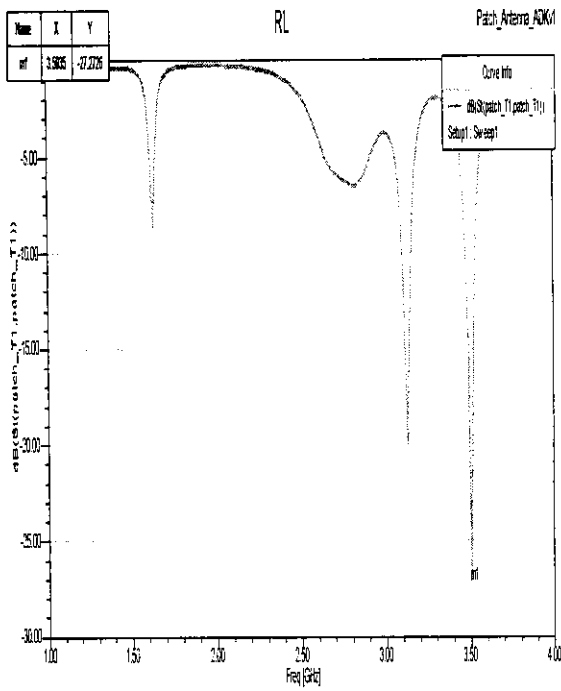


Figure 4.2 Structure of rectangular inset feed patch antenna on HFSS.

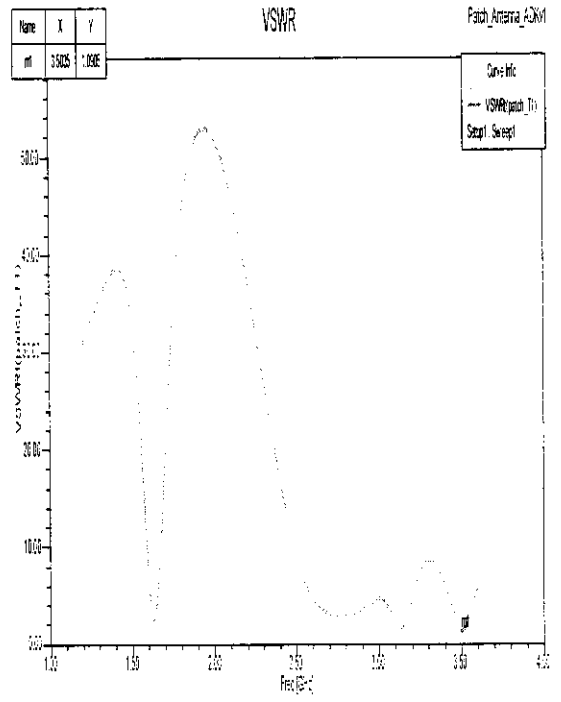
Table 4.2: Microstrip Rectangular Patch Antenna Design Parameters

Parameter	Value (cm)
PatchX	5.1
PatchY	4.3
Feedwidth	0.485
Feedlength	3.807
InsetDistance	1.263
InsetGap	0.243
SubX	8.4
SubY	12.34

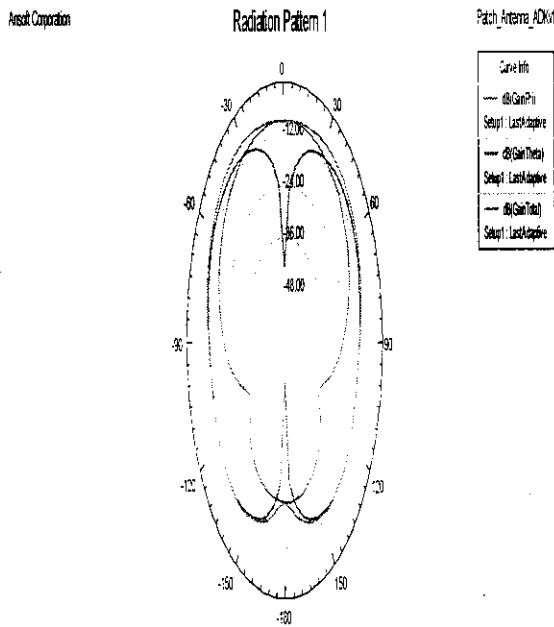
4.2.1. FR4 of 1mm thickness



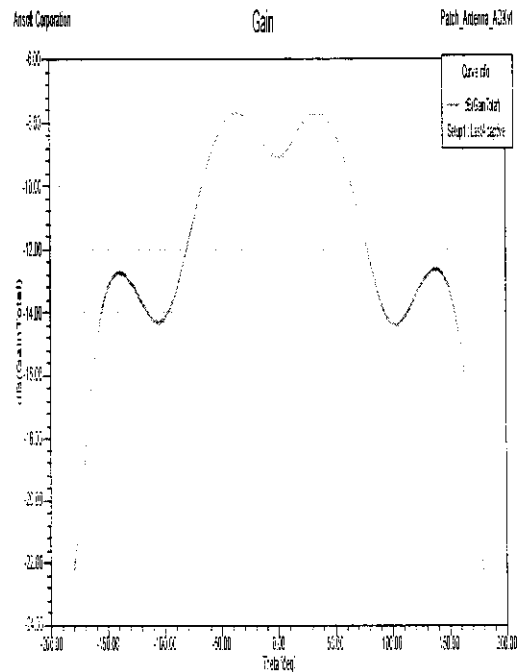
(a)



(b)



(c)



(d)

Figure 4.2.1: Simulated results of Rectangular inset feed patch antenna with FR4 of thickness 1mm (a) Return Loss (b) VSWR (c) Radiation Pattern (d) Gain

4.2.2. FR4 of 1.6mm thickness

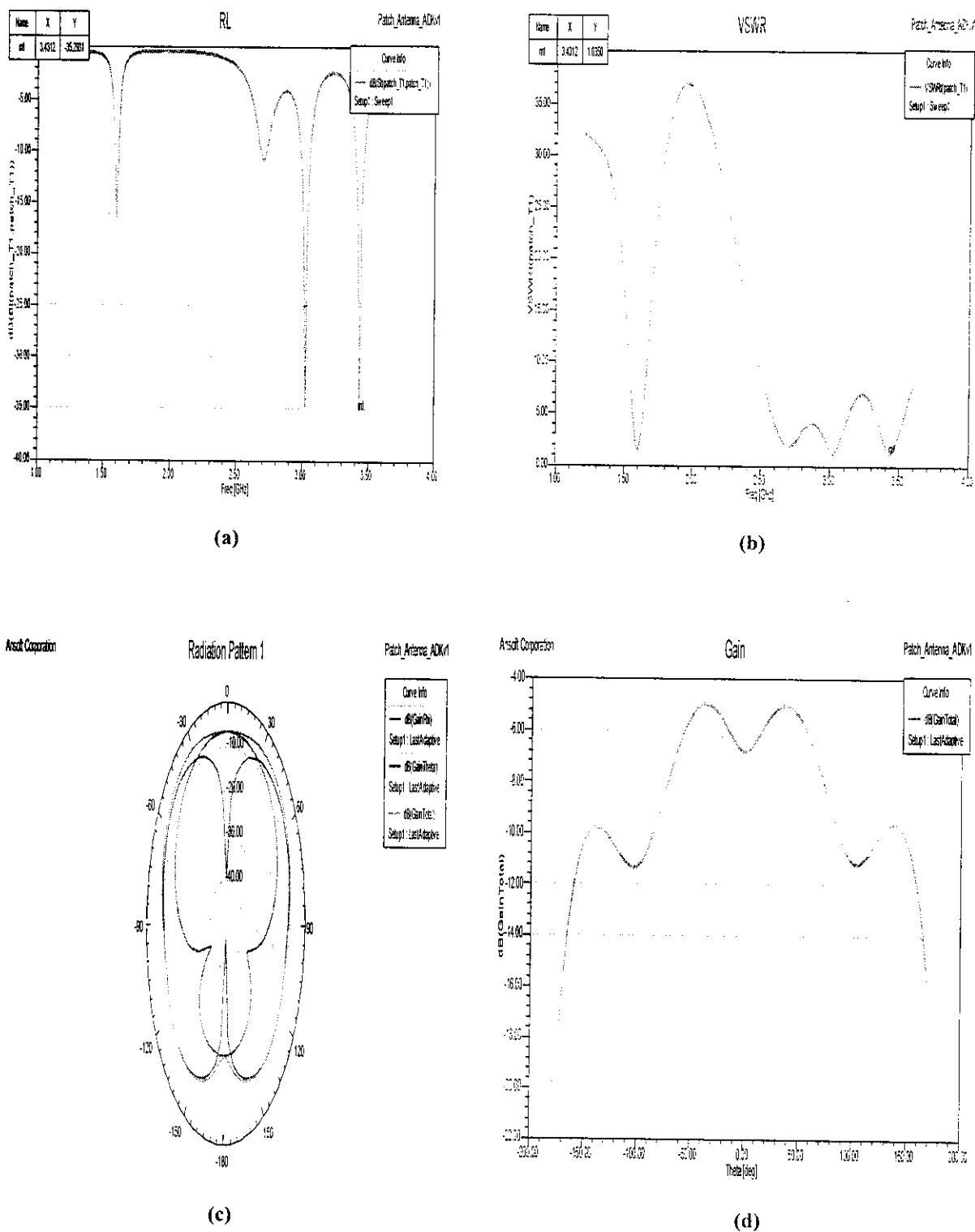


Figure 4.2.2: Simulated results of Rectangular inset feed patch antenna with FR4 of thickness 1.6mm (a) Return Loss (b) VSWR (c) Radiation Pattern (d) Gain

4.2.3 DUROID 5880 of 1.575mm thickness

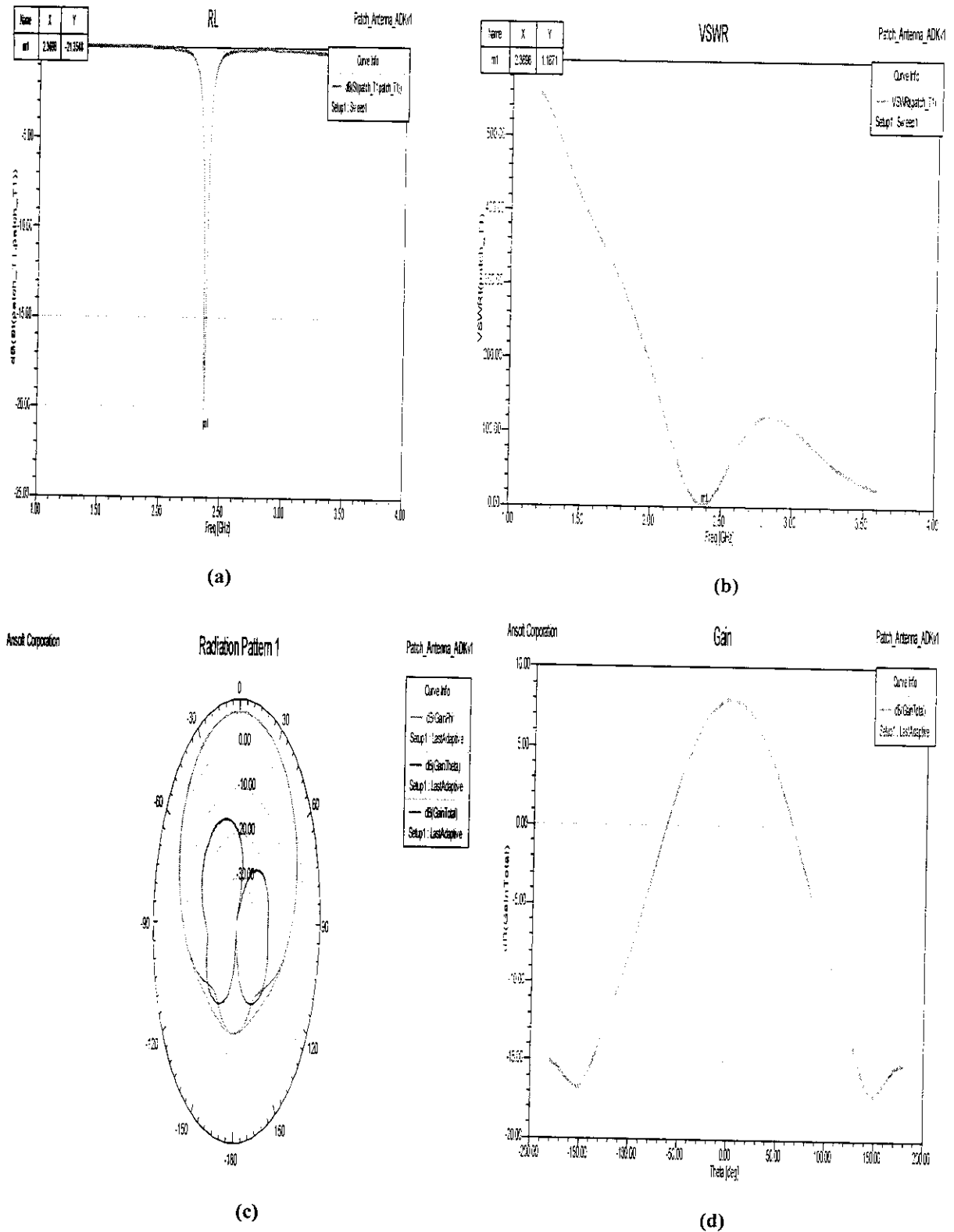


Figure 4.2.3: Simulated results of Rectangular inset feed patch antenna with Duroid 5880 (a) Return Loss (b) VSWR (c) Radiation Pattern (d) Gain

4.2.4. ROGERS RO 4350 of 1.524mm thickness

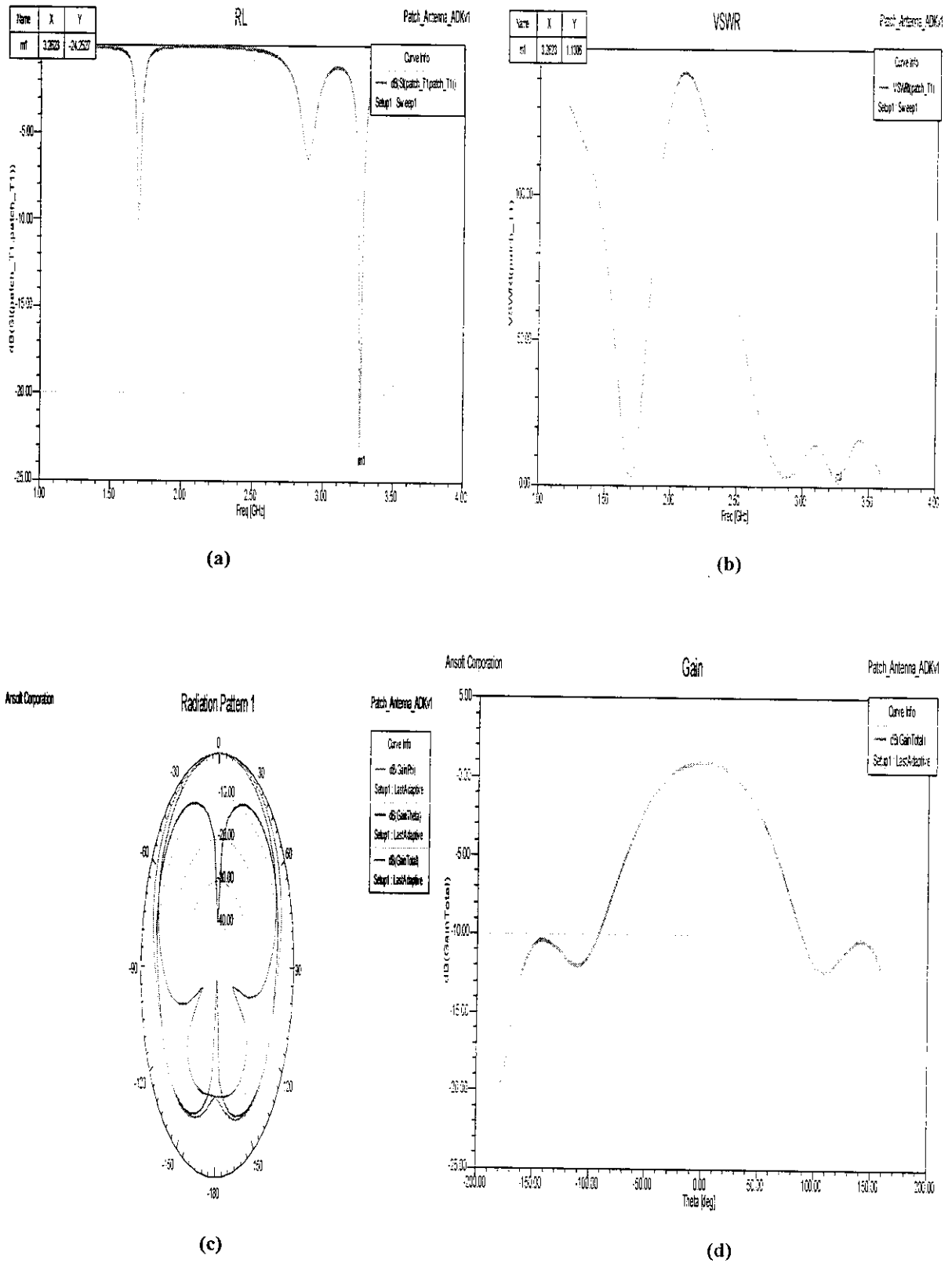


Figure 4.2.4: Simulated results of Rectangular inset feed patch antenna with RO 4350 (a) Return Loss (b) VSWR (c) Radiation Pattern (d) Gain

4.3 ELLIPTICAL INSET FEED PATCH ANTENNA USING DIFFERENT SUBSTRATE MATERIAL

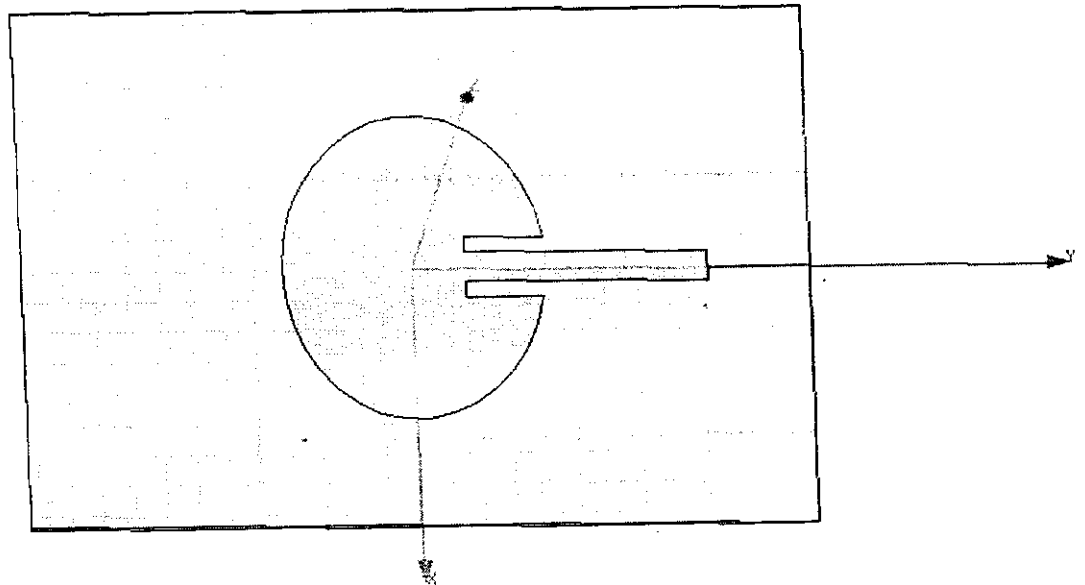


Figure 4.3: Structure of elliptical inset feed patch antenna on HFSS.

Table 4.3: Microstrip Elliptical Patch Antenna Design Parameters

Parameter	Value (cm)
PatchX	4.94cm
PatchY	4.14cm
Feedwidth	0.485cm
Feedlength	3.807cm
InsetDistance	1.263cm
InsetGap	0.243cm
SubX	8.4cm
SubY	12.34cm

4.3.1. FR4 of 1mm thickness

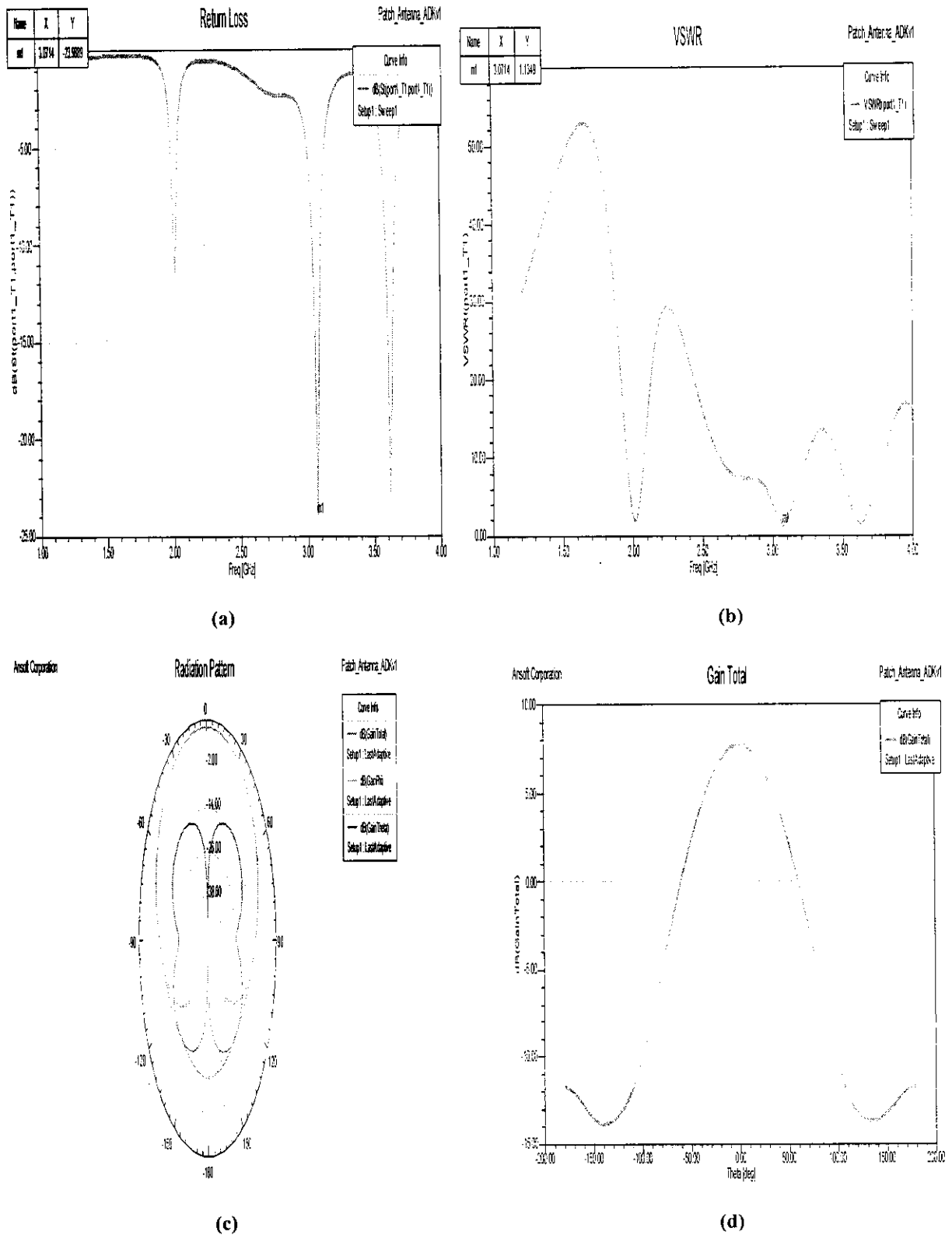


Figure 4.3.1: Simulated results of Elliptical inset feed patch antenna with FR4 of thickness 1mm (a) Return Loss (b) VSWR (c) Radiation Pattern (d) Gain

4.3.2. FR4 of 1.6mm thickness

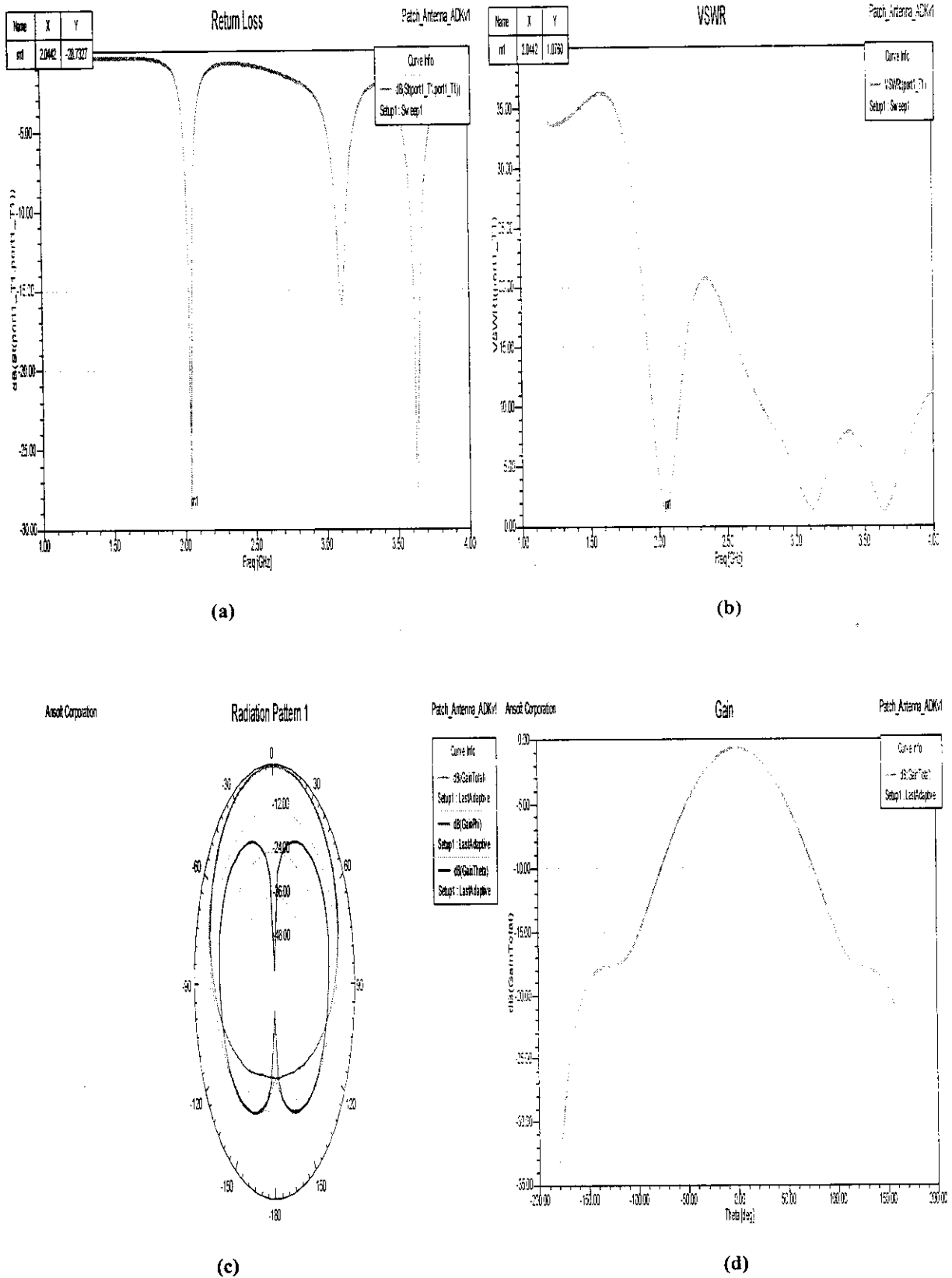


Figure 4.3.2: Simulated results of Elliptical inset feed patch antenna with FR4 of thickness 1.6mm (a) Return Loss (b) VSWR (c) Radiation Pattern (d) Gain

4.3.3 DUROID 5880 of 1.575mm thickness

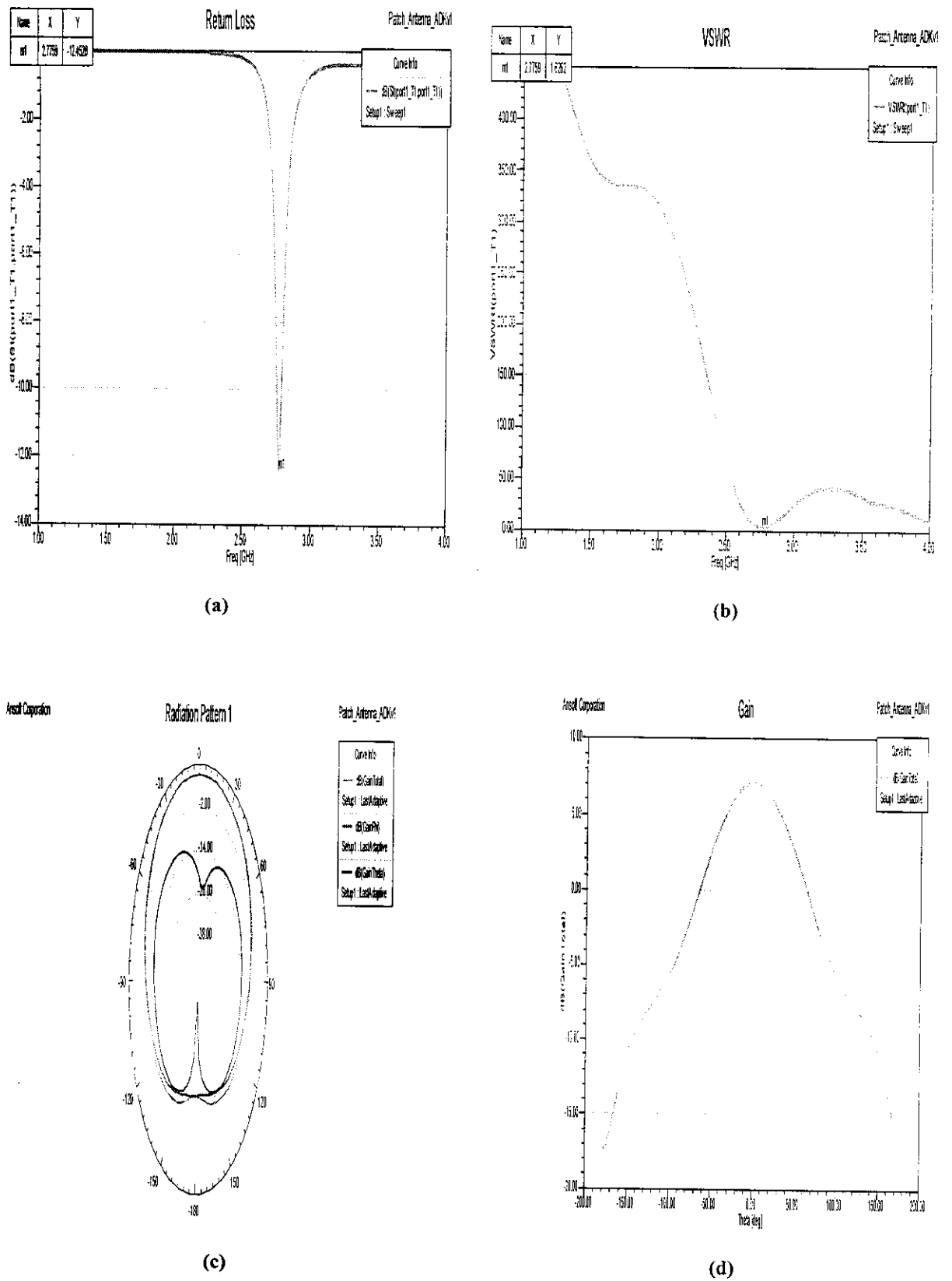
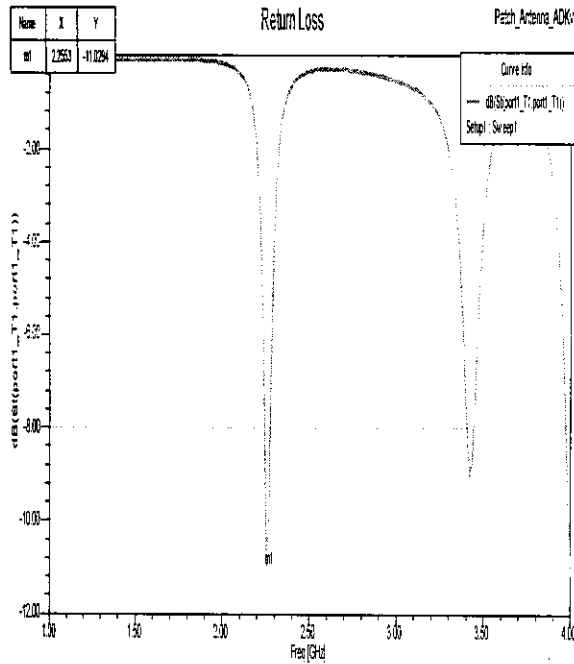
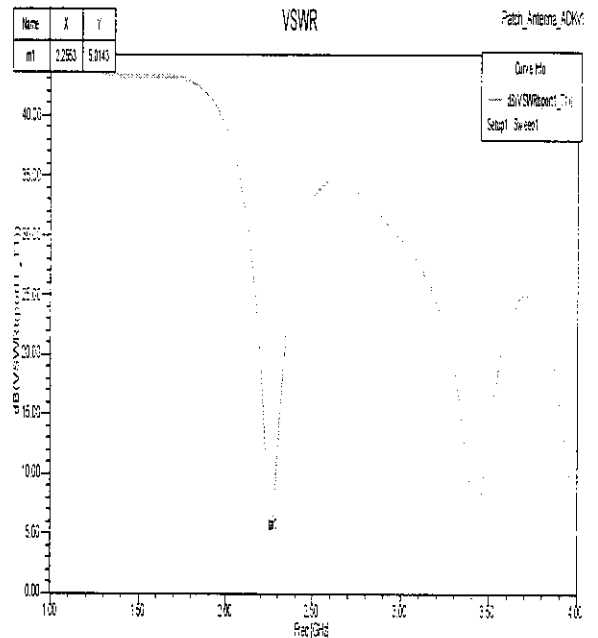


Figure 4.3.3: Simulated results of Elliptical inset feed patch antenna with Duroid 5880 (a) Return Loss (b) VSWR (c) Radiation Pattern (d) Gain

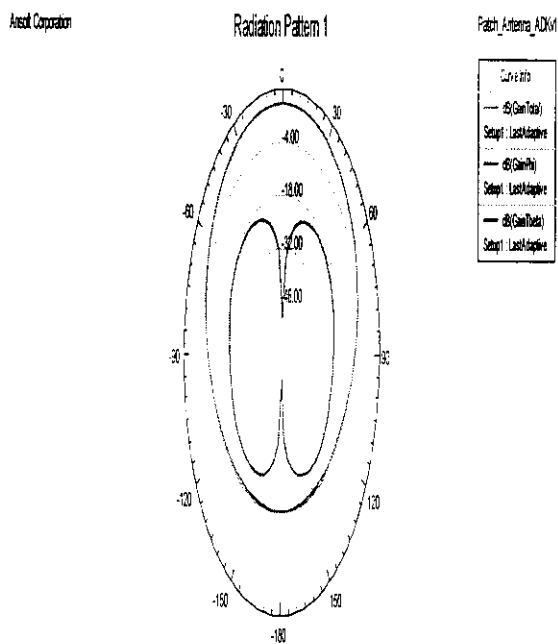
4.3.4. ROGERS RO 4350 with 1.524mm thickness



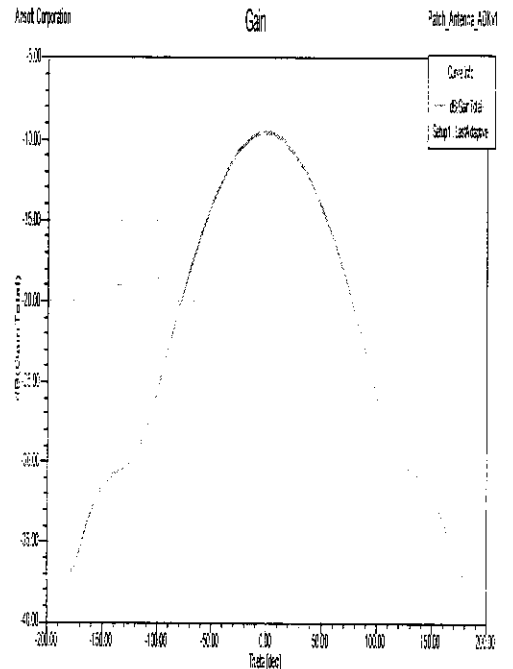
(a)



(b)



(c)



(d)

Figure 4.3.4: Simulated results of Elliptical inset feed patch antenna with RO 4350 (a) Return Loss (b) VSWR (c) Radiation Pattern (d) Gain

4.4 PLANAR INVERTED F - ANTENNA (PIFA) USING DIFFERENT SUBSTRATE MATERIAL

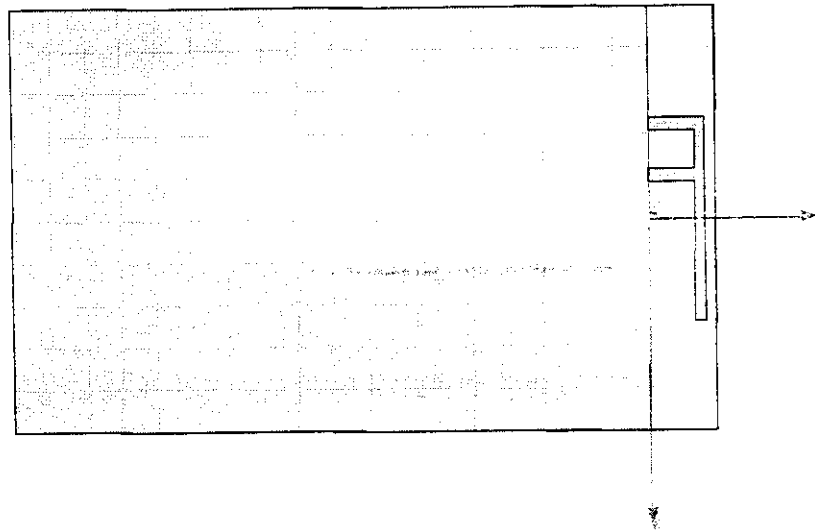


Figure 4.4: Structure of PIFA antenna on HFSS.

Table 4.4: Microstrip PIFA Antenna Design Parameters

Parameter	Value (cm)
Length1	2.217
Length2	0.786
Feedwidth	0.140
Feedlength	0.009
Feedoffset	0.517
Antenna trace width	0.140
Antenna offset	0.468
SubX	5
SubY	10

4.4.1. FR4 of 1mm thickness

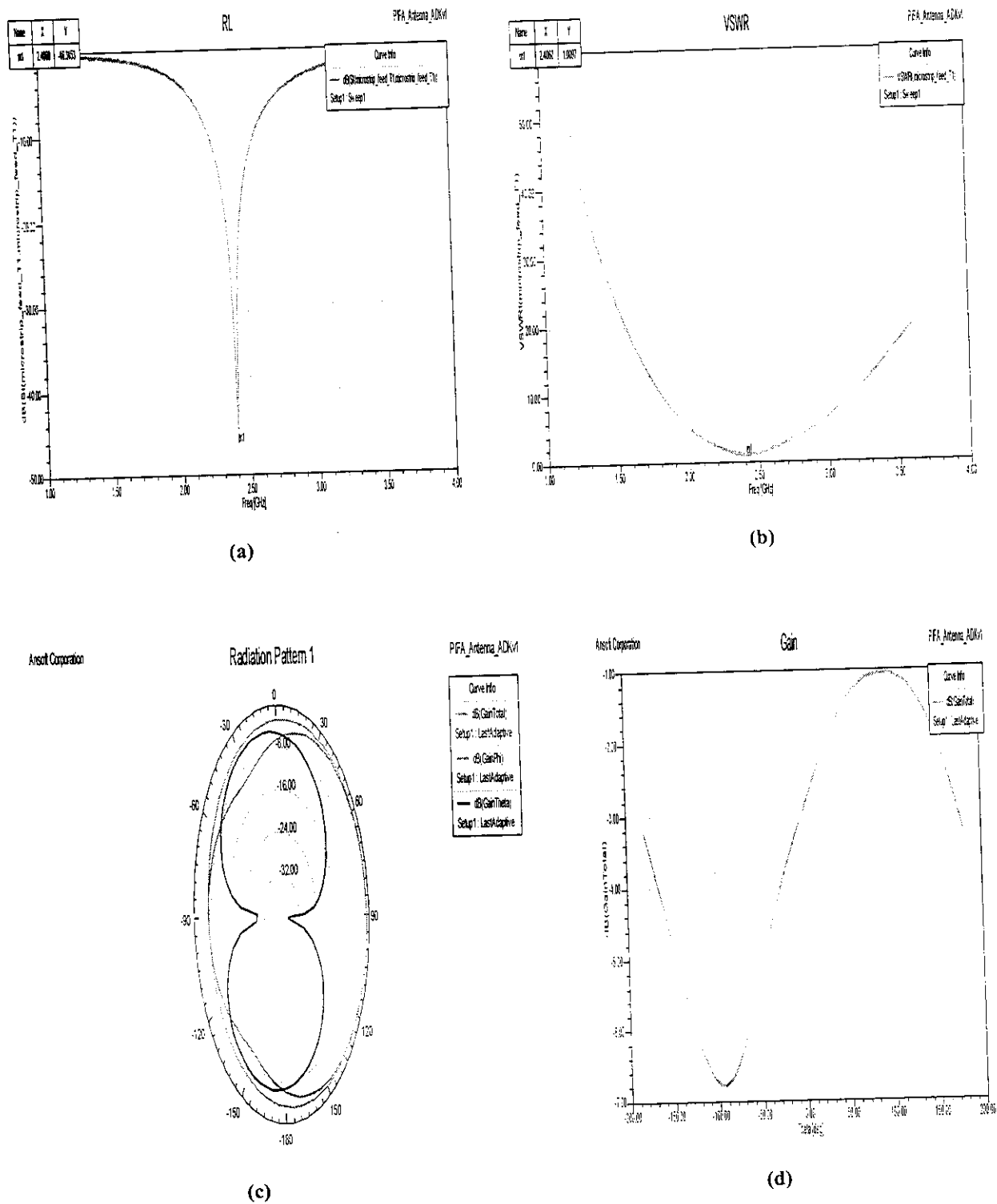
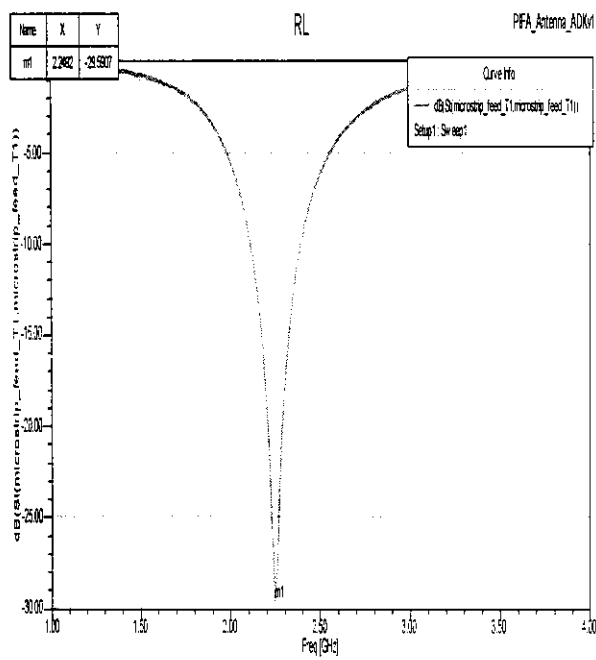
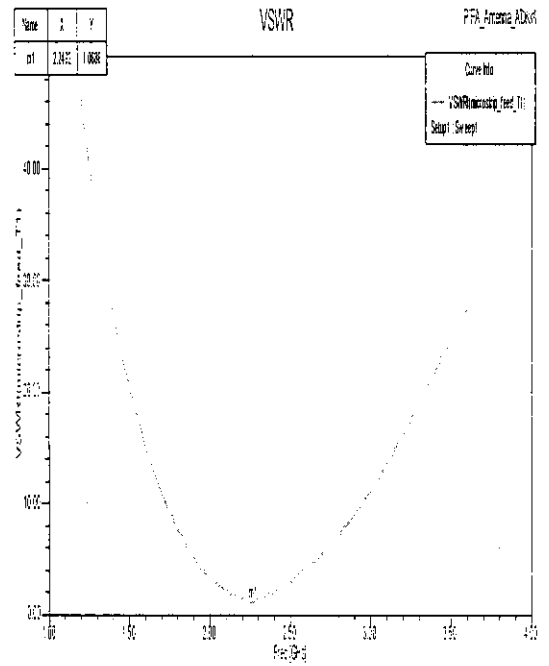


Figure 4.4.1: Simulated results of PIFA antenna with FR4 of thickness 1mm (a) Return Loss (b) VSWR (c) Radiation Pattern (d) Gain

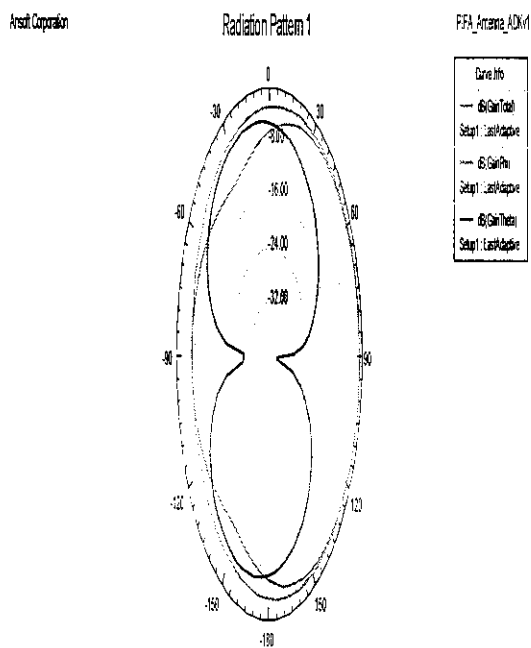
4.4.2. FR4 of 1.6mm thickness



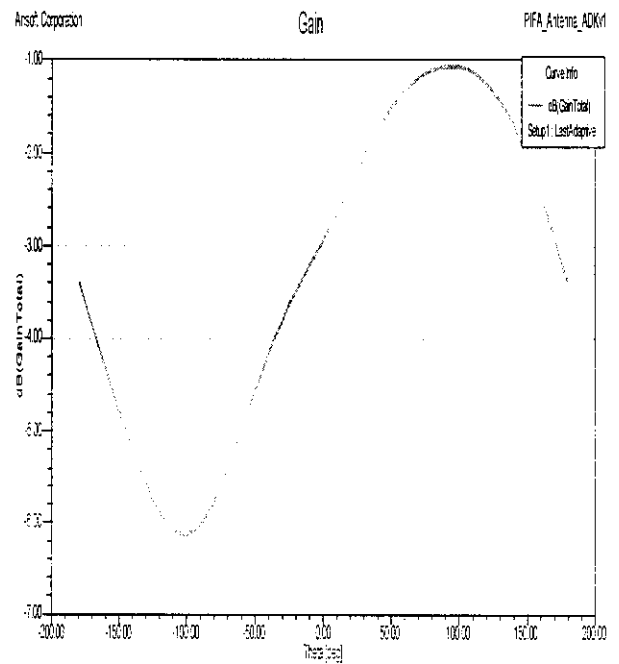
(a)



(b)



(c)



(d)

Figure 4.4.2: Simulated results of PIFA antenna with FR4 of thickness 1.6mm (a) Return Loss (b) VSWR (c) Radiation Pattern (d) Gain

4.4.3. DUROID 5880 of 1.575mm thickness

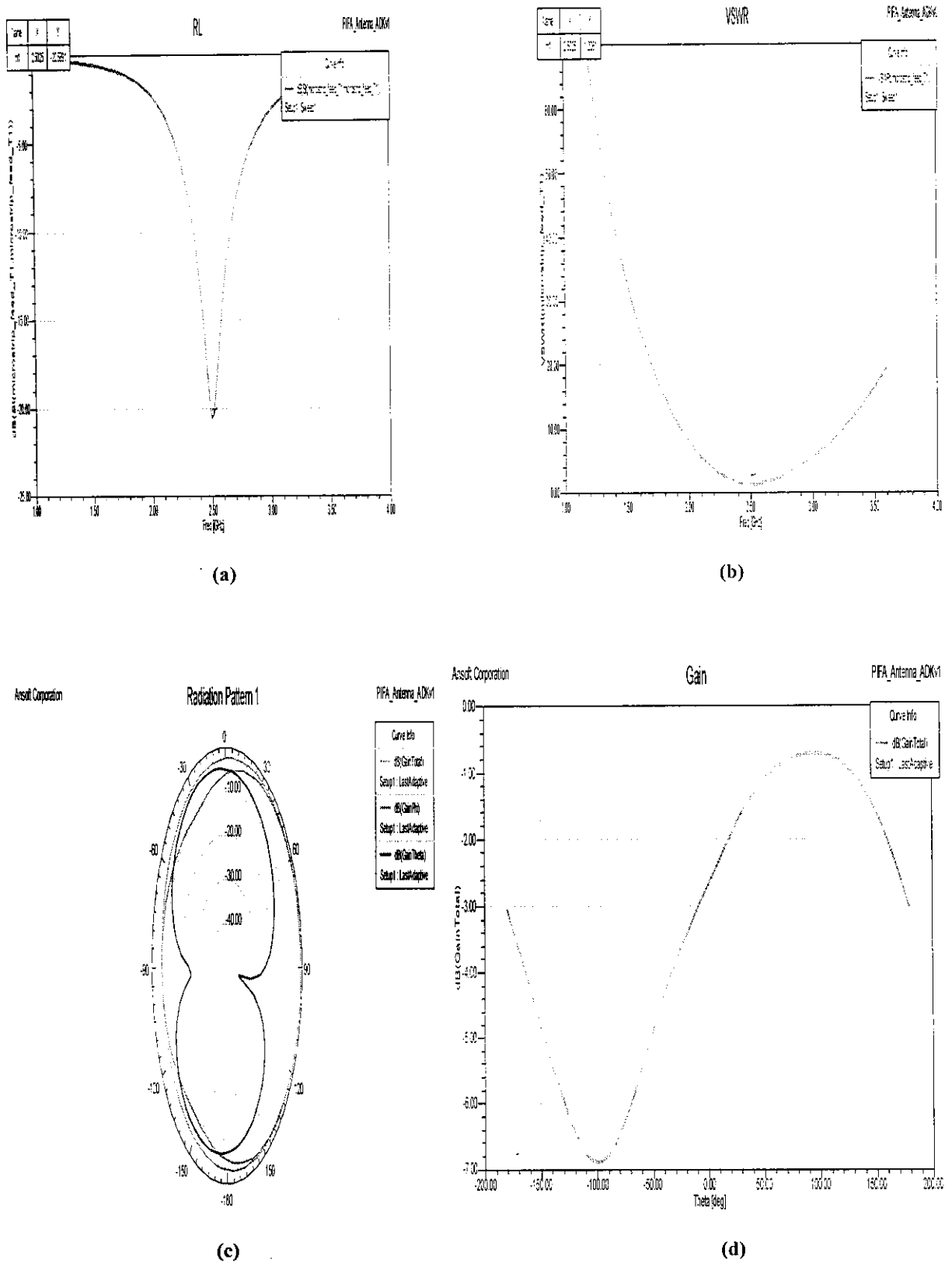


Figure 4.4.3: Simulated results of PIFA antenna with Duroid 5880 (a) Return Loss (b) VSWR (c) Radiation Pattern (d) Gain

4.4.4. ROGERS RO 4350 of 1.524mm thickness

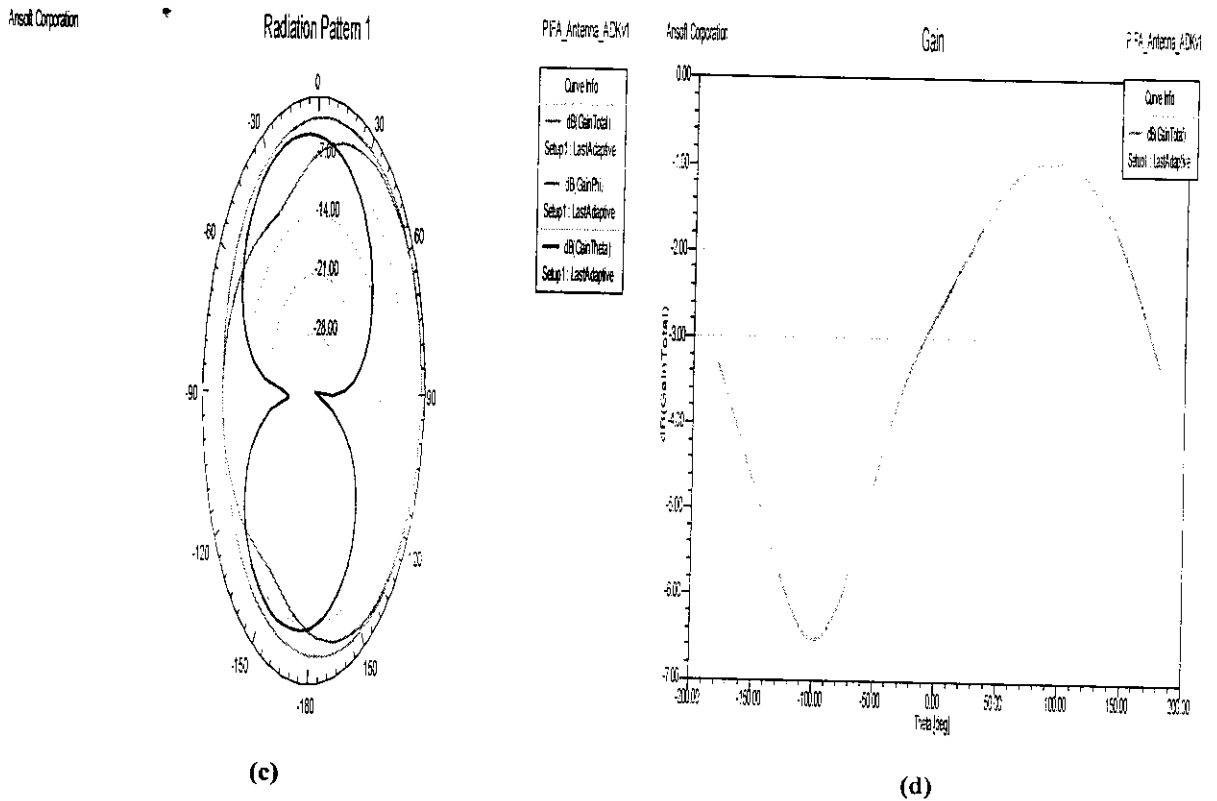
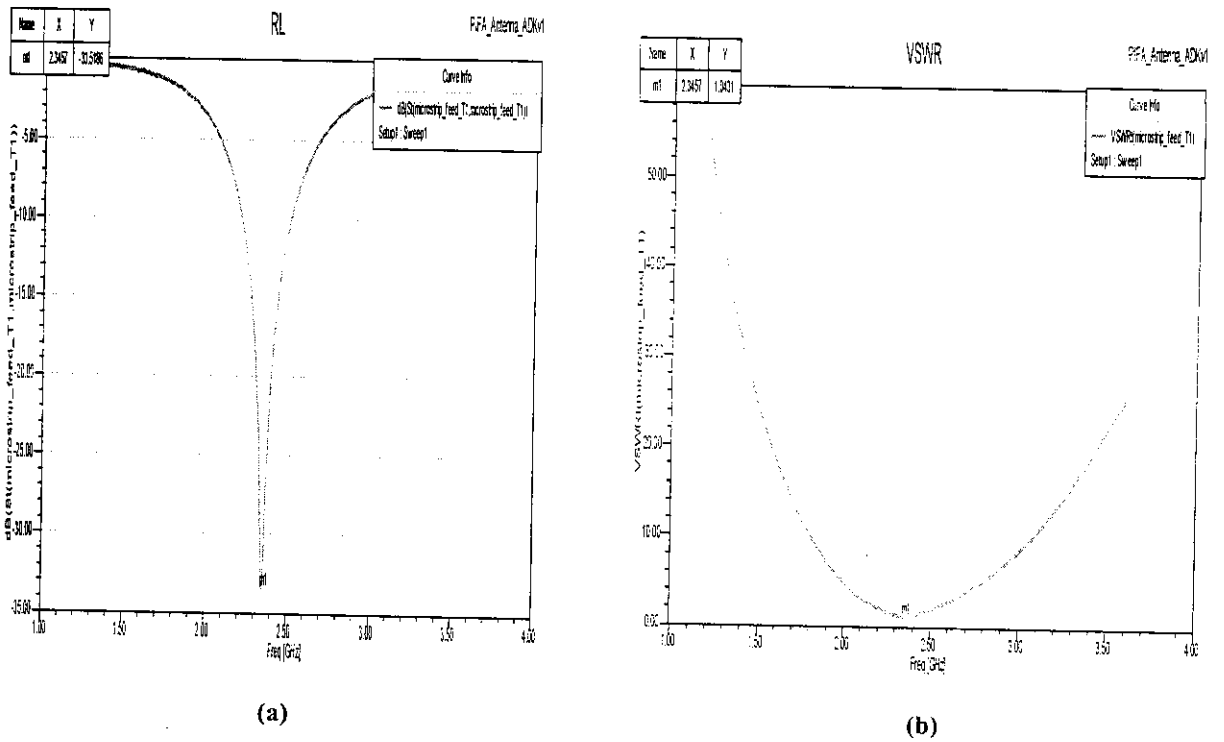


Figure 4.4.4: Simulated results of PIFA antenna with RO 4350 (a) Return Loss (b) VSWR (c) Radiation Pattern (d) Gain

4.5 F-MONOPOLE ANTENNA USING DIFFERENT SUBSTRATE MATERIAL

4.5.1 F-antenna of $10 \times 15 \text{mm}^2$ integrated on substrate dimension- $45 \times 80 \text{mm}^2$

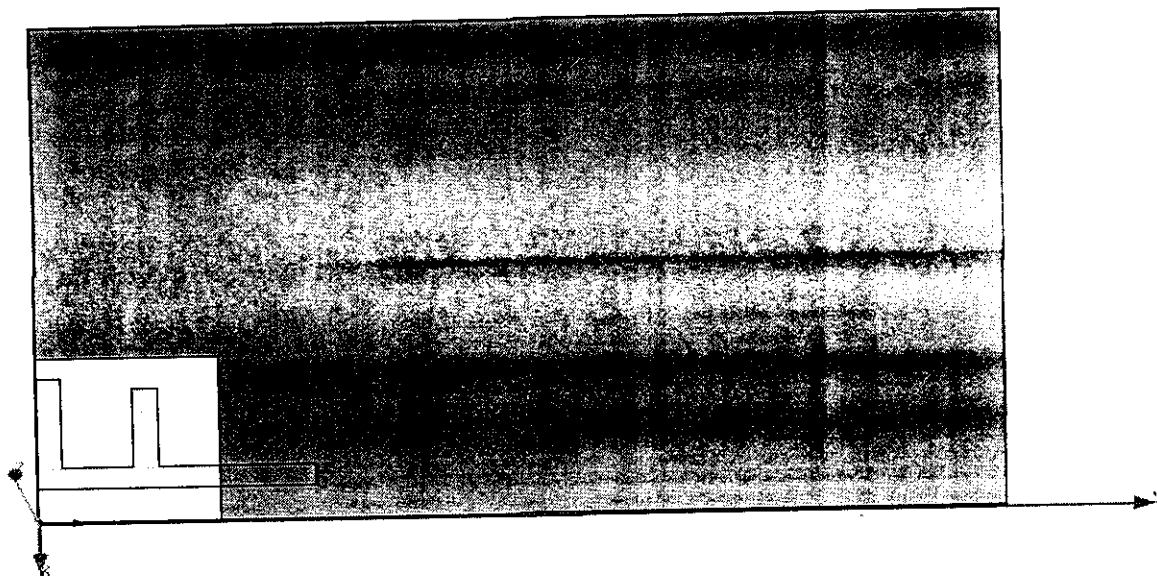
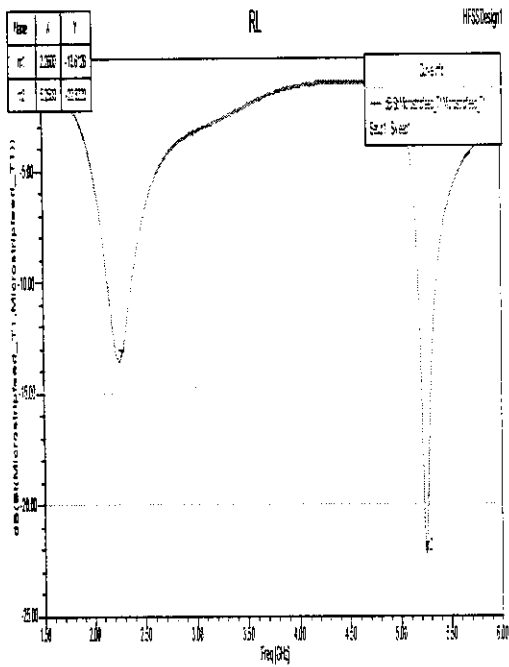


Figure 4.5.1 : Structure of F- antenna of substrate dimension $45 \times 80 \text{mm}^2$ on HFSS.

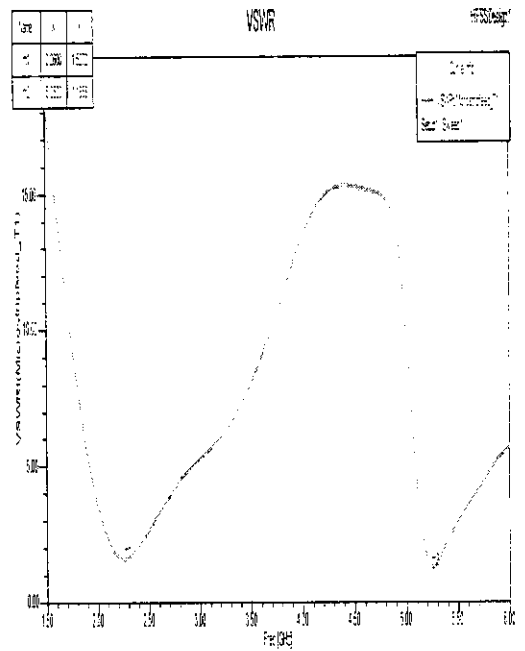
Table 4.5.1: Microstrip F Antenna of substrate dimension $45 \times 80 \text{mm}^2$ Design Parameters

Parameter	Value (cm)
Length 1	1.5
Length 2	1
Length 3	0.9
Antenna width	0.2
Antenna X shift	0.3
Feedwidth	0.2
Cut out X	1.5
Cut out Y	1.5
SubX	4.5
SubY	8

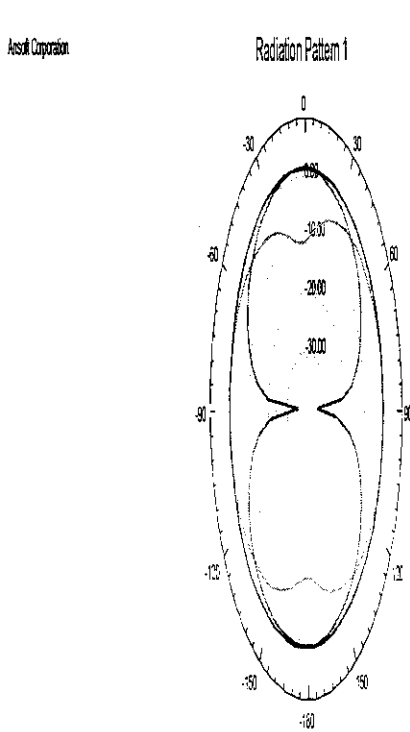
4.5.1.1. FR4



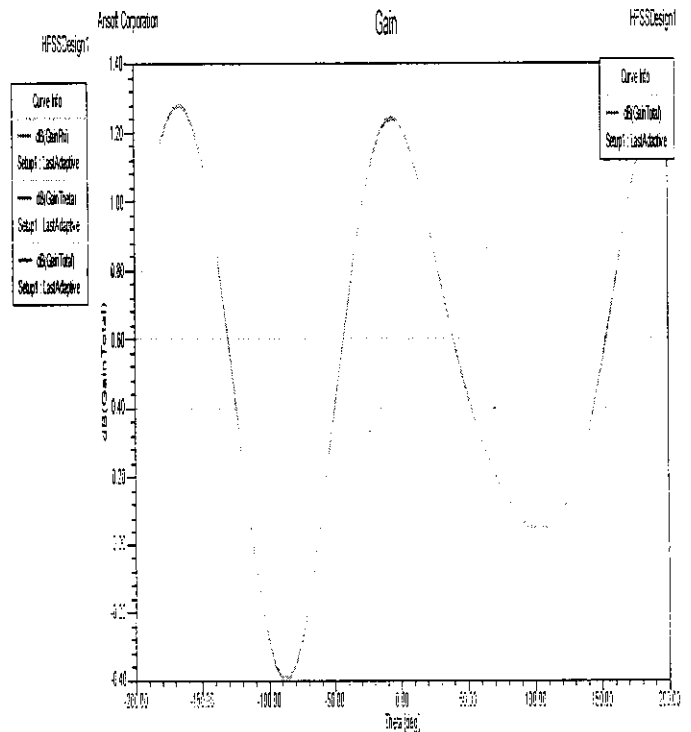
(a)



(b)



(c)



(d)

Figure 4.5.1.1: Simulated results of F antenna of $10 \times 15 \text{mm}^2$ integrated on substrate dimension- $45 \times 80 \text{mm}^2$ with FR4 (a) Return Loss (b) VSWR (c) Radiation Pattern (d) Gain

4.5.1.2. DUROID 5880 of 1.575mm thickness

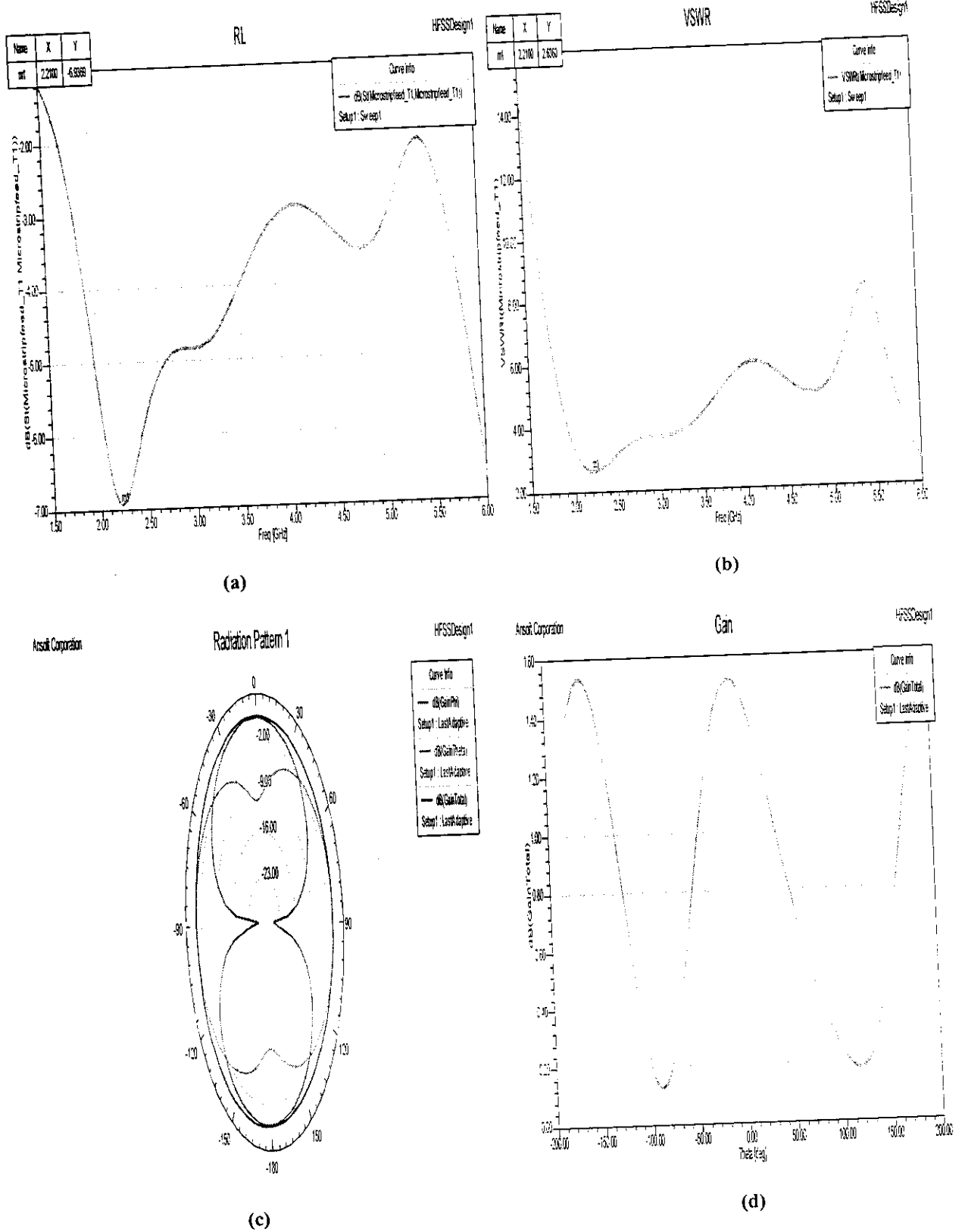
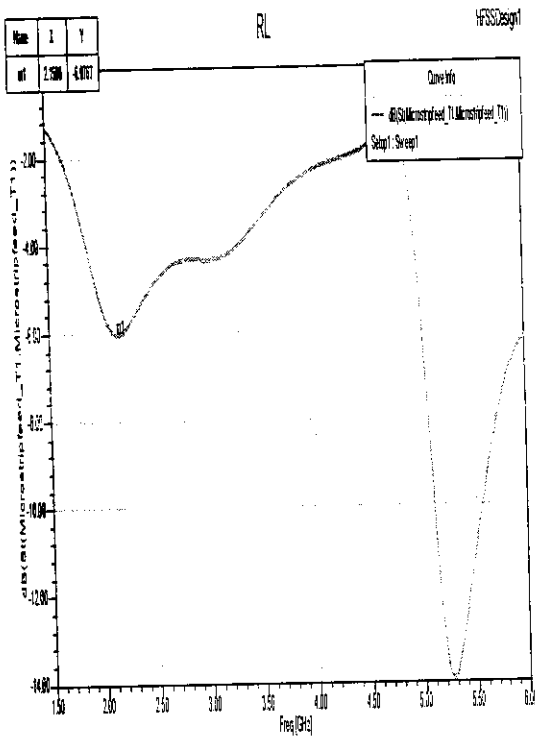
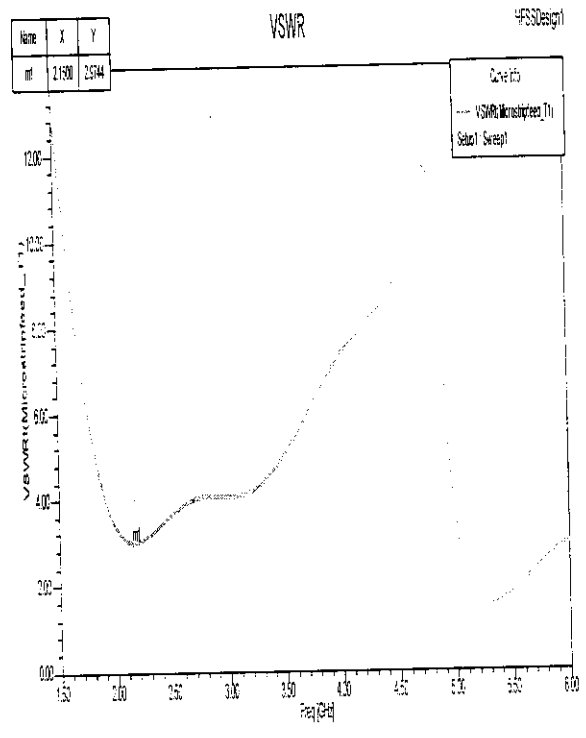


Figure 4.5.1.2: Simulated results of F antenna of $10 \times 15 \text{mm}^2$ integrated on substrate dimension- $45 \times 80 \text{mm}^2$ with Duroid 5880 (a) Return Loss (b) VSWR (c) Radiation Pattern (d) Gain

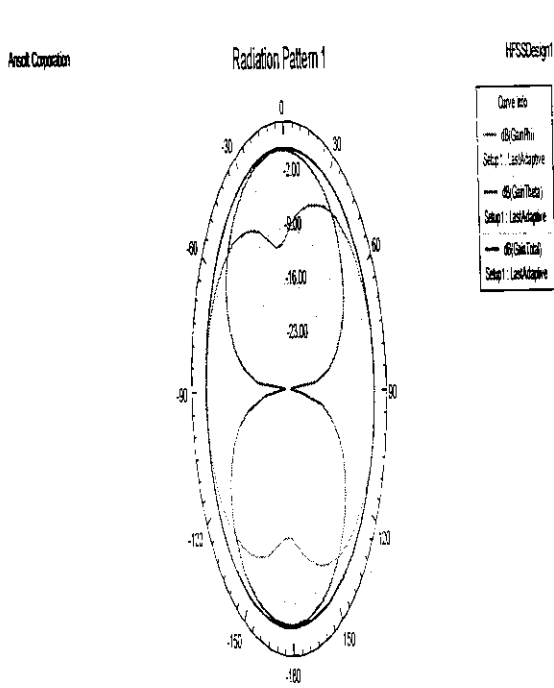
4.5.1.3. ROGERS RO 4350 of 1.524mm thickness



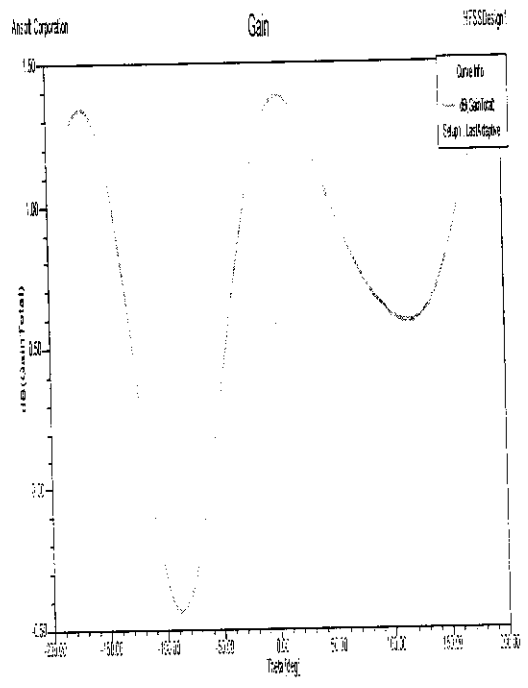
(a)



(b)



(c)



(d)

Figure 4.5.1.3: Simulated results of F antenna of $10 \times 15 \text{ mm}^2$ integrated on substrate dimension- $45 \times 80 \text{ mm}^2$ with RO 4350 (a) Return Loss (b) VSWR (c) Radiation Pattern (d) Gain

Gain

4.5.2 F-antenna of $9 \times 15 \text{mm}^2$ integrated on FR4 substrate (1mm) of dimension $50 \times 35 \text{mm}^2$ and cutout $15 \times 15 \text{mm}^2$

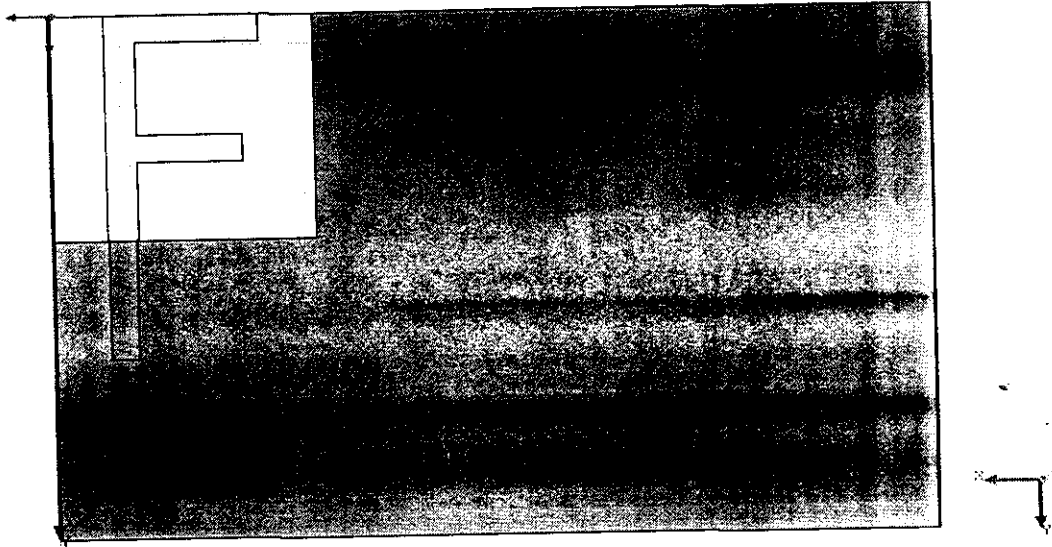
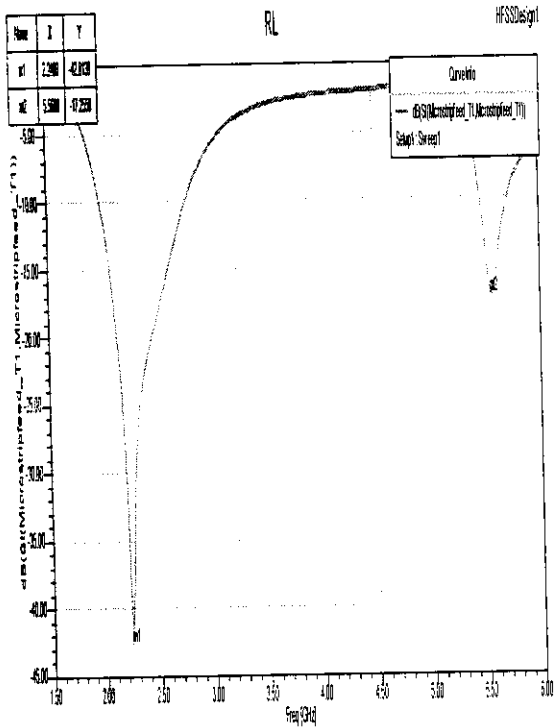


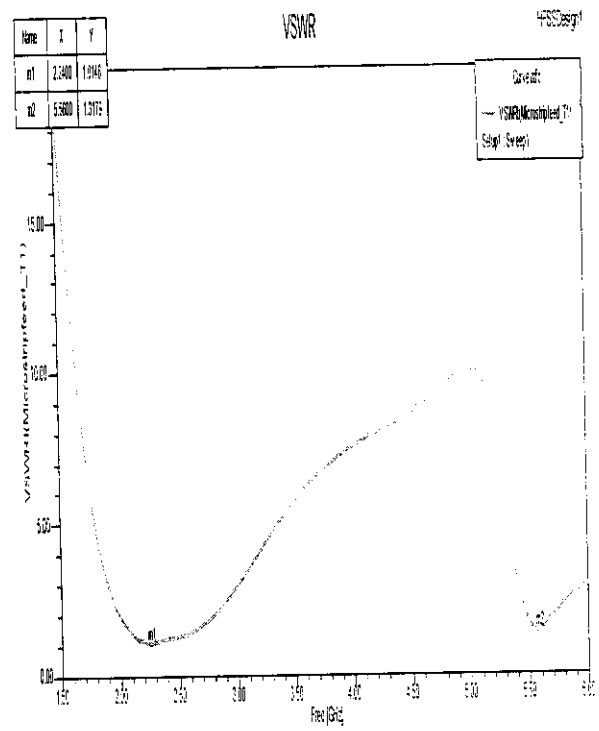
Figure 4.5.2: Structure of F- antenna of substrate dimension $50 \times 35 \text{mm}^2$ and cutout $15 \times 15 \text{mm}^2$ on HFSS.

Table 4.5.2: Microstrip F Antenna of substrate dimension $50 \times 35 \text{mm}^2$ and cutout $15 \times 15 \text{mm}^2$ Design Parameters

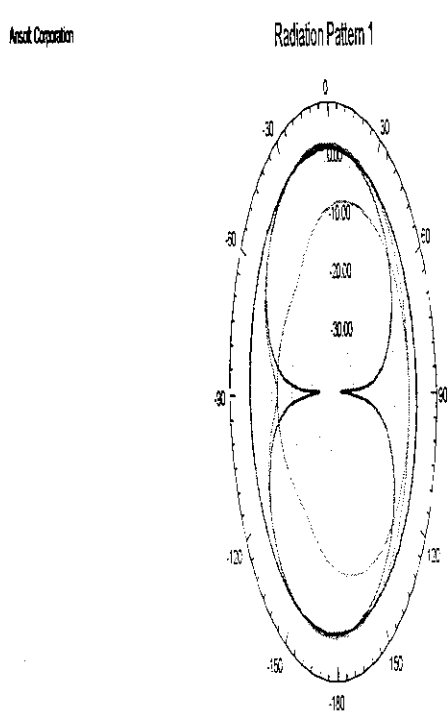
Parameter	Value (cm)
Length 1	1.5
Length 2	0.88
Length 3	0.78
Antenna width	0.18
Antenna X shift	0.3
Feed width	0.16
Cut out X	1.5
Cut out Y	1.5
SubX	5
SubY	3.5



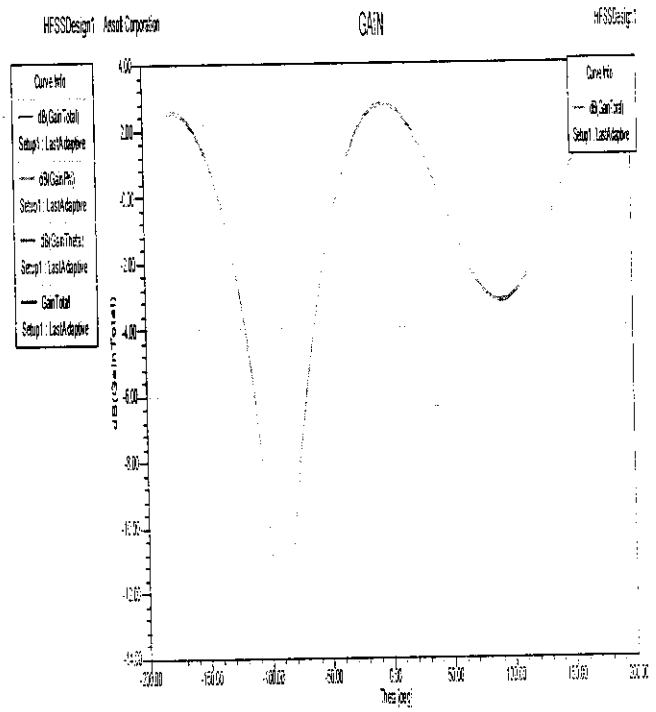
(a)



(b)



(c)



(d)

Figure 4.5.2.1: Simulated results of F antenna of substrate dimension $50 \times 35 \text{mm}^2$ and cutout $15 \times 15 \text{mm}^2$ with FR4 of thickness 1mm (a) Return Loss (b) VSWR (c) Radiation Pattern (d) Gain

4.5.3. F-antenna of $9 \times 15 \text{mm}^2$ integrated on substrate dimension of $50 \times 35 \text{mm}^2$ and cutout $50 \times 18 \text{mm}^2$

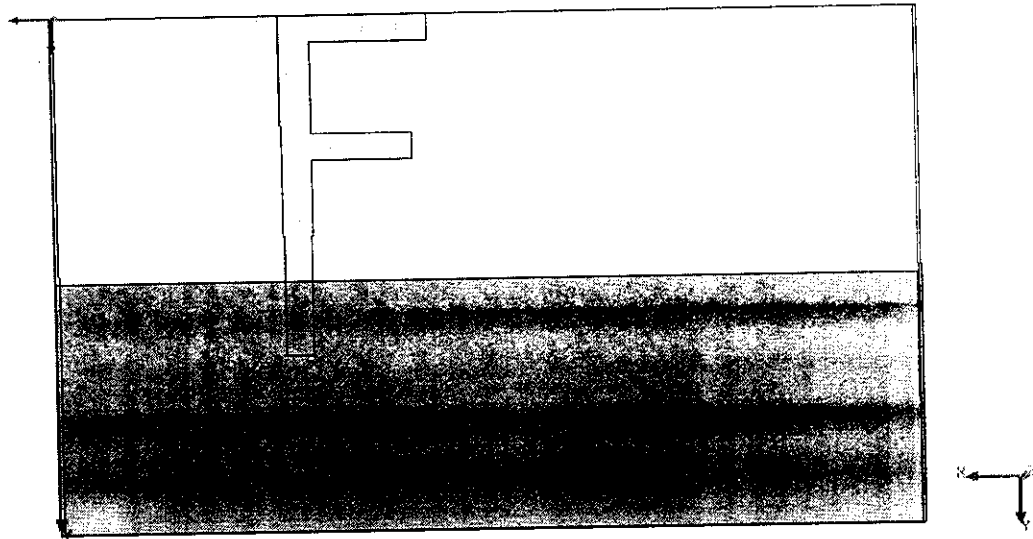


Figure 4.5.3: Structure of F- antenna of substrate dimension $50 \times 35 \text{mm}^2$ and cutout $50 \times 18 \text{mm}^2$ on HFSS.

Table 4.5.3: Microstrip F Antenna of Substrate Dimension $50 \times 35 \text{mm}^2$ and Cutout $50 \times 18 \text{mm}^2$ design Parameters

Parameter	Value (cm)
Length 1	1.5
Length 2	0.86
Length 3	0.76
Antenna width	0.18
Antenna X shift	1.3
Feed width	0.16
Cut out X	5
Cut out Y	1.8
SubX	5
SubY	3.5

4.5.3.1. FR4 of 1mm thickness

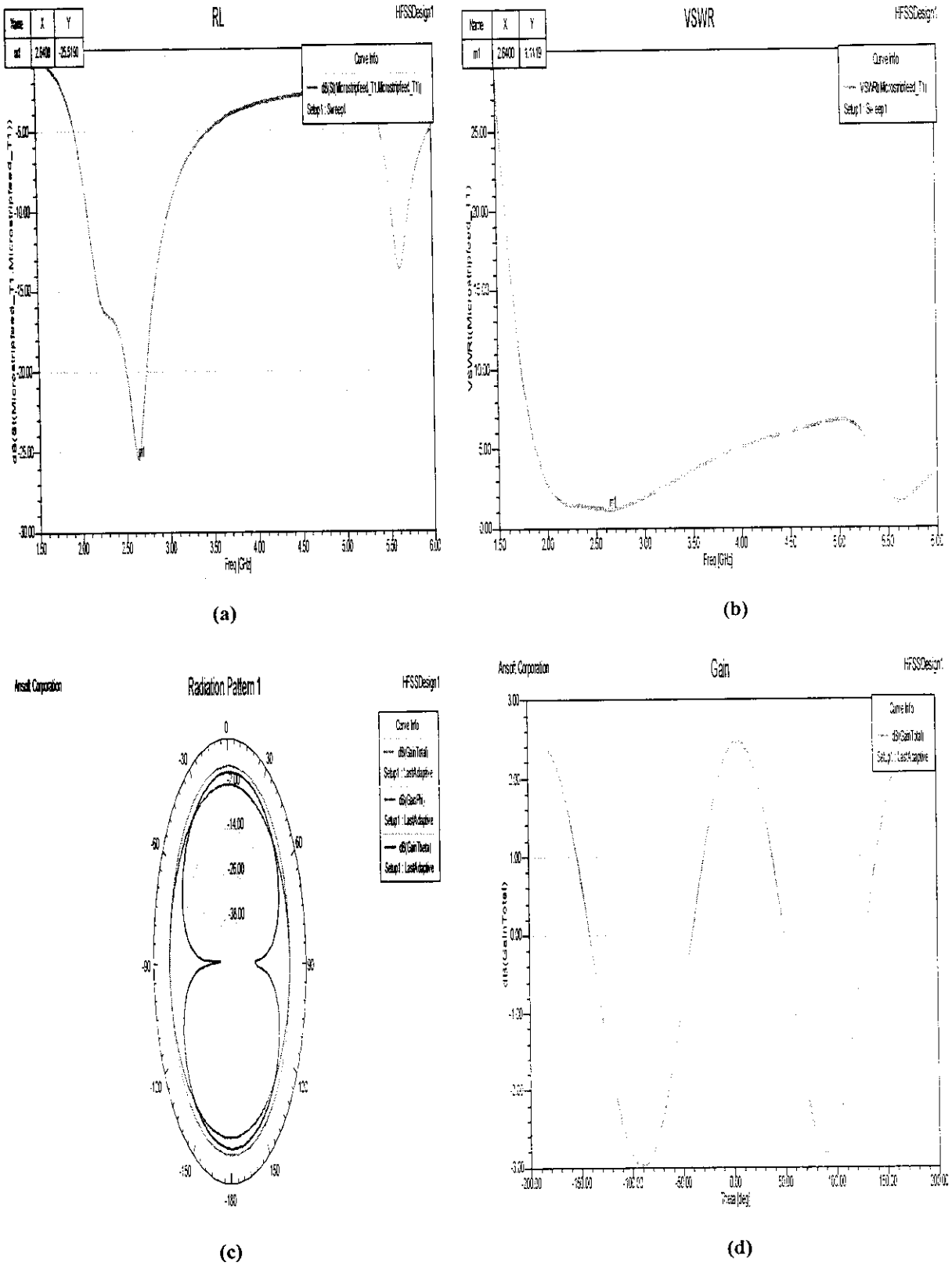


Figure 4.5.3.1: Simulated results of F antenna of substrate dimension $50 \times 35 \text{mm}^2$ and cutout $50 \times 18 \text{mm}^2$ with FR4 of thickness 1mm (a) Return Loss (b) VSWR (c) Radiation Pattern (d) Gain

4.5.3.2. FR4 of 1.6mm thickness

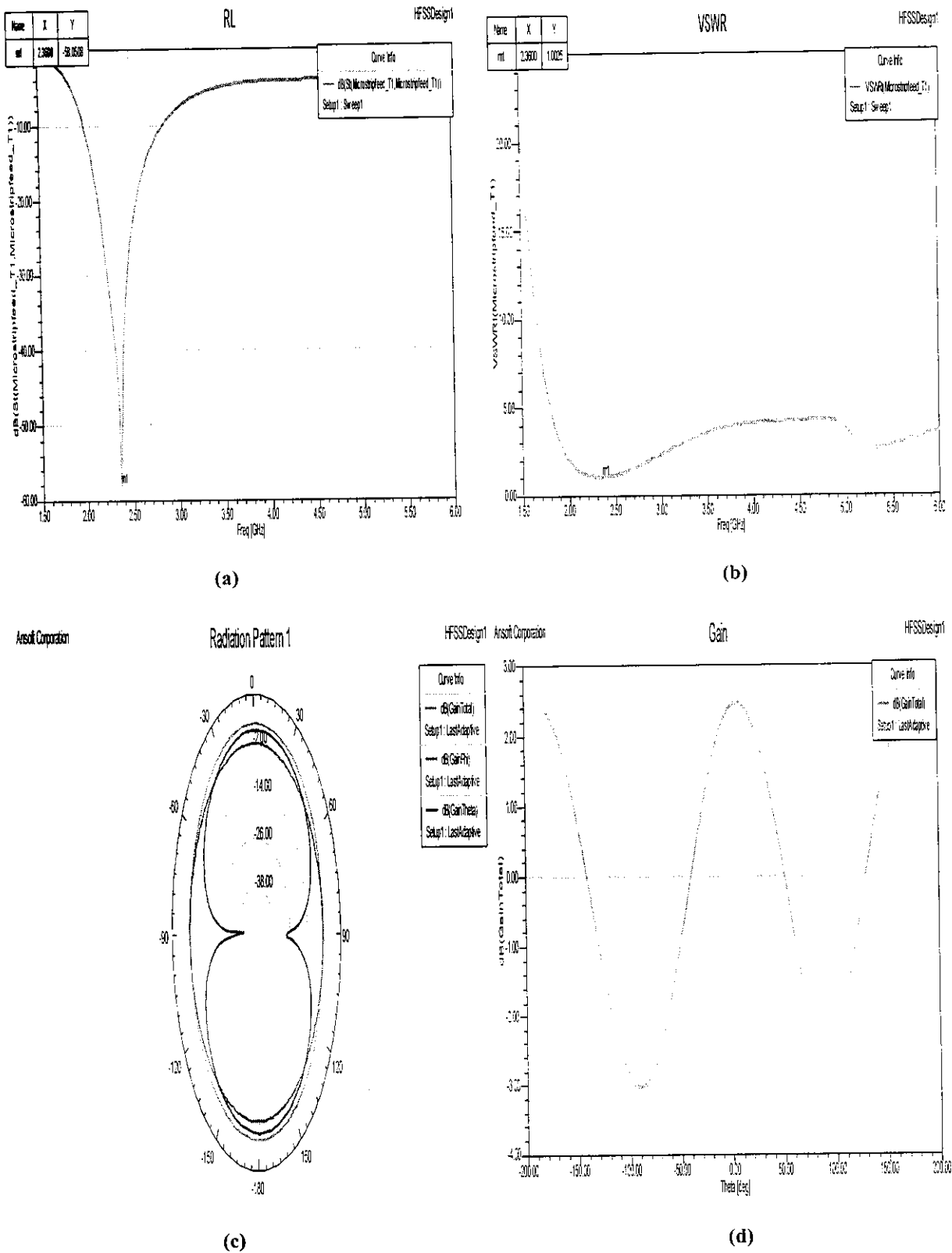


Figure 4.5.3.2: Simulated results of F antenna of substrate dimension $50 \times 35 \text{mm}^2$ and cutout $50 \times 18 \text{mm}^2$ with FR4 of thickness 1.6mm (a) Return Loss (b) VSWR (c) Radiation Pattern (d) Gain

4.5.4. F-antenna of $9 \times 15 \text{mm}^2$ integrated on FR4 substrate (1mm) dimension $47 \times 40 \text{mm}^2$ and cutout $15 \times 15 \text{mm}^2$

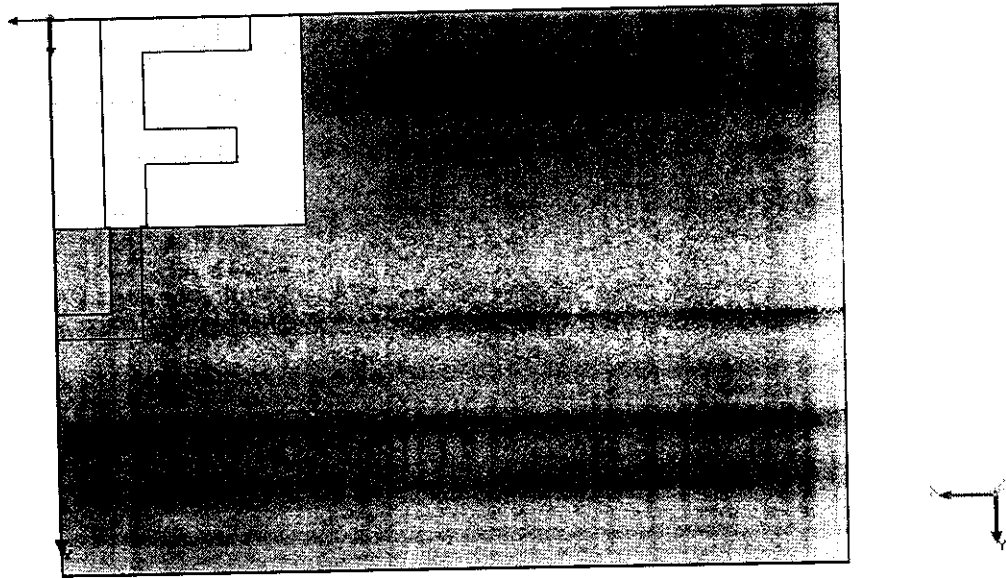
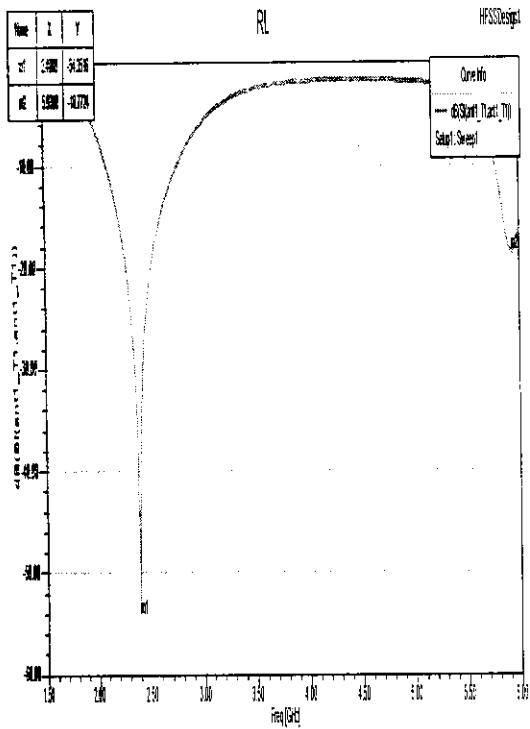


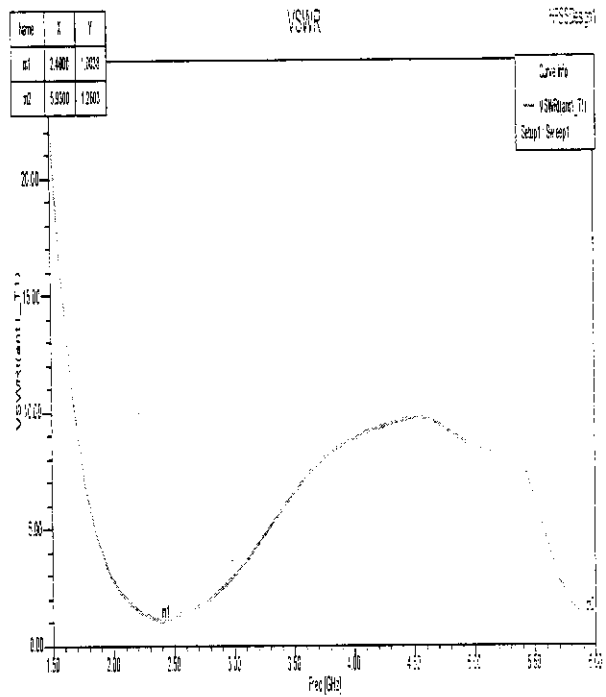
Figure 4.5.4: Structure of F- antenna of substrate dimension $47 \times 40 \text{mm}^2$ and cutout $15 \times 15 \text{mm}^2$ on HFSS.

Table 4.5.4: Microstrip F Antenna of substrate dimension $47 \times 40 \text{mm}^2$ and cutout $15 \times 15 \text{mm}^2$ on Design Parameters

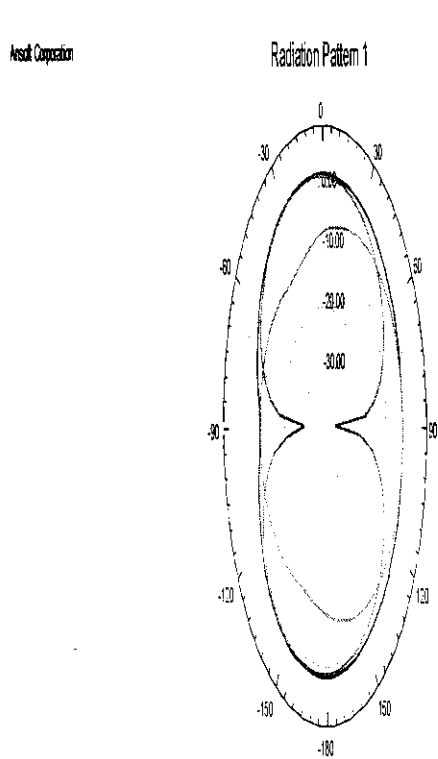
Parameter	Value (cm)
Length 1	1.5cm
Length 2	0.9cm
Length 3	0.8cm
Antenna width	0.25cm
Antenna X shift	0.3cm
Feed width	0.18cm
Cut out X	1.5cm
Cut out Y	1.5cm
SubX	4.7cm
SubY	4cm



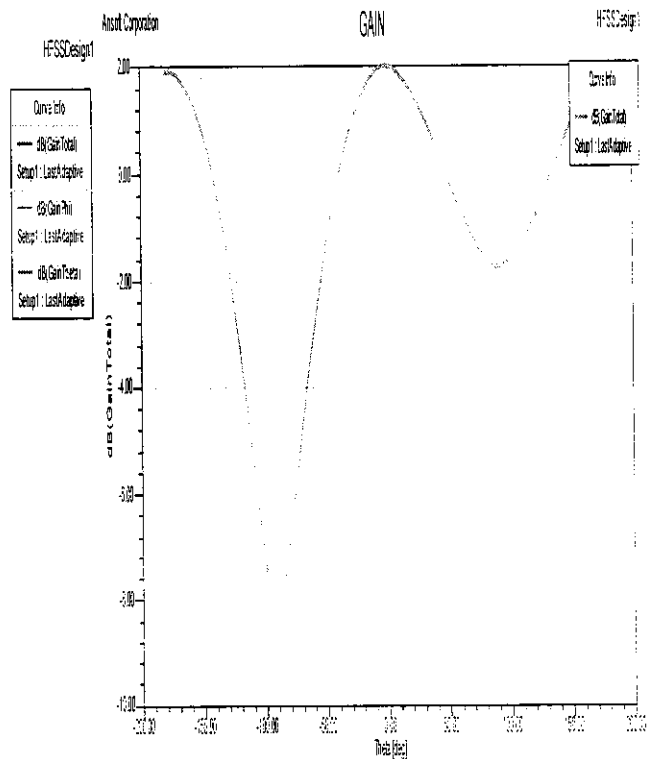
(a)



(b)



(c)



(d)

Figure 4.5.4.1: Simulated results of F antenna of substrate dimension $47 \times 40 \text{mm}^2$ and cutout $15 \times 15 \text{mm}^2$ with FR4 of thickness 1mm (a) Return Loss (b) VSWR (c) Radiation Pattern (d) Gain

4.5.5. F-antenna of $9 \times 15 \text{mm}^2$ integrated on substrate dimension of $47 \times 40 \text{mm}^2$ and cutout $47 \times 18 \text{mm}^2$

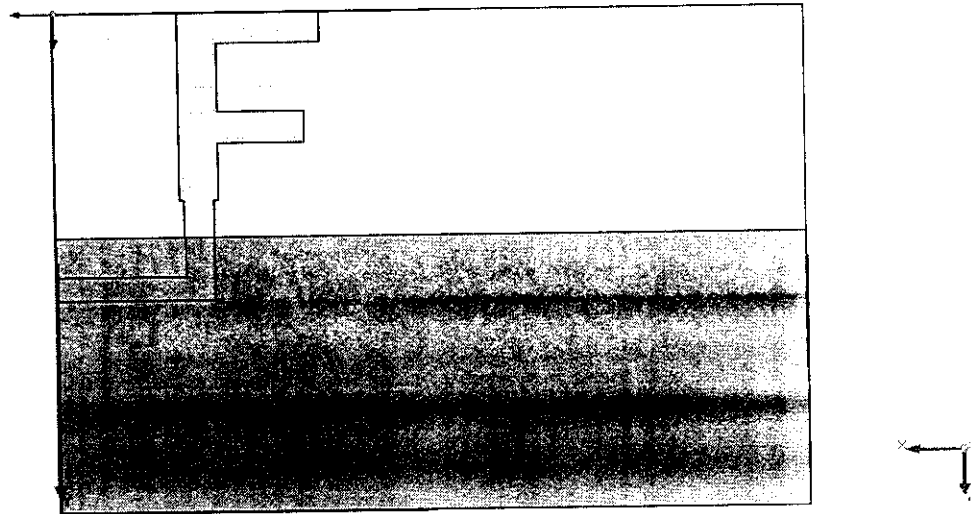


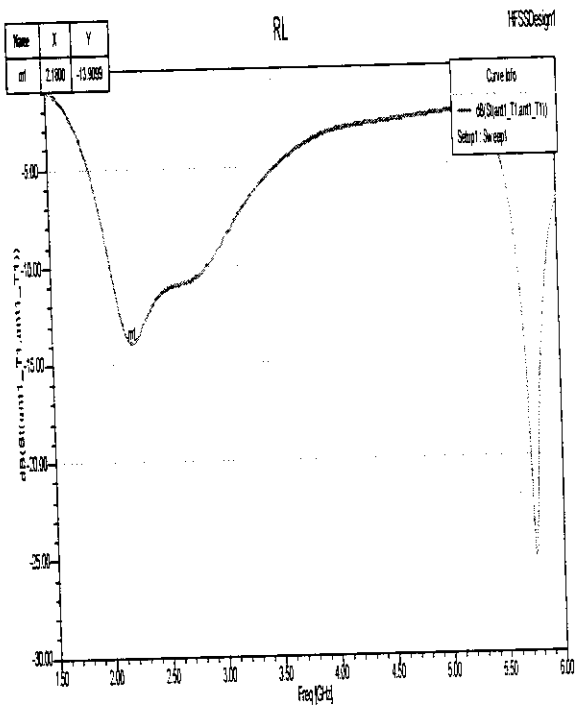
Figure 4.5.5: Structure of F- antenna of substrate dimension $47 \times 40 \text{mm}^2$ and cutout $47 \times 18 \text{mm}^2$ on HFSS.

Table 4.5.5: Microstrip F Antenna of substrate dimension $47 \times 40 \text{mm}^2$ and cutout $47 \times 18 \text{mm}^2$ on Design Parameters

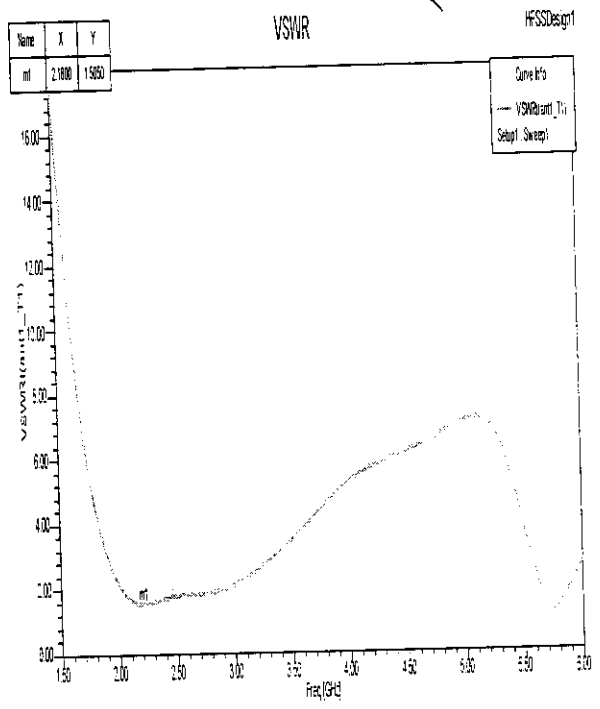
Parameter	Value (cm)
Length 1	1.5
Length 2	0.89
Length 3	0.79
Antenna width	0.25
Antenna X shift	0.77
Feed width	0.18
Cut out X	4.7
Cut out Y	1.8
SubX	4.7
SubY	4



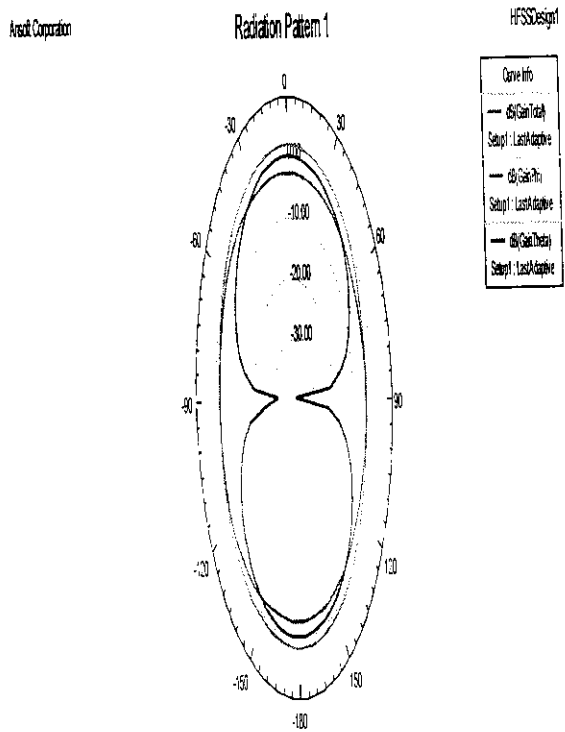
4.5.5.1. FR4 of 1mm thickness



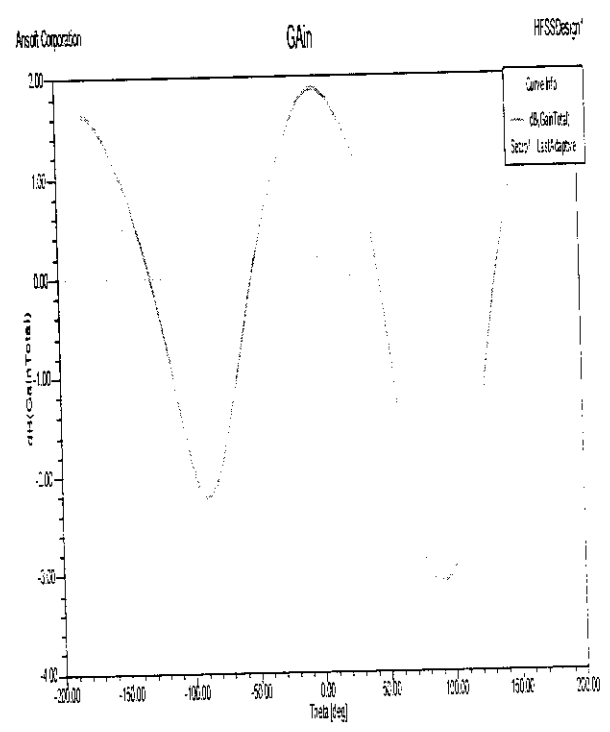
(a)



(b)



(c)



(d)

Figure 4.5.5.1: Simulated results of F antenna of substrate dimension $47 \times 40 \text{mm}^2$ and cutout $47 \times 18 \text{mm}^2$ with FR4 of thickness 1mm (a) Return Loss (b) VSWR (c) Radiation Pattern (d) Gain

4.5.5.2. FR4 of 1.6mm thickness

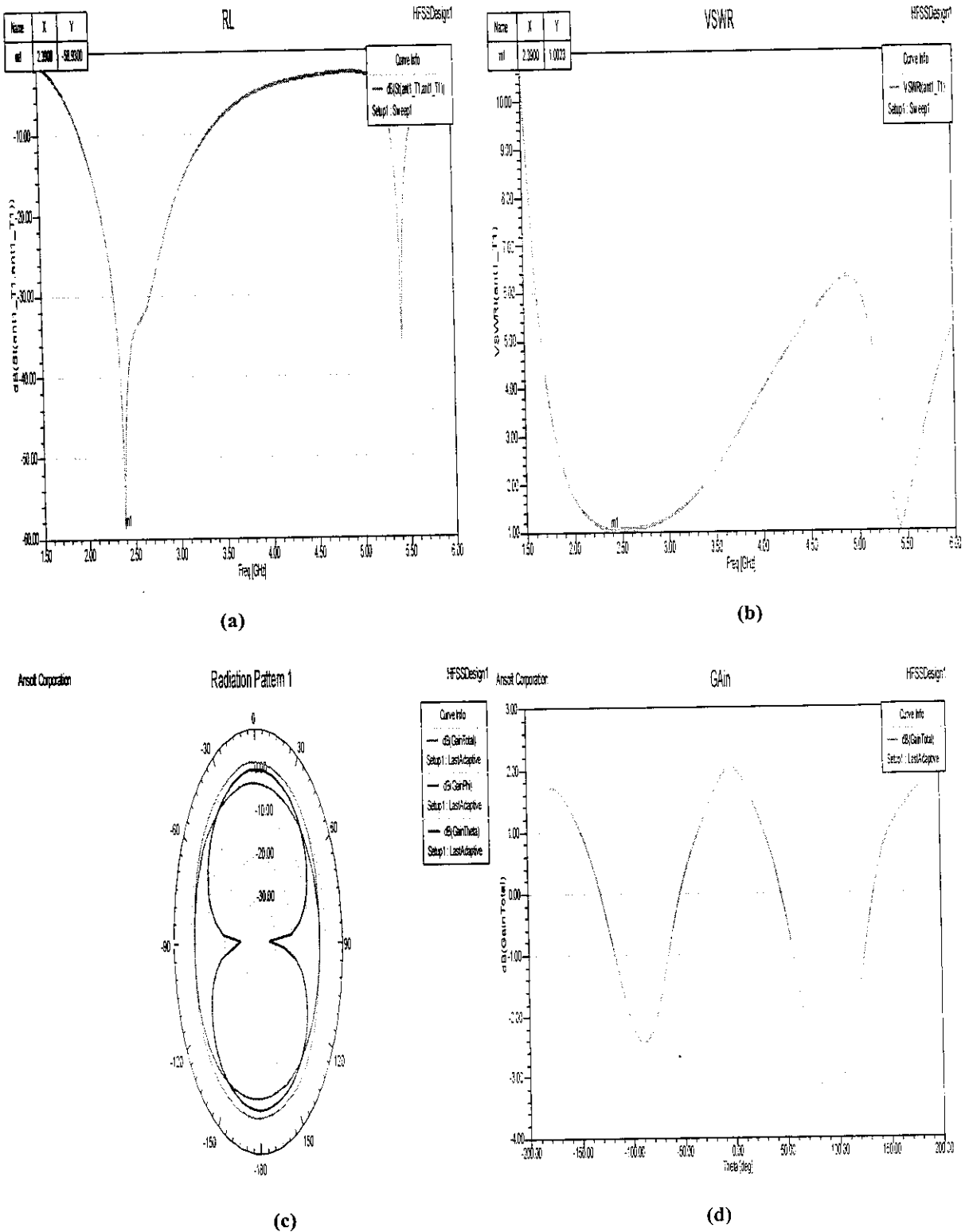


Figure 4.5.5.2: Simulated results of F antenna of substrate dimension $47 \times 40 \text{mm}^2$ and cutout $47 \times 18 \text{mm}^2$ with FR4 of thickness 1.6mm (a) Return Loss (b) VSWR (c) Radiation Pattern (d) Gain

4.6 SPIRAL SHAPED -MONOPOLE ANTENNA USING DIFFERENT SUBSTRATE MATERIAL

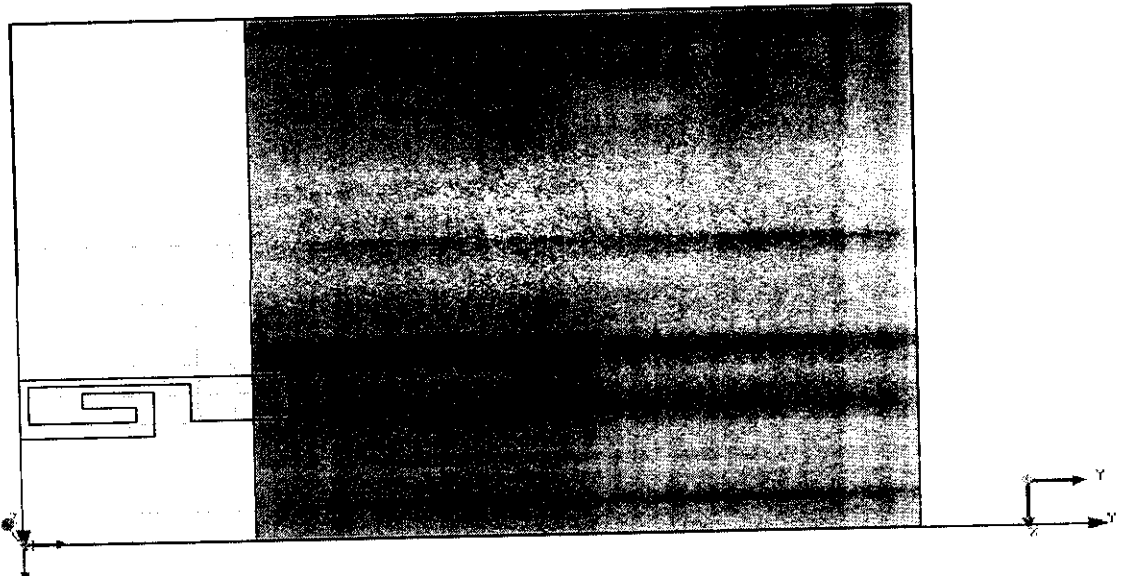


Figure 4.6: Structure of Spiral Antenna on HFSS

Table 4.6: Microstrip Spiral Antenna Design Parameters

Parameter	Value (cm)
Length 1	1
Length 2	0.4
Antenna width1	0.05
Antenna width2	0.1
Antenna X shift	0.71
Feed width	0.3
Cut out X	3.5
Cut out Y	1.3
SubX	3.5
SubY	5

4.6.1. FR4 of 1mm thickness

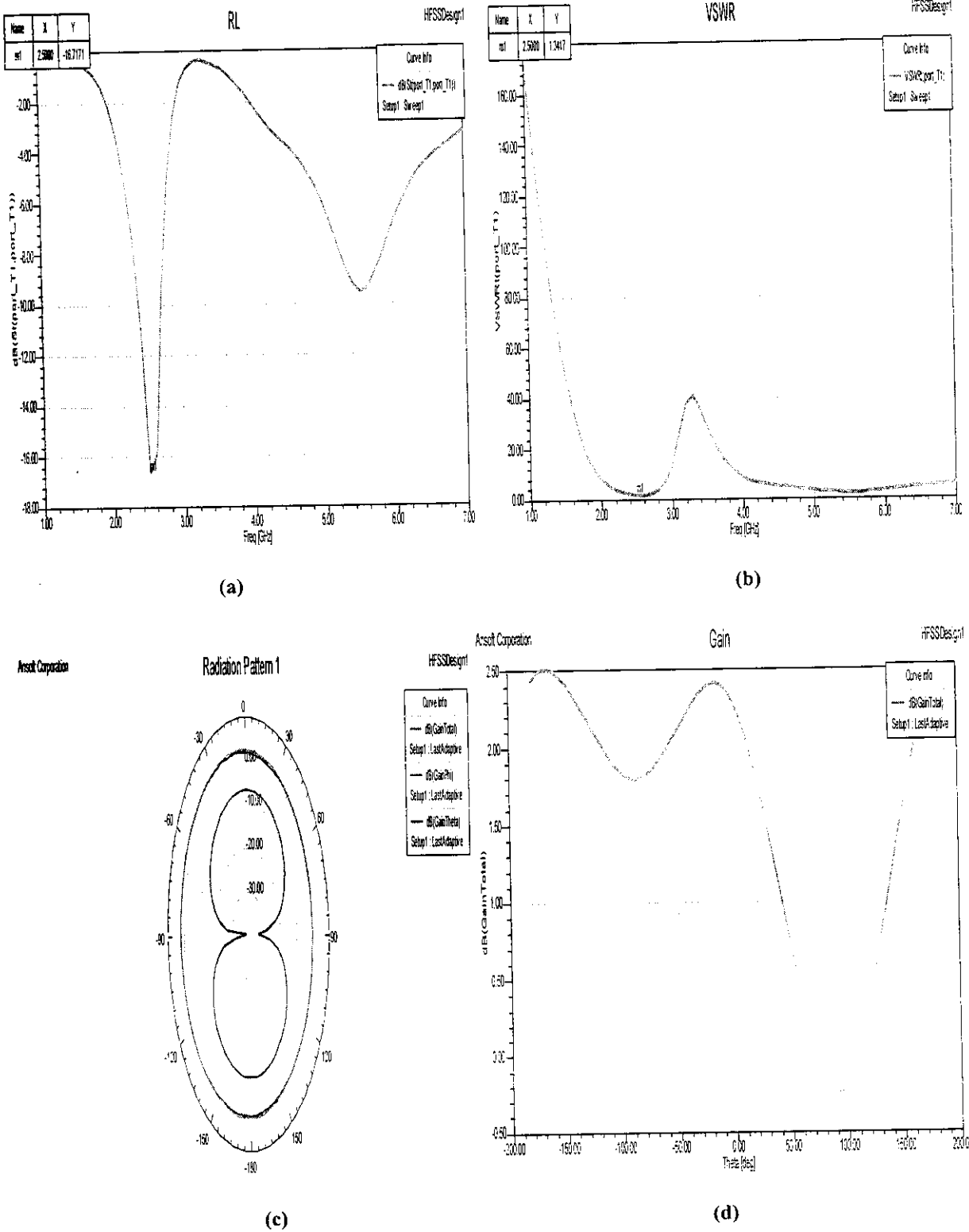


Figure 4.6.1: Simulated results of Spiral antenna with FR4 of thickness 1mm (a) Return Loss (b) VSWR (c) Radiation Pattern (d) Gain

4.6.2. FR4 of 1.6mm thickness

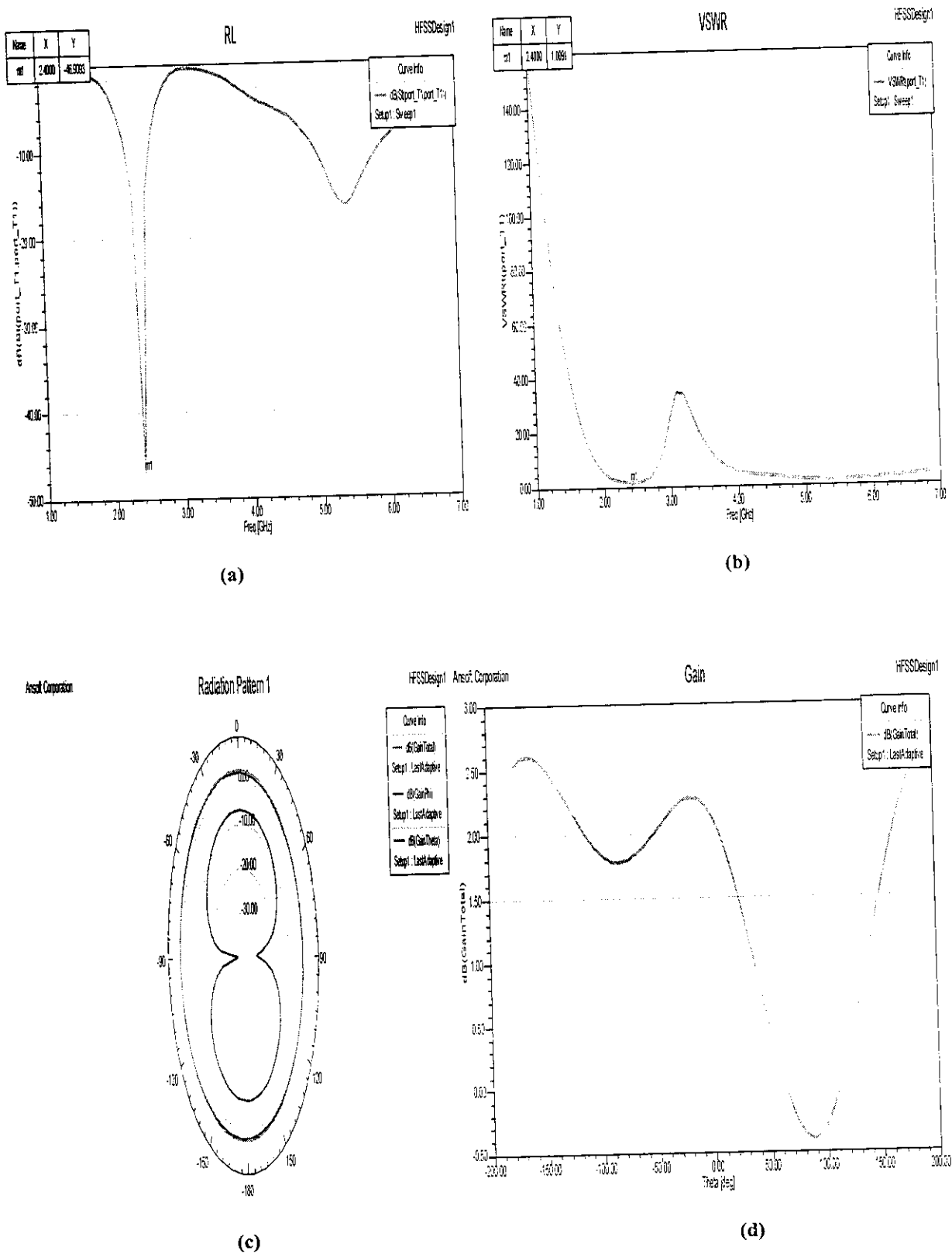


Figure 4.6.2: Simulated results of Spiral antenna with FR4 of thickness 1.6mm (a) Return Loss (b) VSWR (c) Radiation Pattern (d) Gain

4.6.3. DUROID 5880 of 1.575mm thickness

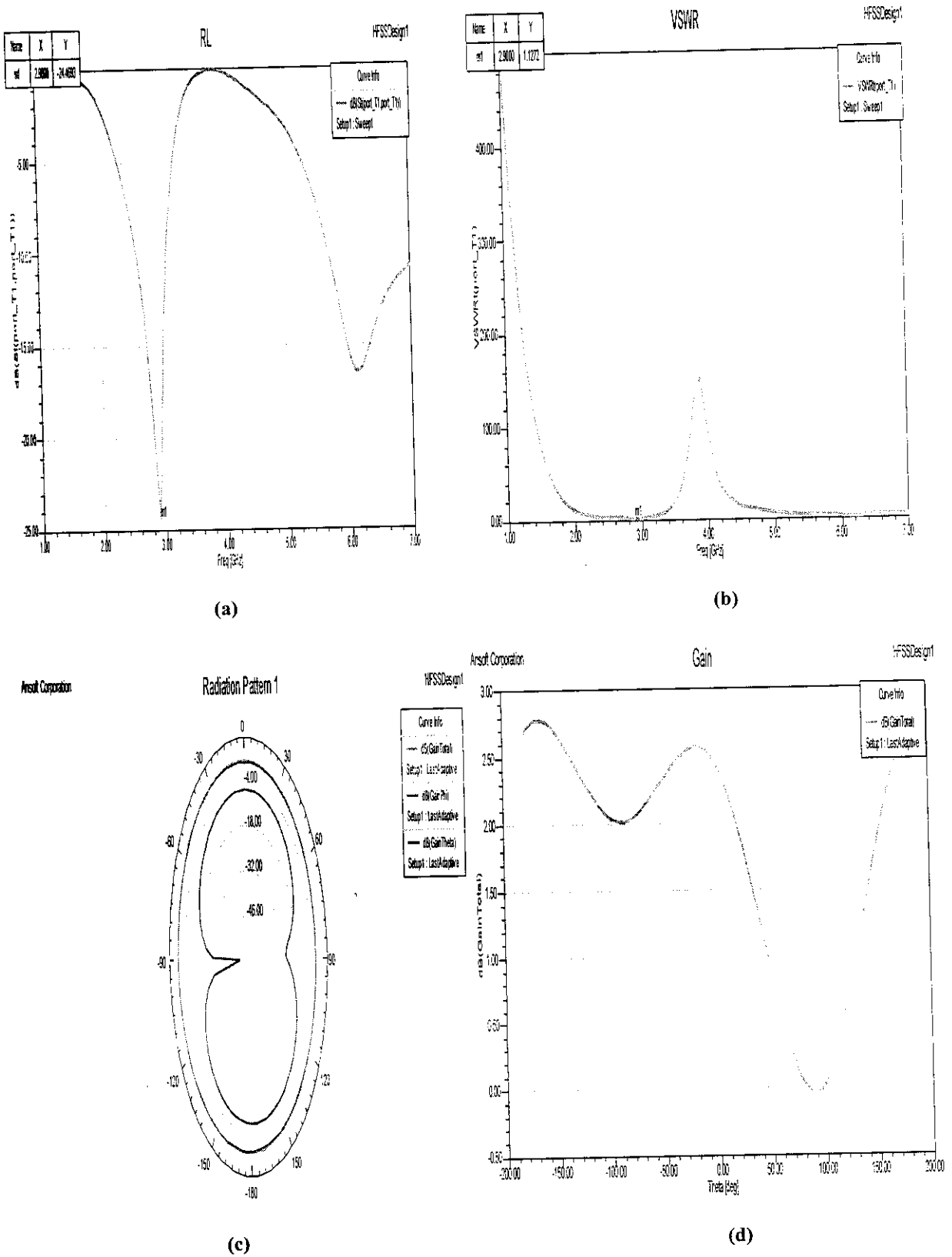
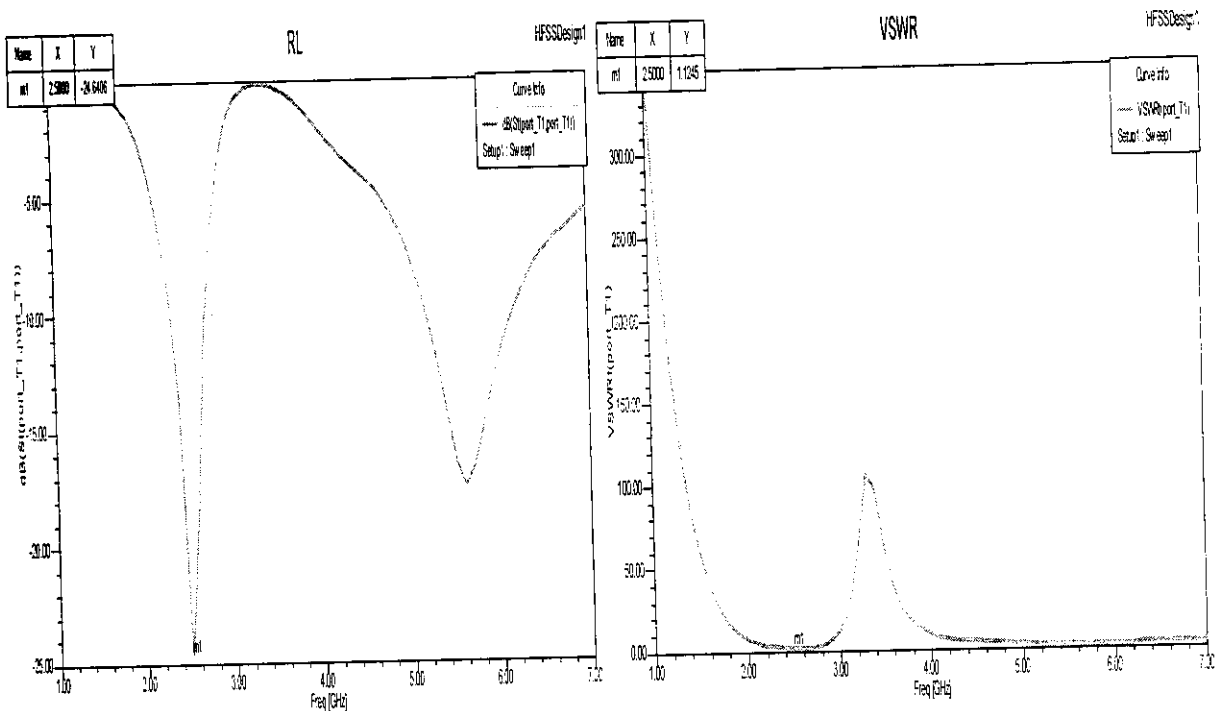


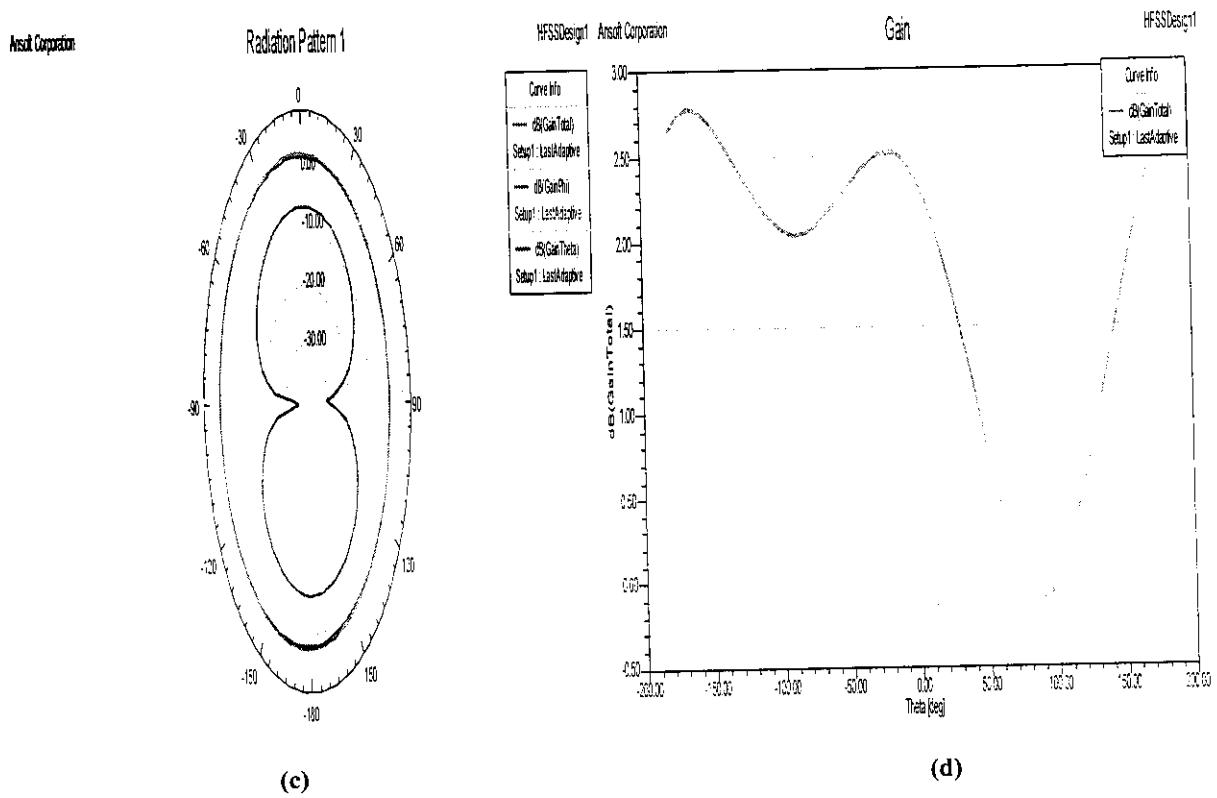
Figure 4.6.3: Simulated results of Spiral antenna with Duroid 5880 (a) Return Loss (b) VSWR (c) Radiation Pattern (d) Gain

4.6.4. ROGERS RO 4350 of 1.524mm thickness



(a)

(b)



(c)

(d)

Figure 4.6.4: Simulated results of Spiral antenna with RO 4350 (a) Return Loss (b) VSWR (c) Radiation Pattern (d) Gain

Table 4.7: Best results based on different substrates for different antenna shapes

Type of Antenna	Substrate Material	Return Loss	VSWR
Planar Dipole Antenna	Rogers 4350	-41.92	1.01
Rectangular Inset Feed Patch Antenna	FR4 (1.6mm)	-35.29	1.02
Elliptical Inset Feed Patch Antenna	FR4 (1.6mm)	-28.73	1.07
PIFA	FR4 (1mm)	-46.35	1.01
F-Monopole of substrate dimension 45x80mm ²	FR4	-13.61	1.52
F-Monopole of substrate dimension 50x35mm ²	FR4 (1.6mm)	-58.05	1.00
F-Monopole of substrate dimension 47x40mm ²	FR4 (1.6mm)	-58.93	1.00
Planar Spiral Antenna	FR4(1.6mm)	-46.90	1.01

From the simulation results it is inferred that F-antenna is having the best performance with FR-4 substrate dimension 47x40mm² of 1.6mm thickness. It is seen that the reduction of the size of the ground plane increases the Return Loss. The ground plane reduces the back lobe radiation.

Array of F antenna with 2 elements and 4 elements was also simulated. In the case of array, it is seen that though it increases the gain, Return Loss and the Omni directional pattern of antenna decreases. All the antennas are fabricated but a few with better Return Loss are studied here. In order to study the practical implications of F-antenna with dimension 50x35mm², 47x40mm² and planar spiral antenna are fabricated.

CHAPTER 5

FABRICATION AND MEASURED RESULTS

The HFSS Simulations were first converted to DXF file and then to the Gerber file using the ORCAD software.

The device used for fabrication is LPKF ProtoMat C30s as shown in the below figure.

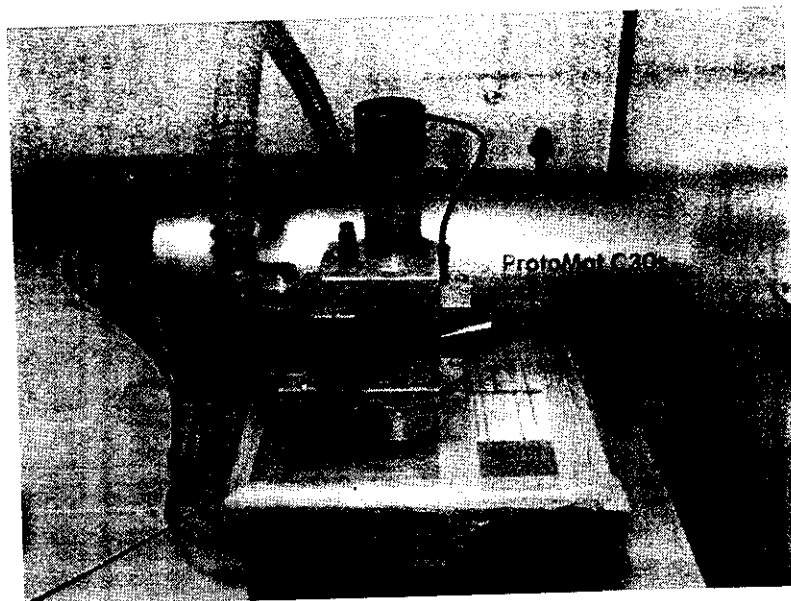


Figure 5.1: Device used for fabrication

The fabricated antennas are

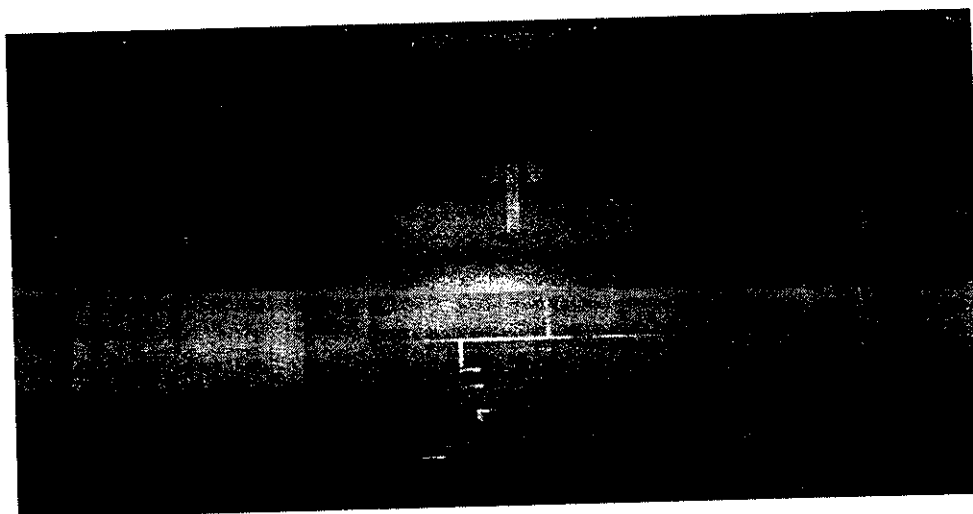


Figure 5.2: Different antenna shapes fabricated

Though all the antenna shapes are fabricated the antenna shapes of rectangular patch, elliptical patch, dipole, PIFA and the array of F shape did not pass the range test. So these shapes were discarded.

The studied antennas are:

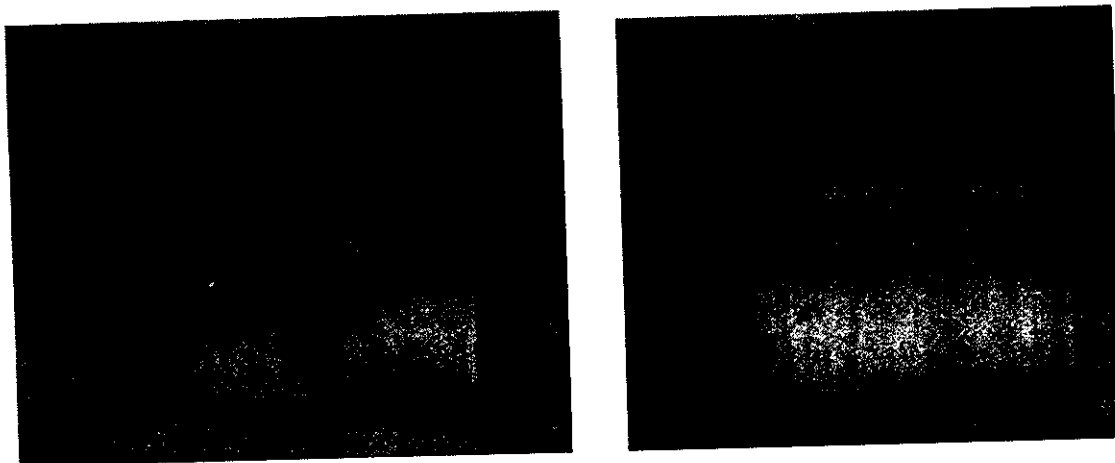


Figure 5.3: Fabricated F-antennas of substrate dimension $47 \times 40 \text{mm}^2$ and $50 \times 35 \text{mm}^2$



Figure 5.4: Planar spiral antenna of substrate dimension $35 \times 50 \text{mm}^2$

The Return Loss and VSWR is measured using Network analyser.

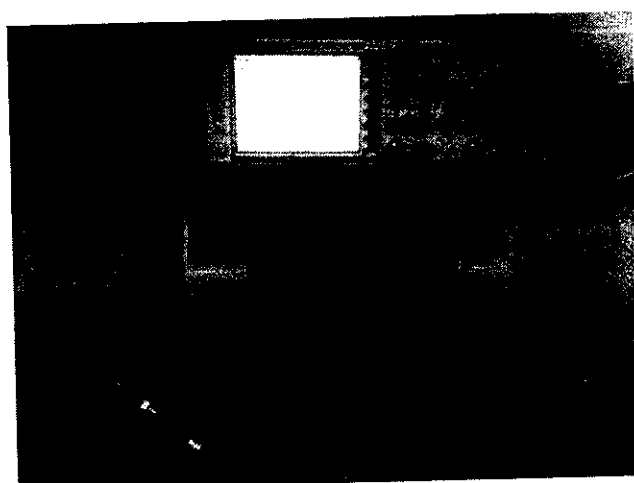
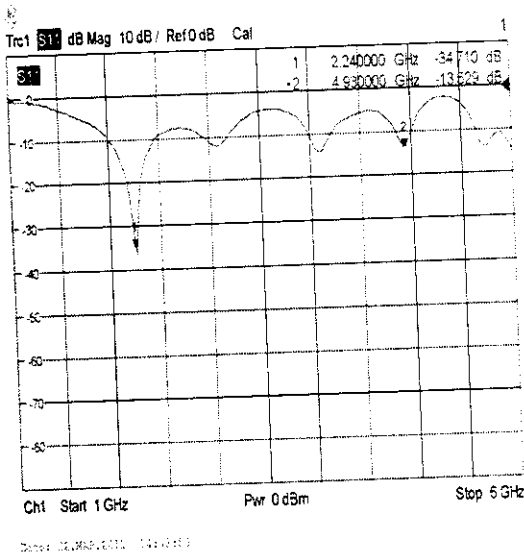


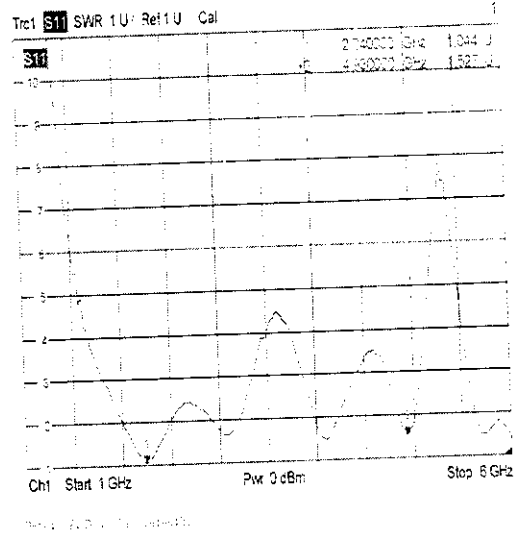
Figure 5.5: Network Analyzer used for measurement of Return Loss and VSWR

5.1 MEASURED RETURN LOSS AND VSWR

5.1.1. F-antenna of $9 \times 15 \text{mm}^2$ integrated on FR4 of 1.6mm thickness substrate dimension- $50 \times 35 \text{mm}^2$



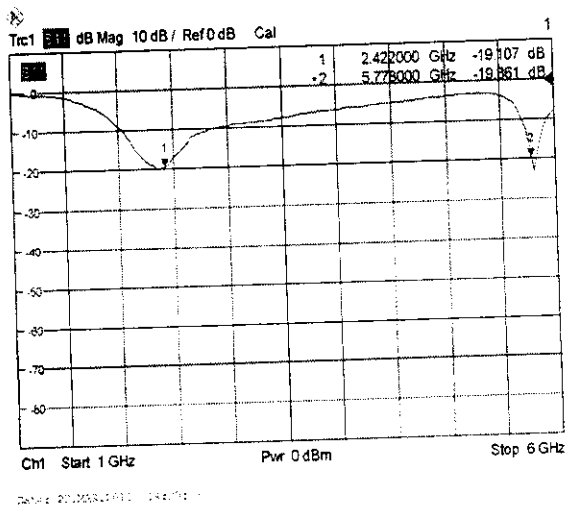
(a)



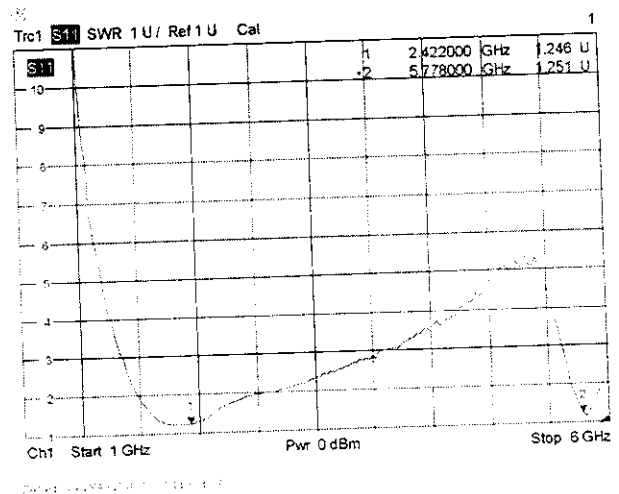
(b)

Figure 5.1.1: Measured Results of F-antenna of $9 \times 15 \text{mm}^2$ integrated on FR4 of 1.6mm thickness substrate dimension- $35 \times 50 \text{mm}^2$ (a) Return Loss (b) Measured VSWR

5.1.2. F-antenna of $9 \times 15 \text{mm}^2$ integrated on FR4 of 1.6mm thickness substrate dimension- $47 \times 40 \text{mm}^2$



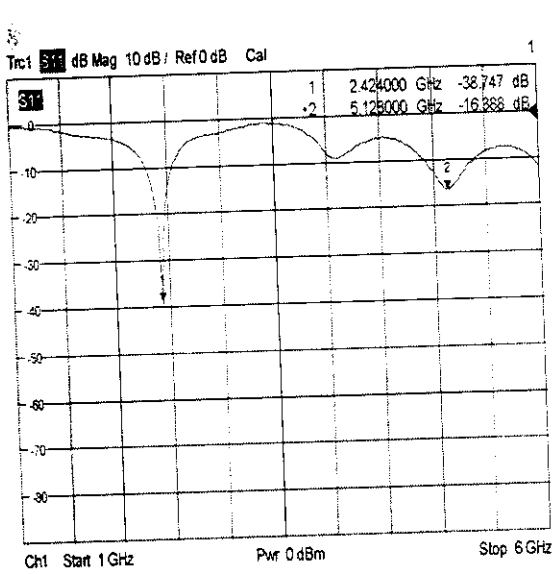
(a)



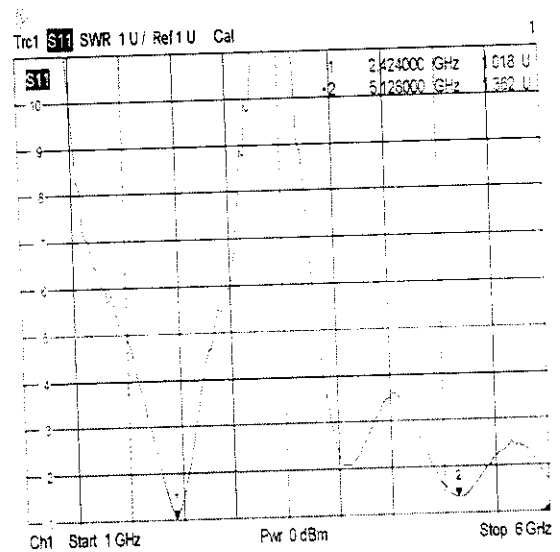
(b)

Figure 5.1.2: Measured Results of F-antenna of $9 \times 15 \text{mm}^2$ integrated on FR4 of 1.6mm thickness substrate dimension- $47 \times 40 \text{mm}^2$ (a) Return Loss (b) Measured VSWR

5.1.3. Planar Spiral of $5 \times 10 \text{mm}^2$ & FR4- $35 \times 50 \text{mm}^2$



(a)



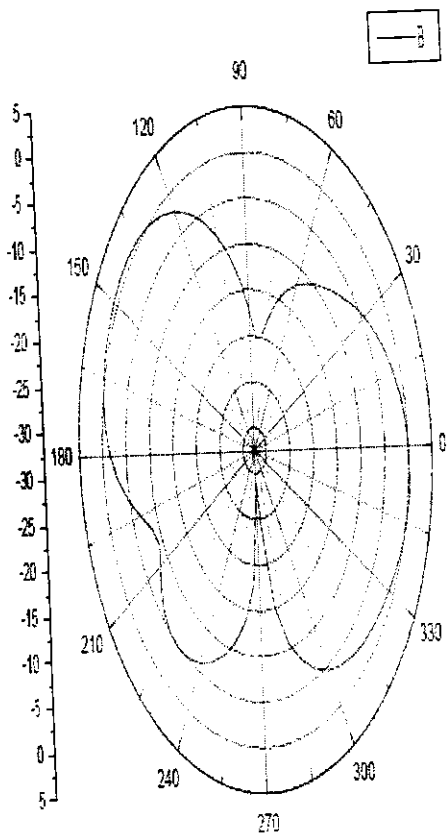
(b)

Figure 5.1.3: Measured Results of Spiral of $5 \times 10 \text{mm}^2$ & FR4- $35 \times 50 \text{mm}^2$ (a) Return Loss (b) Measured VSWR

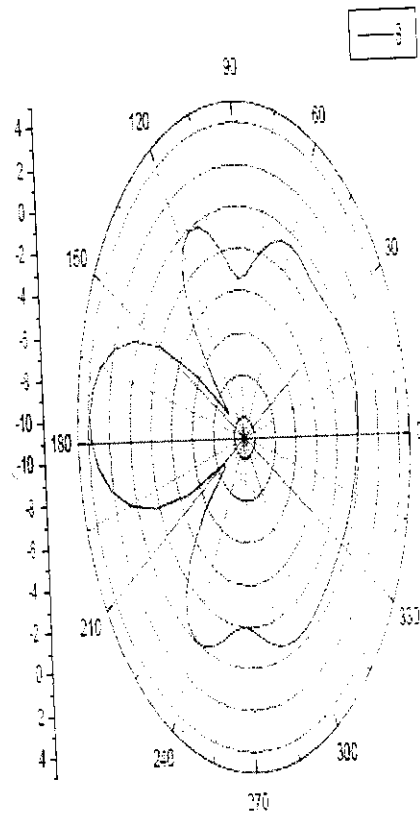
5.2 MEASURED RADIATION PATTERN

The radiation pattern was measured with Horn antenna as the reference antenna, Network Analyzer and a rotating tripod on which the fabricated antenna was placed. One port of the network analyzer was connected to Horn antenna and the other port is connected with the fabricated antenna. The measurements were taken at 5 degree step angle. The Fabricated antenna was connected to a PC where the antenna pattern was measured using CREMA software. The radiation pattern was plotted for four planes namely E-co plane, E-cross plane, H-co plane and H-cross plane.

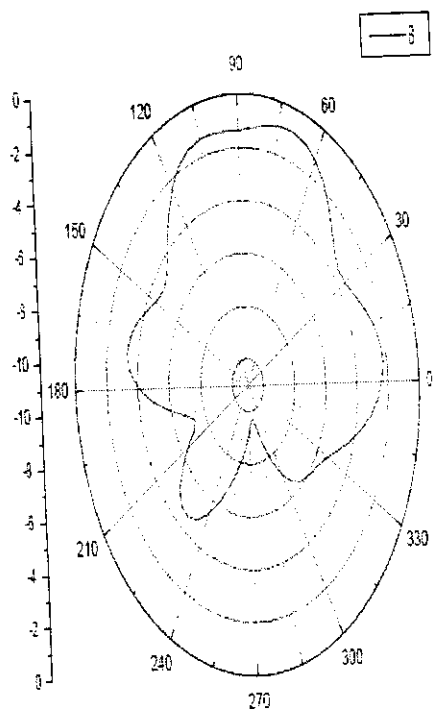
5.2.1. F-antenna of $9 \times 15 \text{mm}^2$ integrated on FR4 substrate dimension- $47 \times 40 \text{mm}^2$



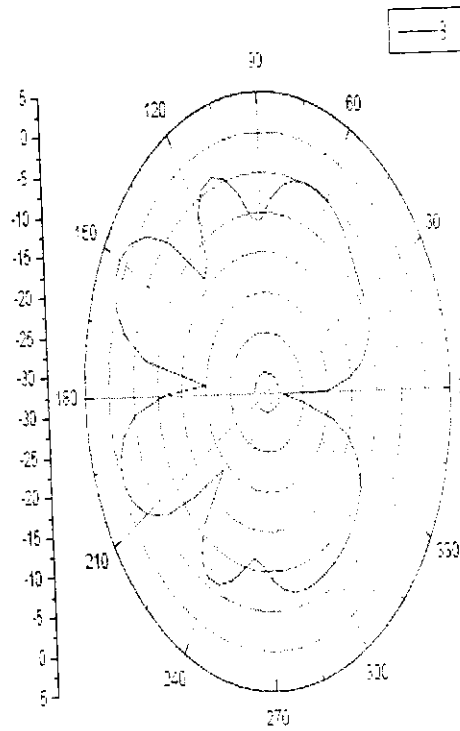
(a)



(b)



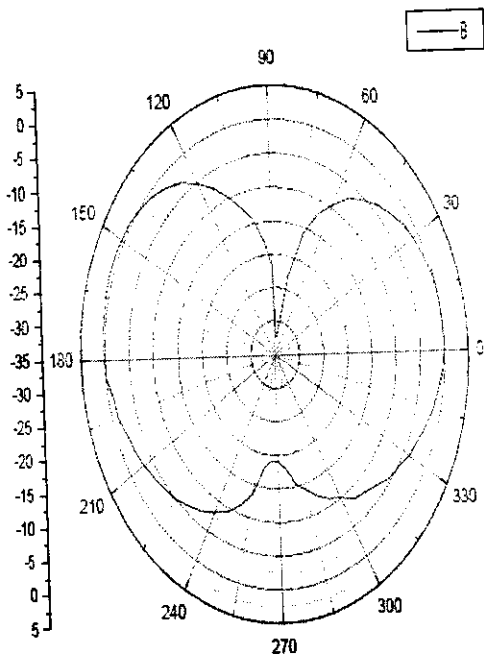
(c)



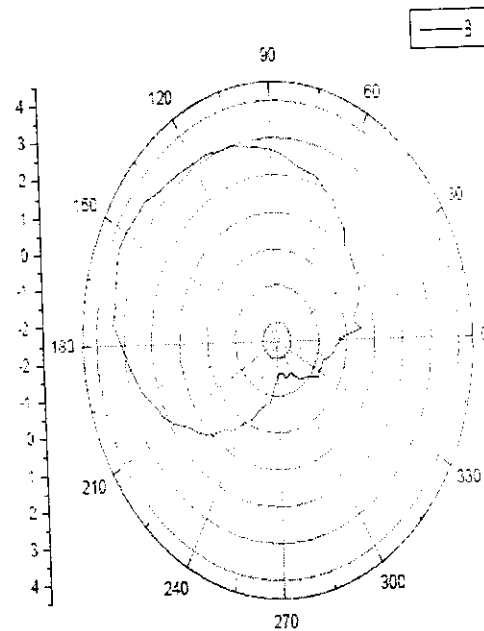
(d)

Figure 5.2.1: Measured Radiation Pattern of F-antenna of $9 \times 15 \text{mm}^2$ integrated on FR4 substrate dimension- $47 \times 40 \text{mm}^2$ in (a) E-co plane (b) H-co plane (c) E-cross plane (d) H-cross plane

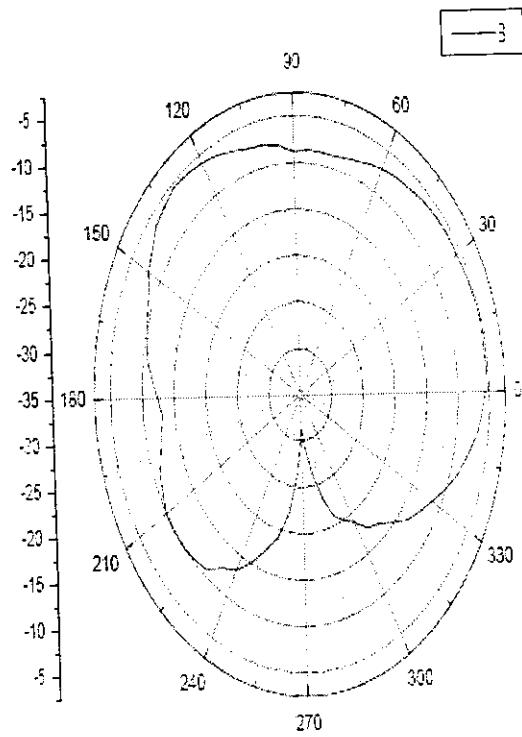
5.2.2. Planar Spiral antenna of $5 \times 10 \text{mm}^2$ & FR4- $35 \times 50 \text{mm}^2$



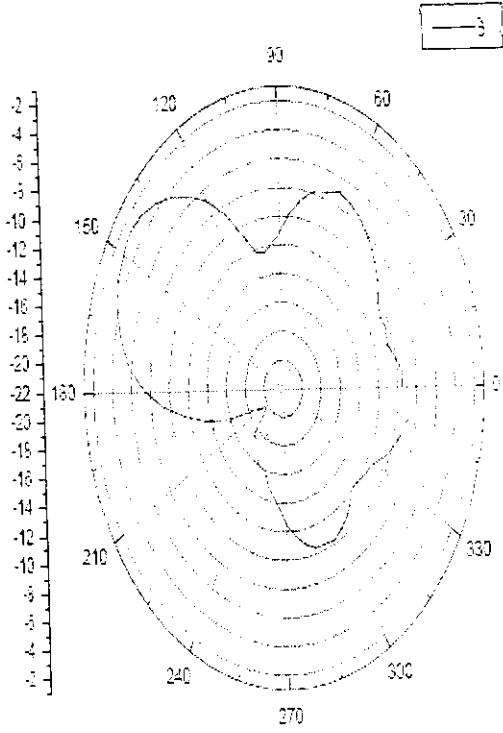
(a)



(b)



(c)



(d)

Figure 5.2.2: Measured Radiation Pattern of Spiral antenna of $5 \times 10 \text{mm}^2$ & FR4- $35 \times 50 \text{mm}^2$ in (a) E-co plane (b) H-co plane (c) E-cross plane (d) H-cross plane

5.3 RANGE RESULTS

For range testing a laptop, Wi-Fi antenna and the scanner device was used. The fabricated antenna was placed inside the scanner device to check the maximum range. The scanner was placed stationary and the Wi-Fi antenna was moved to different distances and the three test were verified.

The device setup is shown below

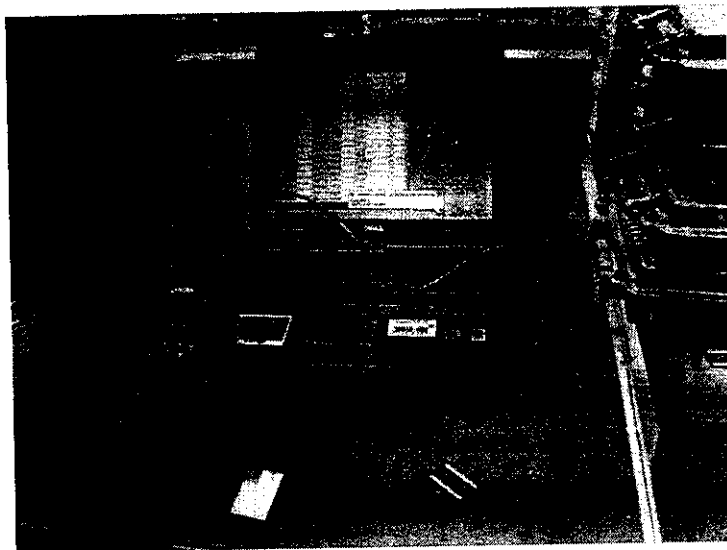


Figure 5.3.1: Device set-up for Range measurement

Measurements are compared with existing RGIS dipole antenna. Different configuration were done here as part of the project work. Two antennas (F-Monopole) and Planar Spiral antenna intended for RGIS requirement were compared below with existing RGIS antenna. Three tests were verified and passed consisting of

1. WLAN Power up
2. Ping Test
3. Test File Download

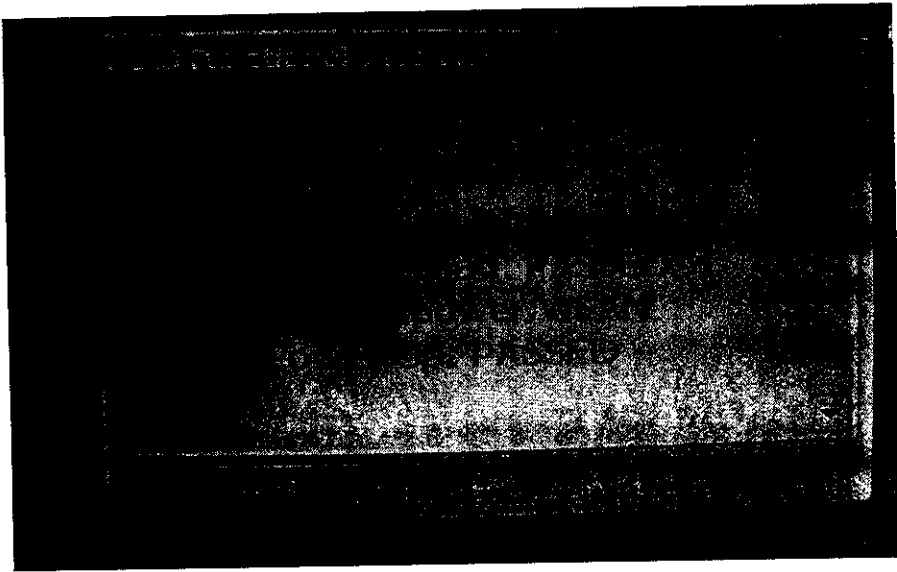


Figure 5.3.2: WLAN Power up test

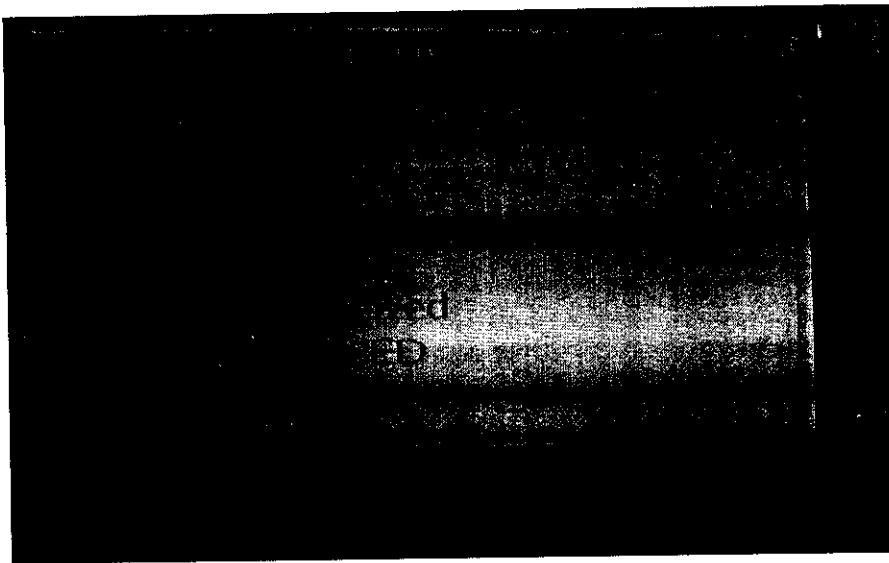


Figure 5.3.3: Ping Test

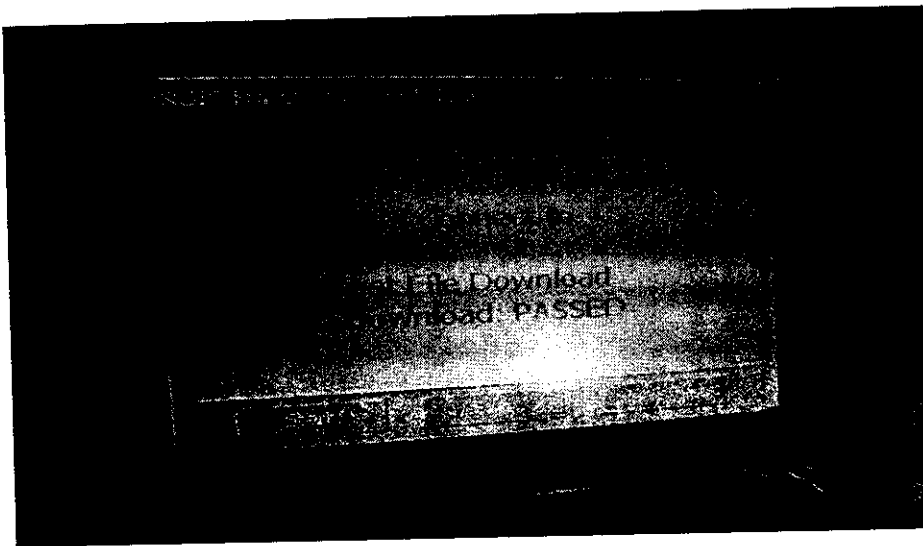


Figure 5.3.3: Test File Download test

Line of Sight: tested up to 144 feet

RGIS Antenna: Passed

F-Monopole and Spiral Antenna: Passed

When scanner with Antenna and Access point placed in two corners:

RGIS Antenna: Passed at 96 feet but failed when verified at 112 feet.

F-Monopole and Spiral Antenna: tested up to 178 feet and passed. (More than 178 feet is possible but not verified).

Distance was measured by counting the no. of floor tiles (2x2 feet).

CHAPTER 6

CONCLUSION

An inventory taking device was having a non satisfactory data communication performance and it was analysed in details and found that the major issue was related to the performance of the attached microstrip antenna. On our measurement, this was confirmed to have bad return loss characteristics. A detailed study was undertaken to arrive at an optimum antenna design, which shall replace the existing one.

Literature survey was done. Simulation studies were carried out for six different antenna shapes namely rectangular patch, elliptical patch, dipole, PIFA, F-Monopole and Spiral. Three different substrate materials and their thickness combinations namely RT/Duroid 5880 with thickness of 1.575mm, Rogers 4350 with thickness of 1.524mm and FR-4 with thickness of 0.8mm, 1mm and 1.6mm were designed and simulated for the performance. Except dipole all other shapes gave better performance with FR-4 substrate whereas for dipole, substrate Rogers 4350 gave better performance. The targeted device is already having complex electronic circuits on FR4 PCB; it is preferred to have the antenna structure also on FR4. It is also less expensive when compared to other substrate. As a result the different antenna shapes were fabricated on FR4 with thickness 1mm and 1.6mm and studied.

Though the measured return loss result of the rectangular patch, elliptical patch, dipole and PIFA gave matching shape to the simulated results, these antennas did not pass the range test. These were attributed to the poor gain performance of these antennas. So these shapes were discarded and F-shape and spiral Antenna were selected.

Table 6.1: Comparison of simulated and measured result of F and spiral antenna

Type of antenna	RL (dB)		VSWR	
	Measured	Simulated	Measured	Simulated
F-antenna	-34.71	-58.09	1.04	1.002
Spiral	-38.78	-46.96	1.02	1.018

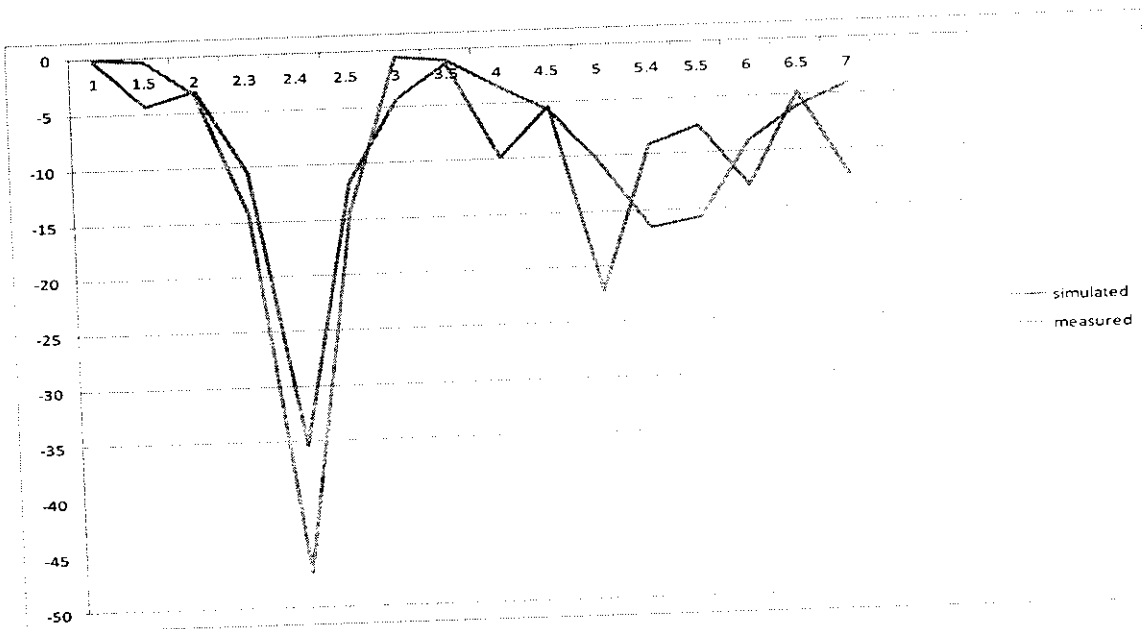


Figure 6.1: Comparison of simulated and measured Return Loss of spiral antenna

Figure 6.1 shows the simulated and measured return loss of the constructed spiral antenna. Satisfactory agreement between the measurement and the AnSoft HFSS simulation is obtained. Two separate wide bandwidths at about 2.4 and 5.2 GHz are obtained. A return loss below -10 dB looks to be good for use. The lower band has an impedance bandwidth of 210MHz, and covers the required 3-dB bandwidth of the 2.4GHz band. The upper band has a bandwidth of 141MHz.

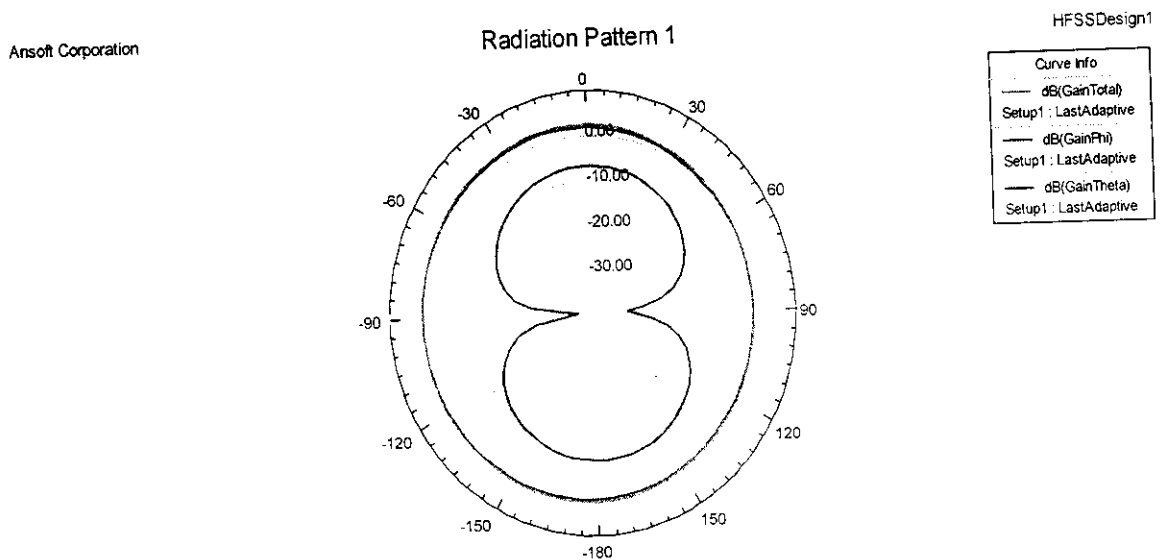


Figure 6.2: Simulated Radiation Pattern of Spiral Antenna in terms of Theta and Phi plane

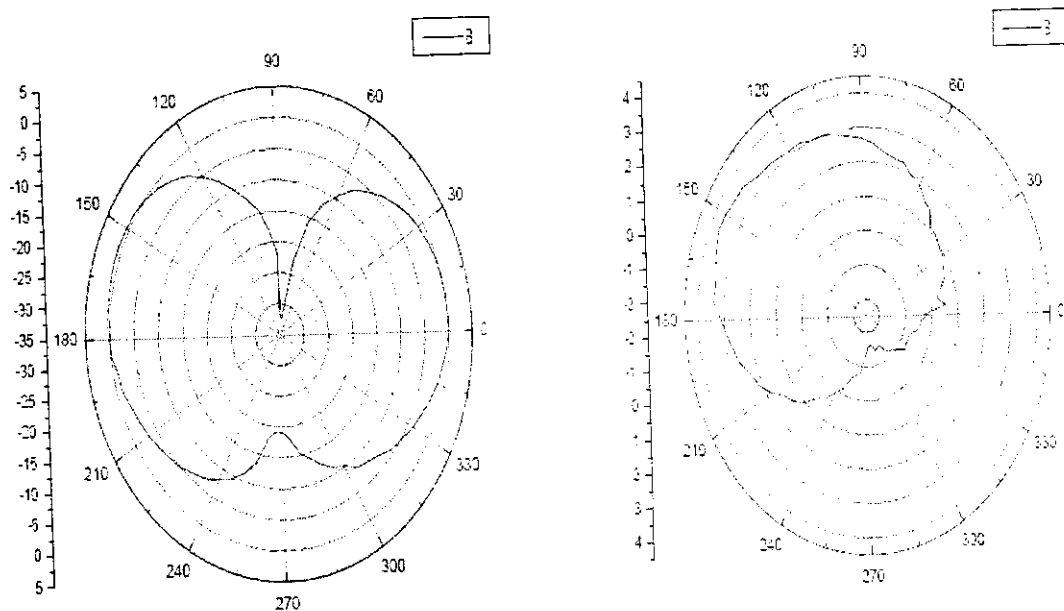


Figure 6.3: Measured Radiation Pattern of Spiral antenna in E-co plane and H-co plane resp.

From the range measurement, it is inferred that both Spiral Antenna and F-Antenna gives a range of more than 178feet. But Radiation pattern of Planar Spiral is more Omni-directional than F-antenna. Considering the return loss, VSWR and radiation pattern, the planar spiral antenna is giving the better performance.

This spiral antenna fabricated in house was attached to the inventory taking device, by replacing the earlier existed microstrip antenna which gave poor performance. Real life test was done on this device with our designed antenna and could see a considerable improvement in performance. The size of the antenna is comparable with the existing one, and a direct replacement is possible without any changes in the mechanical structure or fit.

It is satisfying to note that the antenna has been selected for further use in these devices and a volume production is planned. The customer is based in USA, and the result of these studies has become part of a device which will be used globally.

BIBLIOGRAPHY

- [1]. Constantine A. Balanis "Antenna Theory Analysis and Design"(2nd ed.),JOHN WILEY & SONS,INC,New York,1997
- [2]. M.H.Jamaluddin,M.K.A Rahim, M.Z.A Abd. Aziz,A.Asrokin ,"Microstrip dipole antenna for wlan application" 2005 IEEE
- [3]. M.K.A Rahim, M.Z.A Abd. Aziz,A.Asrokin "Dual band microstrip antenna for wlan" 2005 Asia-Pacific Conference on Applied Electromagnetics,December 20-21,2005
- [4]. Amritesh& Kshetrimayum Milan Singh, "Design of Square Patch Microstrip Antenna for Circular Polarization using IE3D Software"
- [5]. C. Vishnu Vardhana Reddy&Rahul Rana," Design Of Linearly Polarized Rectangular Microstrip Patch Antenna Using IE3D/PSO" National Institute of Technology,Rourkela,2009.
- [6].Shih-huang Yeh And Kin-lu Wong "Integrated F-shaped Monopole Antenna for 2.4/5.2 GHz Dual-band Operation" Microwave and optical technology letters, Vol. 34, No. 1, July 5 2002
- [7]. Kin- Lu Wong "Planar Antennas for wireless communication", A John Wiley & Sons, INC., Publication, 2003.
- [8]. Evangelos S. Angelopoulos, Antonis I. Kostaridis, And Dimitra I. Kaklamani," A Novel Dual-band F-inverted antenna printed on a PCMCIA card" Microwave and optical technology letters, Vol. 42, No. 2, July 20 2004
- [9]. H.C.Tung, W.S.Chen an spird K.L.Wong, "Integrated rectangular spiral monopole antenna for 2.4/5.2GHz dual band operation". in 2002 IEEE Antennas Propagations Soc. Int. Symp. Dig. Vol 3, pp 446-449.
- [10]. Dr. Ryan S. Adams, "Ansoft HFSS Tutorial: Stripline" March 12, 2008
- [11]. Lakshmi Achutha and Dr.Jayanti Venkatraman,"Ansoft HFSS Tutorial Rectangular Waveguide", (Rochester Institute Of Technology),Rochester ,NY

- [12]. Asok De, N.S. Raghava, Sagar Malhotra, Pushkar Arora, Rishik Bazaz.” Effect of different substrates on Compact stacked square Microstrip Antenna” Journal Of Telecommunications, Volume 1, Issue 1, February 2010
- [13]. Ansoft High Frequency Structure Simulator v10 User’s Guide, Ansoft Corporation
- [14]. www.k5rmg.org/tech/rtn-loss.html
- [15]. www.microwaves101.com/encyclopedia/vswr.cfm
- [16]. www.HFSS-Tutorial.htm



Karunya UNIVERSITY

(Karunya Institute of Technology and Sciences)
Declared as Deemed to be University Under sec. 3 of the UGC Act, 1956
Karunya Nagar, Coimbatore 641 114, India


Department of Electronics and Communication Engineering

CERTIFICATE

This is to certify that Dr/Mr/Ms/Mrs..... *Ria Maxia George*..... of *Kumaraguru College of Technology, Coimbatore*..... has participated / presented a paper titled *Design and development of High efficiency microstrip antenna for*..... in the International Conference "Communication and Signal Processing (ICCOS '11)" on 17th & 18th March 2011 organized by the School of Electrical Sciences, Department of Electronics and Communication Engineering, Karunya University, Coimbatore, India.


Dr. A. Ravi Sankar
Convener


Dr. (Mrs.) Anne Mary Fernandez
Patron


Dr. Paul P. Appasamy
Patron